ERDC/CHL TR-12-24

Coastal and Hydraulics Laboratory

US Army Corps of Engineers®
Engineer Research and Development Center

Wave Runup Prediction for Flood Hazard Assessment

Jeffrey A. Melby

October 2012

ERDC/CHL TR-12-24
October 2012

Wave Runup Prediction for Flood Hazard Assessment

Jeffrey A. Melby

Coastal and Hydraulics Laboratory
U.S. Army Engineer Research and Development Center
3909 Halls Ferry Road
Vicksburg, MS 39180–6199

Final report

Prepared for U.S. Army Engineer District, Detroit
477 Michigan Avenue
Detroit, MI 48226

and Federal Emergency Management Agency
536 Clark Street, 6th Floor
Chicago, IL 60605

Great Lakes Coastal Flood Study,
2012 Federal Inter-Agency Initiative

Abstract

Wave runup determines the extent over which waves act. Wave runup is therefore an important parameter to determine flood inundation extents from coastal storms. Cross-shore and longshore sediment transport are a function of the hydrodynamics on the beach and are therefore related to wave runup. In this report, several benchmark wave runup data sets are summarized and used to evaluate the available tools for predicting wave runup for flood hazard assessment. Benchmark data cover a range of shoreline conditions including sandy beaches on the Pacific and Atlantic coasts, dissipative to reflective beaches, as well as structures ranging from impermeable smooth levees to rough permeable rubble mounds. Data include laboratory and prototype measurements. Tools for predicting wave runup are analyzed including empirical equations, computer programs based on empirical equations, and the CSHORE numerical hydrodynamic model. Most of the tools show fairly high degrees of skill but some do not. The study recommends using the numerical hydrodynamic program CSHORE to model runup for most beach and structure conditions. However, CSHORE is not likely to predict wave runup on infragravity-dominated dissipative beaches well. For these cases, it is recommended that one of the recommended empirical equations for beaches be used.

Table of Contents

List of Figures and Tables

Figures

Tables

Preface

The study summarized in this report was conducted at the request of the U.S. Army Corps of Engineers (USACE), Detroit District (LRE). Greg Mausolf was the primary engineering point of contact at LRE. The study was funded by the Federal Emergency Management Agency (FEMA) through LRE and conducted at the U.S. Army Engineer Research and Development Center (ERDC), Coastal and Hydraulics Laboratory (CHL), Vicksburg, MS, during the period November 2010 – November 2011. The FEMA Lead was Ken Hinterlong, Chief, Risk Analysis Branch, Mitigation Division, FEMA Region V. Julie Tochor, Accenture, was the Program Management Lead for FEMA Region V.

This report was prepared by Dr. Jeffrey A. Melby, Harbors, Entrances, and Structures (HES) Branch, CHL. Bruce Ebersole, Chief, Flood and Storm Protection Division; Prof. Nobuhisa Kobayashi, University of Delaware; and Mausolf (LRE), provided thorough reviews. In addition, CSHORE code, example input files, and general support were provided by Jill Pietropaolo, a Civil Engineering student at the University of Delaware. The beach runup data were provided by Hilary Stockdon (U.S. Geological Survey).

Dr. Melby was under the general supervision of Dr. Jackie Pettway, Chief, HES Branch, and Dr. Rose Kress, Chief, Navigation Division.
Dr. William D. Martin was Director, CHL, and Jose Sanchez was Deputy Director, CHL.

COL Kevin J. Wilson was Commander and Executive Director of ERDC.
Dr. Jeffery P. Holland was Director.

Unit Conversion Factors

A sponsor requirement for this study was the use of English Customary units of measurement. Most measurements and calculations were done in SI units and then converted to English Customary. The following table can be used to convert back to SI units.

Multiply	By	To Obtain
cubic feet	0.02831685	cubic meters
feet	0.3048	meters
pounds (force)	4.448222	newtons
square feet	0.09290304	square meters

1 Introduction

1.1 Background

Wave runup determines the extent over which waves act. Wave runup is therefore an important parameter to determine inundation from coastal storms. Cross-shore and longshore sediment transport are a function of the hydrodynamics on the beach and are therefore related to wave runup. Wave runup is required to determine the crest height of coastal structures that will prevent overtopping.

Wave runup, R, is specifically defined as the landward extent of wave uprush measured vertically from the still water level (SWL). Wave runup consists of two parts: wave setup which is a mean (averaged over time) water surface elevation and swash (Figure 1). Swash, S, is the variation of the water-land interface about the mean. So wave runup is often referred to using the following equation (e.g., Stockdon et al. 2006)

$$R = \overline{\eta}_{max} + \frac{S}{2} \tag{1}$$

where the maximum mean setup, $\overline{\eta}_{max}$, is the superelevation of the mean water level at the beach.

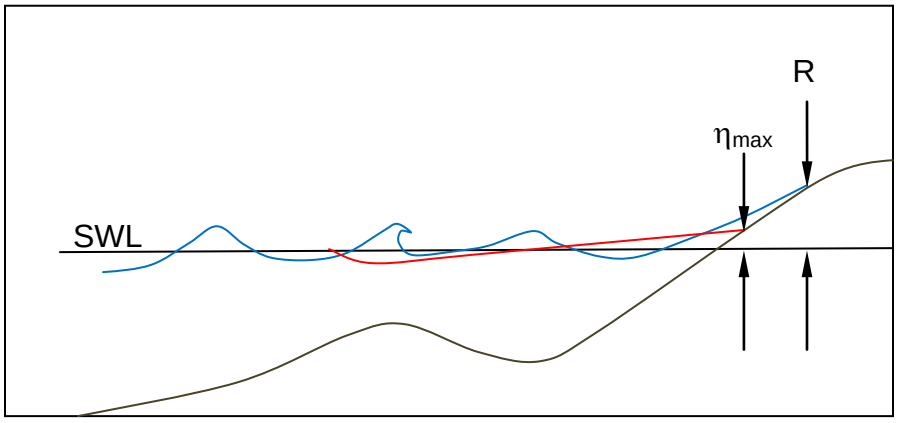

Figure 1. Conceptual sketch of wave runup on a beach (blue line) and setup (red shorter line).

Wave setup is a result of the momentum transfer of the radiation stress cross-shore gradient due to breaking waves, and consists of a mean and an oscillating component (Longuet-Higgins and Stewart 1962, 1964). Setup varies across the surf zone, being slightly negative at the wave break point and increasing to a maximum above the still water level. Often, setup is described by a mean component with the time varying components of setup and swash both considered as runup as per Kobayashi (1999), Stockdon et al. (2006), and others. Wave setup variation occurs at periods on the order of 100 sec on natural beaches. For Pacific Coast conditions where the wave spectra can be narrow, the slowly oscillating component of setup may be the dominant portion of runup.

Wave runup has been studied extensively over the last half century. Recent summary works include Kobayashi (1999), the USACE *Coastal Engineering Manual* (CEM) (USACE 2002), and the *EurOtop Manual* (2007). As noted by Kobayashi, wave runup on coastal structures has been studied mostly by engineers using hydraulic physical models whereas wave runup on beaches has been studied mostly by oceanographers using field measurements. Wave runup on coastal structures can be subdivided into impermeable core (levees and revetments), permeable core (rubble mound breakwaters), smooth (grass covered levees or planar slopes in the laboratory), and rough (stone or concrete armored structures). Coastal structures are characterized by relatively steep slopes of 1:4 – vertical. Some structures are shallower sloping or have compound slopes with a berm.

Beaches, on the other hand, are characterized with shallower average slopes of 1:100 – 1:10. Beaches are commonly composed of sand and/or cobble and are typically mobile. However, beaches can be rocky or composed of clay and can be relatively immobile. A beach typically has a relatively complex bathymetry with one or more bars and a nearshore slope roughly conforming to the power law $h = Ay^{2/3}$, where y is the cross-shore dimension and h is the depth. Beach morphology changes with time with beach steepening during storms when sediment and the nearshore bar move offshore. So defining a single average slope for a beach, to estimate runup, can be uncertain. Steeper beaches are wave-reflecting, while shallower beaches are wave-dissipating.

Runup is a function of nearshore wave transformation and wave breaking across the surf zone. Runup on beaches is influenced by local bathymetry,

beach steepness, beach composition, wave steepness, beach permeability, groundwater elevation, and infragravity waves. For structures, runup is influenced by offshore bathymetry, structure geometry, porosity/ roughness, and core permeability. Runup can vary considerably alongshore.

Battjes (1974a, 1974b) classified wave breaking according to the surf similarity or Iribarren parameter $\xi = \tan\alpha/\sqrt{H / L}$ (Iribarren and Nogales 1949) where α is the nearshore slope from horizontal, H is the incident wave height, and L is the incident wave length. Battjes (1974a, 1974b) noted that spilling breakers correspond to $\xi < 0.5$, plunging breakers to $0.5 < \xi < 3.3$ and surging or collapsing breakers occur for $\xi > 3.3$. Madsen et al. (1997a, 1997b) found that ξ also governed the type of shoreline motion. They noted that individual swash oscillations are distinct for breakers of the plunging to surging type ($\xi > 0.5$) but that wave group-induced sub-harmonic motion dominates the swash oscillations for breakers of the spilling type ($\xi < 0.5$). They also described the influence of bound long waves (wave grouping, e.g., Jiabao 1993). Low frequency incident waves from bound long waves and slow time variations of the breaker location generate both bound and free long waves in the surf zone creating what is known as surf beat or slow variations of the shoreline. Incident short waves are mostly dissipated in the surf zone, while free long waves are almost entirely reflected. This low frequency motion of the shoreline is commonly referred to as infragravity waves.

Mase and Iwagaki (1984) and Mase (1989) summarized the impact of wave groupiness on wave runup. Based partly on the work of Carstens et al. (1966) and Johnson et al. (1978) and partly on their own data, they noted that for steep structures, increasing wave groupiness yields higher runup. Conversely, for shallow nearshore slopes, wave groupiness variability has little effect on runup.

Runup at infragravity wave frequencies is commonly defined for frequencies lower than $f = 0.05$ Hz (e.g., Guza and Thornton 1982). They note that the progressive wave component of runup is saturated so that the infragravity component can constitute virtually all of the variance in the runup. Holland and Holman (1999) also describe cross-shore standing waves or edge waves resulting from the almost complete reflection of infragravity waves.

The probability distributions of runup and swash have been investigated. Hughes et al. (2010) showed that the probability distribution of swash maxima on a beach is reasonably modeled by the Rayleigh distribution but better modeled by the Normal distribution. However, they noted that the empirical distribution of swash skewness is not captured by the Normal distribution. Nielsen and Hanslow (1991) suggested that the Rayleigh distribution is reasonable for runup on beaches. These two studies though computed the probabilities differently and used different measurements. Kobayashi (1997) summarized several studies that showed runup on structures to be approximately Rayleigh distributed.

1.2 Problem

There are a number of empirical relations, general computer programs, and numerical hydrodynamic models available for computing wave runup. Unfortunately there is no consensus on model use. Some of the computational tools are dated but still in use, and there are several new empirical models and numerical hydrodynamic models that look promising but that have not been independently evaluated.

1.3 Purpose

The purpose of this report is to evaluate the most popular tools available for computing wave runup and make recommendations for use in flood risk assessments. In addition, a number of high-quality benchmark data sets for runup are summarized. These data sets are useful in evaluating any new runup estimating techniques.

1.4 Contents of this report

Chapter 2 describes the select benchmark data sets that are contained in Appendices A–D. These data sets cover the following nearshore conditions: smooth or grass-covered impermeable structures with a range of slopes from steep to mild including a berm, stone-armored impermeable structures, permeable rubble-mound structures, and sandy beaches with a variety of profiles and incident wave conditions.

Hunt (1959) suggested that relative runup is proportional to the surf similarity parameter or Iribarren number:

$$\frac{R}{H_0} = \xi_0 \tag{2}$$

where H_0 is the average deep water regular wave height, $\xi_0 = \tan\alpha / \sqrt{H_0 / L_0}$, $L_0 = gT^2/2\pi$, and T = the regular wave period. This simple expression states that wave runup increases with increasing shore steepness and decreasing wave steepness. In the following, we discuss this relation as it has been carried forward in present day design equations.

Chapter 3 describes several popular empirical models for predicting wave runup on structures and beaches including the Hunt (1959)-based formulations of Holman (1986), Ahrens (1981), Mase (1989), van der Meer and Stam (1992), van Gent (1999a, 1999b), the momentum flux method of Hughes (2004), and the formulation for beaches by Stockdon et al. (2006). The models are compared to the benchmark data sets. In this process, several standard measures of model skill are computed including bias, scatter index, and root-mean-square (rms) error. Minor variations to the Hunt-based formulas are suggested based on improved fits to the beach data. Two computer programs, ACES and Runup 2.0, based on empirical equations, are also evaluated. The models covered in Chapter 3 are fits to data as opposed to models of the fundamental processes. As such, the predictive capability of these models is usually limited to the range of data used to fit the models.

Recently, numerical models of the hydrodynamic processes based on shallow water wave equations and Boussinesq equations have been proposed for predicting complex nearshore hydrodynamics and beach processes including runup. CSHORE (Johnson et al., in preparation) solves the time-averaged equations for mass, momentum, and energy in the surface and swash zone, and has been well documented in the many references of Kobayashi and his students as well as other authors (e.g., Kobayashi 2009). CSHORE has the option of including cross-shore sediment transport and beach profile change. Nwogu (1993) discussed a new formulation of Boussinesq equations which has since become the productized software BOUSS-1D and BOUSS-2D (Nwogu and Demirbelik 2001). These programs provide consistent prediction of runup from steep to shallow slopes, include structure/beach porosity and roughness, and account for complex nearshore processes on irregular bathymetry. CSHORE and BOUSS-1D are transect models. CSHORE runs extremely

fast – a few seconds per storm per transect is typical. It is also stable. So, it is very attractive for running hundreds to thousands of runs for regional flood risk assessments. A horizontally two-dimensional version of CSHORE is called C2SHORE. The programs have been validated for limited data sets as described in the many references. However, the models have not been validated for the range of runup data given in the attached appendices, and specific parameter settings are somewhat uncertain. In Chapter 4, runup predictions from CSHORE are compared to both structure and beach data. The Boussinesq-based models are not evaluated herein due to time and funding constraints but have been shown to predict runup well. However, they require much greater computational resources per storm and transect and they require more expertise and experience to model the wide variety of shore profiles. Therefore, the Boussinesq-based models are likely to be attractive in the future as their usability improves.

Chapter 5 provides a summary and conclusions for this study.

The models evaluated herein are primarily transect models. As such, they model wave runup along a line perpendicular to the shoreline at a single location. Because the models evaluate runup along a transect, they assume some level of alongshore uniformity. In reality, the swash is not uniform alongshore (Birkemeier and Hathaway 1996). More sophisticated models are available that can model the three-dimensional surf and swash zone as discussed above; however, these models are presently too computationally demanding for bulk application in flood risk assessment. Additionally, the transect models have been used successfully for years to model inundation extents, probably because the alongshore variability of runup does not significantly influence the maximum inundation extent and flooding.

The models evaluated herein assume that the still water level in the absence of waves is known. This water level includes tides, storm surge and other variations. The models also characterize the incident wave climate with unidirectional wave height and wave period, with a single statistic of each. In reality, the nearshore wave spectra can be quite complex, composed of multi-directional, multi-modal spectra, and infragravity waves all contributing to runup (Elgar et al. 1993). For engineering applications, the somewhat idealized models in this report have shown to provide reasonable prediction of runup.

Some empirical equations in existing design manuals and computer programs for predicting runup are based on studies completed prior to the late 1990s, when laboratory techniques improved considerably. In particular, active wave absorption and second order wave correction to correct for generation of bound sub-harmonics and super-harmonics were key technologies implemented over the last 20 years. Re-reflected long waves and spurious bound harmonics in a wave flume can yield significant bias in runup measurements. In addition, the wave and runup statistics and methods of computing the statistics have varied historically but have become more uniform over the last 15 years. Runup measurement and data analysis methods vary considerably. Most authors report runup as per Equation 1, to include setup, but a few authors subtract out setup. Finally, laboratory and prototype measurement and analysis techniques routinely differ. So interpretation and comparison of runup measurements and predictive techniques can be a challenge. These issues will be further addressed in this report.

2 Benchmark Data Sets

2.1 Summary

Laboratory data sets were acquired, tabulated in appendices, and assembled into Microsoft Excel spreadsheets for a number of studies. Mase (1989) conducted small-scale tests of runup on smooth impermeable slopes of 1:5 to 1:30 and those data are summarized in Appendix A. The equations of de Waal and van der Meer (1992) are based on data summarized in Appendix B. More recent studies of runup on coastal structures were completed by van Gent as part of the European Union-funded OPTICREST research program (van Gent 1999a,b).These studies include full-scale prototype and small-scale laboratory measurements of runup on a barred-bathymetry/levee profile. These measurements are summarized in Appendix C. All physical model experiments summarized herein were modeled using Froude similitude where the geometry was undistorted and the temporal scale was $N_T = 1/\sqrt{N_L}$ where N_T is the ratio of prototype to model temporal parameters, such as wave period and storm duration, and N_L is the ratio of prototype to model length parameters, such as wave height and structure height.

Prototype-scale measurements of runup on beaches have been reported by a number of authors (e.g., Holman and Sallenger 1985; Holman 1986; Holland et al. 1995; Raubenheimer and Guza 1996; Holland and Holman 1999; and Stockdon et al. 2006). Empirical equations for predicting runup on beaches were reported by Holman 1986, Mase 1989, Douglass 1992, Raubenheimer and Guza 1996, Stockdon et al. 2006, and others. Stockdon et al. (2006) assembled nine of the beach data sets and those data are summarized in Appendix D. These data sets are from sandy beach sites in central Oregon, southern California, and North Carolina in the U.S. and one in Terschelling, NL (The Netherlands). Near full-scale measurements of runup in a large-scale wave flume were reported from the Supertank study by Mayer and Kriebel (1994) and Kriebel (1994). Unfortunately, the Supertank data have some uncertainty related to the laboratory wave generation technology described above. Seiching in the wave flume was a noted problem for these data making data interpretation more difficult.

In this chapter, we summarize the data sets. All of these studies utilized irregular waves, a primary requirement of this study. The two primary wave parameters are the energy-based significant wave height $H_{m0} = 4\sqrt{m_0}$, where m_0 is the zeroth moment of the wave energy density spectrum, and peak wave period $T_p = 1/f_p$, where f_p is the peak frequency of the wave energy density spectrum. The deep water wave length is $L_{0p} = gT_p^2/2\pi$, g is the acceleration of gravity, h_t is the toe depth for structures, wave steepness is $s_{0_p} = H_{m0}/L_{op}$, surf similarity or Iribarren parameter is $\xi_{0p} = \tan\alpha/\sqrt{s_{0_p}}$, and α is the structure or beach slope. Any wave parameters that differ are noted.

2.2 Mase data set

Mase and Iwagaki (1984) and Mase (1989) conducted laboratory experiments of smooth uniform slopes ranging from 1:30 to 1:5. The offshore bathymetry was flat for these idealized tests. Irregular waves were measured on the flat portion of the flume in intermediate depth. There was no mention of active wave absorption or second order wave correction in any of the publicly available papers. Swash was measured at the level of the slope in a channel using a capacitance wire gage. The runup gage channel was 0.033 ft (1 cm) deep and 0.098 ft (3 cm) wide. Runup statistics $R_{\max}$, $R_{2\%}$, $R_{1/10}$, $R_{1/3}$, and $\overline{R}$ were computed by dividing the number of runups by the number of incident waves and then rank ordering the result. Here, $R_{\max}$ is the maximum, $R_{2\%}$, is the 2 percent exceedance, $R_{1/10}$ is the average of the highest 10 percent, $R_{1/3}$ is the average of the highest 1/3, and $\overline{R}$ is the mean. Runup included setup. The small-scale model experiment was not to any specific scale as it was a generalized model. The experimental conditions are further described in Mase and Iwagaki (1984) (Table 1). This data set is limited to the following ranges of parameters:

Number of Experiments: 120 total: 30 experiments per slope, 4 slopes
Spectrum Type: Pierson-Moskowitz
Spectral Groupiness Factors: 0.74 and 0.53
Offshore Bathymetry: flat

The Mase and Iwagaki (1984) data are plotted in Figure 2 where normalized (or relative) runup is plotted versus surf similarity number.

Table 1. Summary of Mase and Iwagaki (1984) experiment.

Parameter	Series A	Series B	Series C	Series D
tan α	1/5	1/10	1/20	1/30
H_{m0} in ft	0.13 – 0.36	0.10 – 0.36	0.09 – 0.33	0.09 – 0.33
T_p in sec	0.84 – 2.39	0.84 – 2.29	0.92 – 2.28	0.82 – 2.25
s_{0p}	0.004 – 0.058	0.004 – 0.059	0.003 – 0.063	0.004 – 0.066
ξ_{0p}	0.83 – 3.02	0.41 – 1.65	0.20 – 0.85	0.13 – 0.56
h_t in ft	1.48	1.48	1.48	1.41
$R_{2\%}$ in ft	0.30 – 0.71	0.18 – 0.41	0.12 – 0.24	0.09 – 0.18

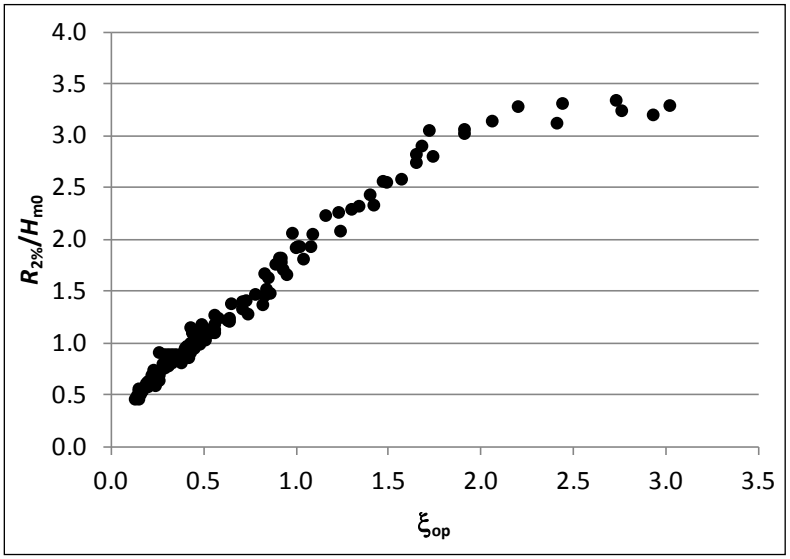

Figure 2. Relative runup versus surf similarity parameter for Mase and Iwagaki (1984) data set.

2.3 Van der Meer and Stam data set

Van der Meer (1988) and van der Meer and Stam (1992) summarized generalized irregular wave laboratory experiments on a variety of permeable and impermeable rock-armored coastal structures and the data are summarized in Appendix B. The experiments were generalized and so not scaled to any specific structure. The related studies of de Waal and van der Meer (1992) and van der Meer and Stam (1991, 1992) were used to generate empirical runup equations in the USACE *Coastal Engineering Manual* (USACE 2002) and the *Dutch Wave Runup and Wave Overtopping at Dikes Manual* (TAW 2002). They give significant wave height as a time domain parameter $H_{1/3}$. These data correspond to structures where the toe is in relatively deep water ($h_t > 3H_{1/3}$) with no surf zone

seaward of the structure so $H_{1/3}$ can be set equal to H_{m0} for these data with very little error. Here h_t is the toe depth. The details of wave and runup measurements were not included in any publicly available report but the experiments are generally described in van der Meer (1988). A system was used to compensate for re-reflection at the wave generator and incident and reflected waves were resolved with a 2-wave-gage array. Tables 2 and 3 summarize the data from these experiments that are plotted in Figure 3. *Permeability* in Tables 2 and 3 is a notional permeability of the structure as defined by van der Meer (1988). The data set is limited to the following ranges of parameters:

Irregular waves on rubble mound structures
Spectrum Type: Pierson-Moskowitz
Offshore Bathymetry slope: flat

Table 2. Summary of van der Meer and Stam (1991, 1992) experiments with impermeable slopes.

Parameter	Series 1	Series 2	Series 3
Number of Tests	18	40	43
tan α	1/2	1/3	1/4
Permeability	0.1	0.1	0.1
H_{m0} in ft	0.15 – 0.31	0.23 – 0.62	0.23 – 0.65
T_p in sec	2.08 – 3.85	1.37 – 3.57	1.42 – 3.64
s_{0p}	0.004 – 0.013	0.004 – 0.051	0.004 – 0.057
ξ_{0p}	4.436 – 8.316	1.483 – 5.161	1.047 – 4.119
h_t in ft	2.62	2.62	2.62
$R_{2\%}$ in ft	0.37 – 0.84	0.41 – 0.94	0.36 – 0.84

Table 3. Summary of van der Meer and Stam (1991, 1992) experiments with permeable slopes.

Parameter	Series 4	Series 5	Series 6	Series 7
Number of Tests	14	19	21	13
tan α	1/3	1/2	2/3	1/2
Permeability	0.4	0.4	0.4	0.6
H_{m0} in ft	0.37 – 0.59	0.29 – 0.52	0.28 – 0.49	0.33 – 0.62
T_p in sec	1.44 – 3.51	1.39 – 3.51	1.42 – 3.51	1.40 – 3.64
s_{0p}	0.006 – 0.052	0.005 – 0.048	0.006 – 0.043	0.006 – 0.056
ξ_{0p}	1.47 – 4.35	2.29 – 6.79	3.20 – 8.87	2.12 – 6.69
h_t in ft	2.62	2.62	2.62	2.62
$R_{2\%}$ in ft	0.37 – 1.02	0.41 – 1.14	0.46 – 1.01	0.60 – 1.15

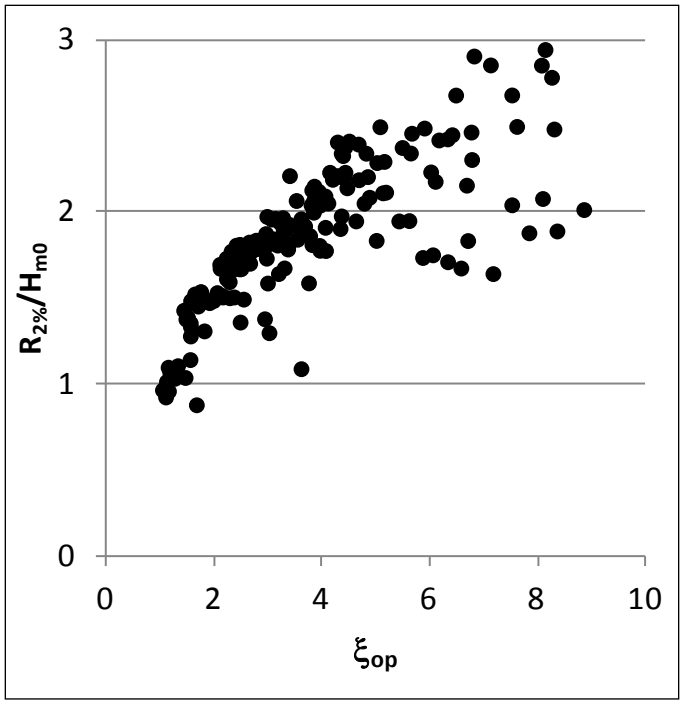

Figure 3. Relative runup versus surf similarity parameter for van der Meer and Stam (1991, 1992) for rubble mound structure experiments.

2.4 Van Gent data set

Van Gent (1999a, 1999b, 2001) conducted laboratory and prototype experiments of relatively smooth uniform and bermed impermeable dike slopes. The experiments consisted of two parts: (a) full-scale measurements from the Petten Sea Defense site with associated small-scale physical model experiment (Series P); and (b) generalized small-scale model experiments with systematic variation of parameters (Series A – C). Series P is reported in detail in van Gent (1999a). Series A – C are reported in detail in van Gent (1999b, 2001). The small-scale model study was conducted using undistorted geometry at a length scale of 1:40. The sectional profiles and other details are shown in Appendix C.

Active wave absorption at the wave generator was used in these experiments. For all test series, irregular waves were measured on the flat portion of the flume in intermediate depth and across the shallow surf zone to the structure toe. Swash was measured using a step gage at an elevation of 0.082 ft (2.5 mm) above the slope. The probes were spaced at 0.82 ft (25 mm). In addition, a continuous runup gage was placed parallel to the slope at an elevation of 0.164 ft (5 mm) above the slope. Runup $R_{2\%}$ was computed by dividing the number of runups by the number of incident

waves and then rank-ordering the result. These data are limited to the ranges of parameters given below and in Table 4. The data are plotted in Figures 4-7.

Spectrum Type: single peaked and double peaked JONSWAP
Spectral Groupiness Factors: varied
Offshore Bathymetry Slope: flat

Table 4. Summary of van Gent experiments.

Parameter	Series P	Series A	Series B	Series C
Number of Tests	6 full scale, 34 small scale	42 at small scale	31 at small scale	24 at small scale
tan α	2/9 lower, berm at 1/20, and 1/3 upper	1/4	2/5	2/5
H_{m0} in ft	6.6 – 20.3	0.45 – 0.50	0.45 – 0.50	0.43 – 0.50
T_p in sec	6.8 – 18.5	1.3 – 2.5	1.3 – 2.6	1.5 – 2.5
s_{0p}	0.007 – 1.42	0.014 – 0.055	0.014 – 0.057	0.014 – 0.039
ξ_{0p}	1.42 – 3.90	1.06 – 2.09	1.68 – 3.39	2.01 – 3.41
h_t in ft	6.3 – 20.4	0.15 – 1.16	0.15 – 1.16	0.15 – 1.16
$R_{2\%}$ in ft	10.8 – 26.9	0.39 – 1.35	0.46 – 1.61	0.33 – 1.57

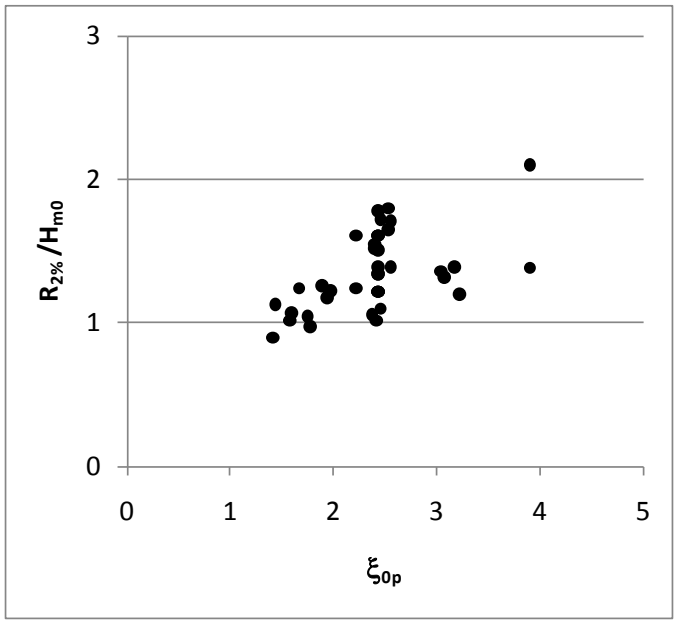

Figure 4. Relative runup versus surf similarity parameter for van Gent Series P.

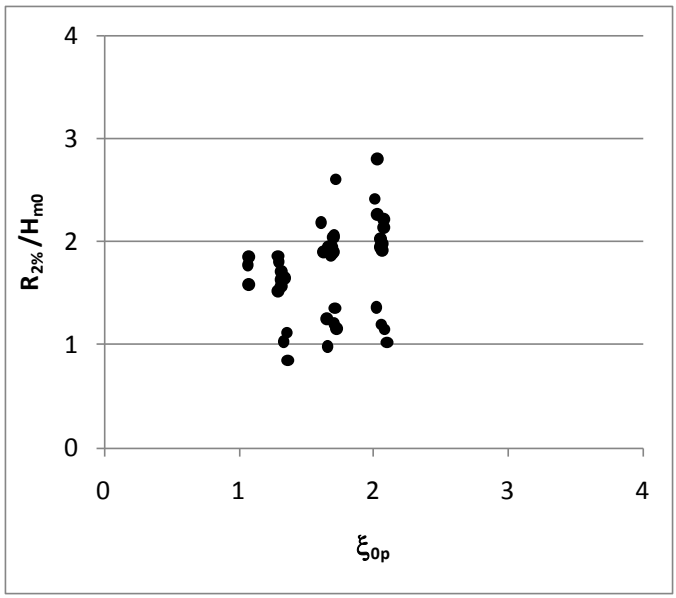

Figure 5. Relative runup versus surf similarity parameter for van Gent Series A.

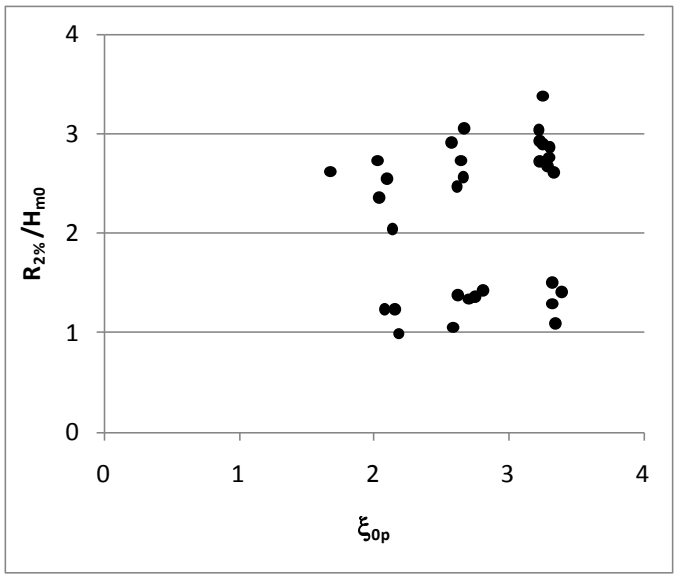

Figure 6. Relative runup versus surf similarity parameter for van Gent Series B.

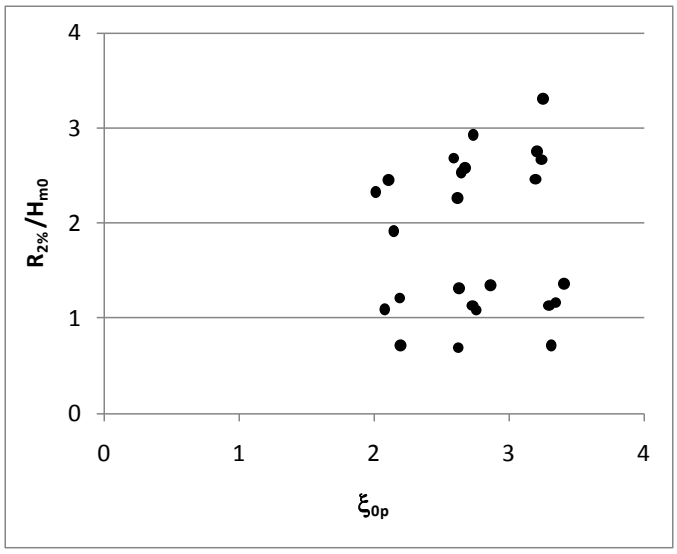

Figure 7. Relative runup versus surf similarity parameter for van Gent Series C.

2.5 Stockdon data set

Stockdon et al. (2006) reported a large data set consisting of data from nine full-scale experiments conducted between 1982 and 1996. The experiments and summary information are listed in Table 5 and in Appendix D. Here, the column labeled *Dates* has the dates of the experiment, N is the number of data points for that experiment, β_f is the beach slope at the mean water line, and $\xi_0 \pm \sigma$ is the mean surf similarity parameter ± one standard deviation. The foreshore beach slope β_f is defined as

Table 5. Summary of beach experiments from Stockdon et al. (2006).

Site	Dates	N	Average Conditions			
			H_{m0} (ft)	T_p (s)	β_f	$\xi_0 \pm \sigma$
Duck, NC (Duck 1982)	5-25 Oct 1982	36	5.60	11.9	0.12	1.95, 1.02
Duck, NC (Delilah)	6-19 Oct 1990	138	4.58	9.2	0.09	1.21, 0.59
Duck, NC (Duck 1994)	3-21 Oct 1994	52	6.19	10.5	0.08	1.15, 0.50
Duck, NC (SandyDuck)	3-30 Oct 1997	95	4.51	9.5	0.09	1.70, 0.53
San Onofre, CA	16-20 Oct 1993	59	2.64	14.9	0.10	2.44, 1.90
Scripps Beach, CA	26-29 Jun 1989	41	2.26	10.0	0.04	0.68, 0.46
Agate Beach, OR	11-17 Feb 1996	14	8.13	11.9	0.02	0.18, 0.13
Gleneden Beach, OR	26-28 Feb 1994	42	6.77	12.4	0.08	1.08, 0.64
Terschelling, NL	Apr & Oct 1994	14	6.02	8.3	0.02	0.18, 0.09

the average slope over a region between $\pm 2\sigma$ of the mean water level, where σ is defined as the standard deviation of the continuous water level record. In this case, the wave conditions are given by Stockdon et al. (2006) as those in deep water computed by deshoaling waves from a depth of about 8 m using linear wave theory. All of these data sets are plotted in Figure 8 with surf similarity plotted against relative runup using all deep water wave conditions and slopes given in Table 5.

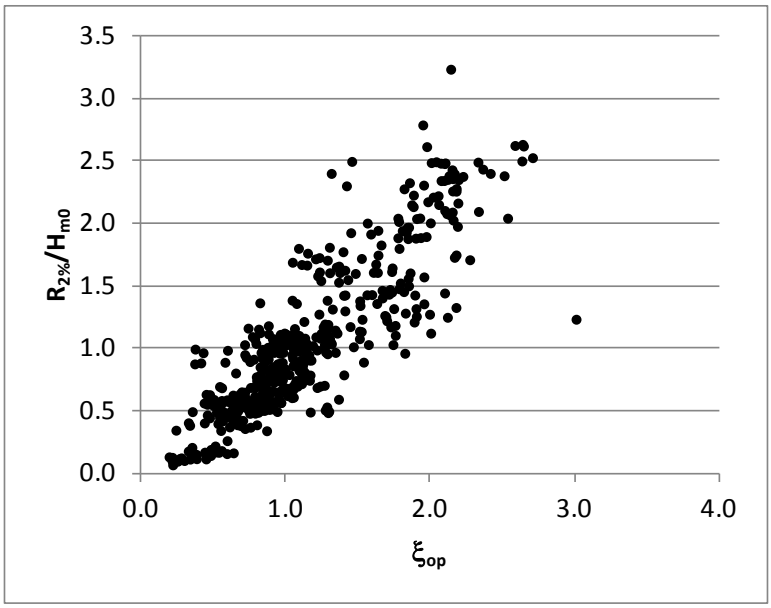

Figure 8. Relative runup versus surf similarity parameter for Stockdon data set.

Most of the measurements were made using shoreline tracking from video. Stockdon et al. (2006) describe the calculation method for $R_{2\%}$ where they rank ordered the runups normalized by the total number of runups. This can be contrasted with the data sets summarized in Appendices A–C where the runups were normalized by the total number of incident waves. There are typically fewer runups than incident waves so Stockdon's resulting runup statistic will be relatively greater. Another thing to note is that for experiments summarized in Appendices A–C, the wave conditions correspond to those of storms, while those in Appendix D correspond to non-storm conditions for most open coast locations. The impact of measuring non-storm conditions is primarily in the proportion of infra-gravity wave energy. It is expected that during storm conditions, incident wave energy will typically dominate the runup response whereas in non-storm conditions, it is possible for infragravity energy to dominate the runup response. Beach slope typically steepens during storms,

accentuating the impact of incident waves on runup. It is expected that the models summarized in this report will better predict runup during storm conditions than is illustrated herein using non-storm data because the models are uniformly less capable of predicting infragravity swash. This is particularly true on dissipative mild-sloping beaches characteristic of quiescent periods of wave activity. The beach profiles shown in Appendix D are average profiles, averaged in time but approximately corresponding to the beach profile at the location of the runup measurement.

3 Empirical Models

3.1 Introduction

The experiments listed in Chapter 2 all included generation of predictive runup equations that were best fits to the empirical data. In this chapter, empirical equations for predicting runup that have found wide spread use are discussed and the generality with respect to the full range of data summarized in this report is reviewed. In the following equations, runup is composed of setup and swash as per Equation 1. So, all of the empirical equations include setup.

3.2 Runup empirical formulae for structures

Battjes (1974a) extended the regular wave Hunt formula to irregular waves using time domain wave parameters. His formula for relative runup was as follows:

$$\frac{R_{2\%}}{H_{1/3}} = C_m \xi_{0m} \tag{3}$$

with C_m = 1.49 – 1.87 and $\xi_{0m} = \tan\alpha / \sqrt{s_{0m}}$, $s_{0m} = H_{1/3} / L_{0m}$, and $L_{0m} = gT_m^2/2\pi$, where $H_{1/3}$ is the average of the highest 1/3 wave heights, α is the structure slope from horizontal, L_{0m} is the linear theory mean wave length in deep water, and T_m is the mean wave period. Other authors have expanded the range of C_m. Ahrens (1981) gave a variation of Equation 3 for a range of structure slopes from 1:1 to 1:4 using frequency domain wave parameters. Ahrens expressed the surf similarity parameter as per Chapter 2 with $\xi_{0p} = \tan\alpha / \sqrt{s_{0p}}$, where $s_{0p} = H_{m0} / L_{0p}$, $L_{0p} = gT_p^2/2\pi$ and T_p is the peak wave period. His coefficient was C = 1.6, roughly in the middle of the range given by Battjes.

3.3 Holman equation

A more generalized form of Hunt's equation was proposed by Holman (1986) for beach data

$$\frac{R_{2\%}}{H_{m0}} = a\xi_{0p}{}^{b} + c \tag{4}$$

Hunt's data suggested that $a = 1$, $b = 1$, and $c = 0$ using deep water regular waves. Holman (1986) fit this equation with $a = 0.83$, $b = 1$, and $c = 0.2$ to field data from Duck, NC, using the intermediate depth H_{m0} and T_p. Holman retained Hunt's linear relation between relative runup and surf similarity parameter.

3.4 Mase equation

Mase (1989) developed predictive equations for irregular wave runup on plane impermeable slopes, based on the laboratory data summarized in Chapter 2 and Appendix A. The relative runup empirical equation was given as:

$$\frac{R_{2\%}}{H_{m0}} = 1.86\xi_{0p}{}^{0.71} \tag{5}$$

where the frequency domain wave parameters are those in deep water. Figure 9 shows the fit of Equation 5 to the Mase data. Similar to the Holman equation, Equation 5 is not universal with very good fit to the roughly linear portion where $\xi_{0p} < 2$ but deviation for cases with higher ξ_{0p} with steeper slopes or lower steepness waves.

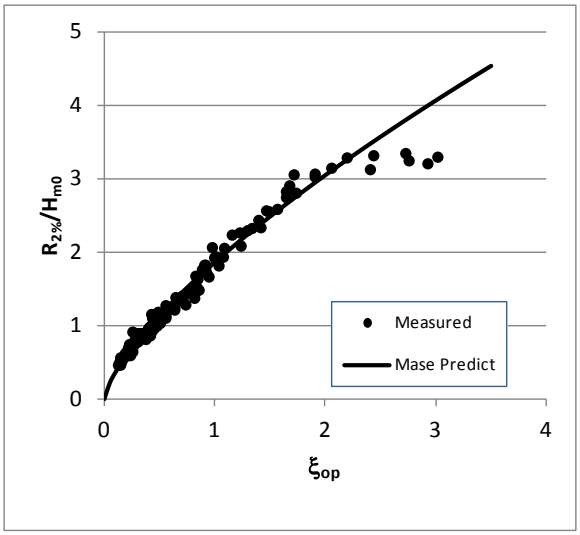

Figure 9. Mase relative runup prediction plotted with Mase and Iwagaki (1984) measurements.

Ahrens and Heimbaugh (1988) extended the range of runup prediction for structures to higher surf similarity numbers where the linear trend between $R_{2\%}/H$ and ξ breaks down. They noted three general regions of wave-structure interaction: (a) $\xi_{0p} < 2$ where the waves plunge directly on the structure, (b) a transition region where $2 < \xi_{0p} < 3.5$, and (c) $\xi_{0p} > 3.5$ where the waves are of the surging type. Ahrens showed a decreasing dependence of relative runup on ξ_{0p} for increasing ξ_{0p}, which Mase's data suggest.

Some authors report H_s and do not report the details of wave measurement and analysis so it is uncertain which statistic H_s represents. As discussed by Melby (2003), most laboratories use Goda and Suzuki (1976) or Mansard and Funke (1987) methodology to determine incident wave characteristics from wave gage array measurements that include both incident and reflected waves. Both of these methods yield frequency domain wave parameters. So, when authors report wave height as H_s from laboratory experiments, they often mean H_{m0}. The wave statistics $H_{1/3}$ and H_{m0} are similar and interchangeable in deep water so, in this case, it doesn't make a difference which statistic is intended for H_s. However, in shallow water, these statistics diverge. In some laboratory experiments, waves are measured in an open channel next to the test section or with no structure in place where wave reflection is low. In this case, incident and reflected waves may not be resolved and analysis may include individual gage time or frequency domain wave parameters or both. Most wave hindcast and wave transformation numerical models and most prototype wave measurements report spectral parameters H_{m0} and T_p. So equations based on spectral wave parameters are preferred and that is the focus herein.

3.5 Van der Meer and Stam equation

Van der Meer and Stam (1991, 1992), analyzed wave runup on rock-armored structures for a range of spectral shapes. Their recommended runup guidance, an extension of Equation 3, was given as:

$$\begin{aligned} \frac{R_{2\%}}{\gamma H_{1/3}} &= A\xi_{0m} \quad \xi_{0m} \le 1.5 \\ \frac{R_{2\%}}{\gamma H_{1/3}} &= B\xi_{0m}^{C} \quad \xi_{0m} \ge 1.5 \\ \frac{R_{2\%}}{\gamma H_{1/3}} &\le 3.2 \end{aligned} \tag{6}$$

where A = 0.96, B = 1.17, and C = 0.46 for mostly rock-armored slopes. An influence factor γ is used to account for various things as described below. The upper limit of relative runup was introduced for permeable-core structures. Equations 3–6 use wave parameters defined in intermediate to deep water resulting in wave conditions that conform to the Rayleigh wave height distribution. As such, $H_{1/3}$ can be interchanged with H_{m0} in Equations 3 and 6. However, these equations are not necessarily valid in shallow water where there is a wide surf zone. For Equation 6, $\xi_{0m} \leq 1.5$ roughly corresponds to Ahrens $\xi_{0p} < 2$ for plunging breakers.

Equation 6 is plotted in Figures 10 and 11 against the van der Meer and Stam (1991, 1992) data. It is clear that the equation fits the range of surf parameters from the linear range, through the transition area, and into the surging region. However, the scatter is increasing in the surging region where the fit is less certain.

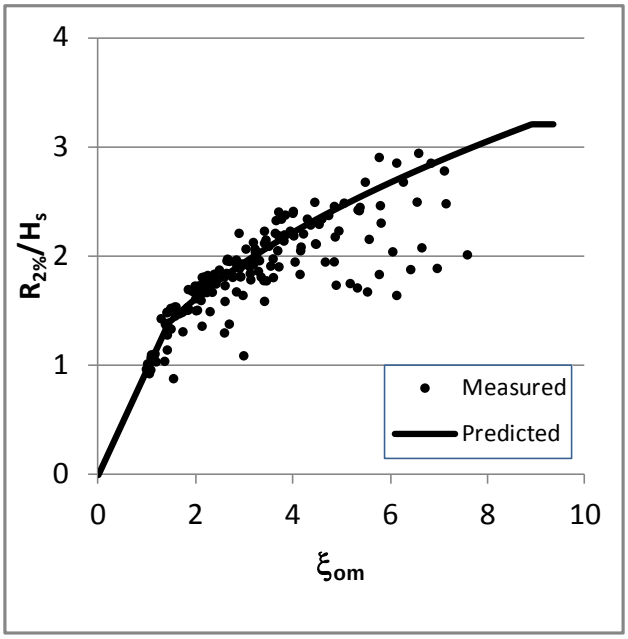

Figure 10. Van der Meer and Stam (1991, 1992) relative runup prediction using Equation 6 plotted with their measurements.

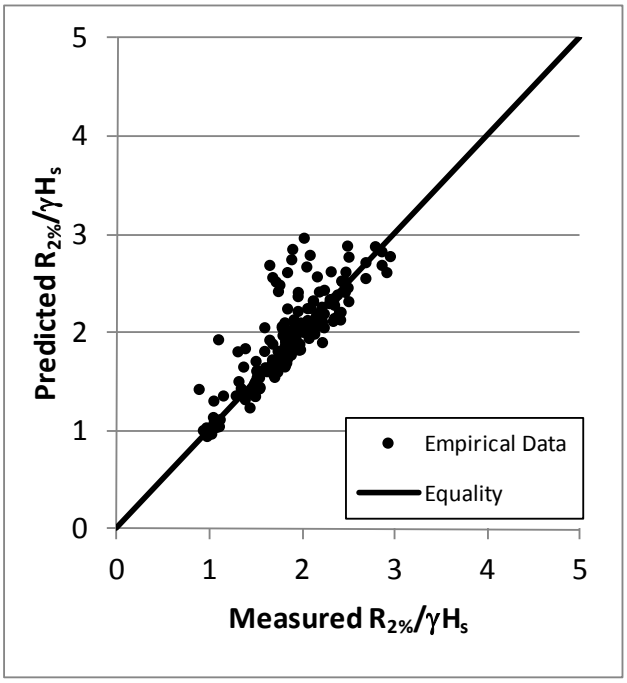

Figure 11. Van der Meer and Stam (1991, 1992) measured relative runup versus Equation 6.

Battjes (1974a) gave runup influence factors that reduce the estimated runup for various structure armor and cross section types including traditional rock structures. In Equation 3, H_s is replaced by γH_s, where, for example, $\gamma = 0.55$ for multi-layer stone armor. The influence factors were republished in the *Shore Protection Manual* (SPM) (USACE 1984). Empirical coefficient $A = 0.96$ in Equation 6 for runup on rock structures due to plunging breakers is roughly 50 percent of the value of $A = 1.86$ in the Mase equation for smooth structures, confirming Battjes factor for rock structures for $\xi_{0p} < 2$. De Waal and van der Meer (1992) gave an update of influence factors where the total influence factor is the product of component influence factors $\gamma = \gamma_b \gamma_f \gamma_h \gamma_\beta$ and the various factors are for berms (γ_b), slope roughness (γ_f), shallow water (γ_h), and angle of wave attack (γ_β). These influence factors have been repeated in the CEM, EurOTop, and TAW manuals.

3.6 Van Gent equation

A number of variations on the Hunt equation have been given in the literature for a wide range of beach and structure conditions. Recently, the Hunt equation was extended by van Gent (1999a, 1999b, 2001) to shallow water where wave heights deviate from the Rayleigh distribution. Van Gent (2001) gave equations to fit his runup data for smooth and rough impermeable structures with varied uniform and compound slopes. The equations are based on shallow water wave conditions at the structure toe and so differ from those equations given above. The primary best-fit equation is:

$$\frac{R_{2\%}}{\gamma H_s} = \begin{cases} c_0 \xi & \xi \le p \\ c_1 - c_2 / \xi & \xi > p \end{cases} \tag{7}$$

where $c_2 = 0.25(c_1)^2/c_0$, $p = 0.5c_1/c_0$, and c_0 and c_1 are given for several different wave period statistics. Van Gent (2001) provides best fits for ξ computed separately for various wave period statistics but the optimal fits were for T_p and $T_{m\text{-}1,0}$, where $T_{m\text{-}1,0} = m_{-1}/m_0$, and m_{-1} and m_0 are the negative first and zeroth moments, respectively, of the wave variance density spectrum and $m_n = \int_0^\infty f^n S(f) df$. Typically, $T_{m\text{-}1,0} \approx T_p/1.1$. The fit coefficients were given as:

T_p:	$c_0 = 1.35$	$c_1 = 4.3$	$c_2 = 3.4$	$p = 1.6$
$T_{m\text{-}1,0}$:	$c_0 = 1.35$	$c_1 = 4.7$	$c_2 = 4.1$	$p = 1.7$

Although not widely available, $T_{m\text{-}1,0}$ provides a more stable parameter than T_p because it is based on the integrated wave variance density spectrum rather than the somewhat uncertain peak of the spectrum. In Equation 7, $\gamma = \gamma_f \gamma_\beta$ is an adjustment for slope roughness (γ_f) and wave directionality (γ_β). Van Gent dropped γ_h and γ_b suggesting that these coefficients are not required. Van Gent incorporated the depth effects into Equation 7 and the berm effect into the slope in the surf similarity parameter. For a berm, van Gent suggests using an average structure slope of $\tan\alpha = 4H_s/L$, where L is the horizontal distance between points on the structure at $2H_s$ below and $2H_s$ above the still water line. Roughness reduction factors are 1.0 for smooth slopes, 0.9 for grass-covered slopes, 0.6 for single layer rock slopes and 0.5 for multi-layer rock slopes. For smooth slopes, the wave directionality factor is given as $\gamma_\beta = 1 - 0.0022\beta$ for $\beta < 80$ deg, where β is the wave angle from shore normal. For rock armored slopes, the 0.0022 coefficient is replaced with 0.0063.

Van Gent's Equation 7 is plotted versus his data in Figures 12 and 13 and against the data from van der Meer and Stam (1991, 1992) in Figure 14. In Figure 12, $\xi_{m\text{-}1,0} = \tan\alpha / \sqrt{s_{m-1,0}}$, where $s_{m\text{-}1,0} = H_{m0}/L_{m\text{-}1,0}$ and $L_{m\text{-}1,0} = g(T_{m\text{-}1,0})^2/2\pi$. Note that $T_{m\text{-}1,0}$ was used for Figures 12 and 13, while T_p was used for Figure 14 because $T_{m\text{-}1,0}$ was not provided with the van der Meer and Stam data. In addition, Figures 12–13 represent wave conditions that were primarily depth limited at the structure toe, while Figure 14 represents experimental conditions where $h_t > 3H_{m0}$ at the toe. For Figure 14, a value of $\gamma_f = 0.55$ was applied to account for roughness of multi-layer rock armor.

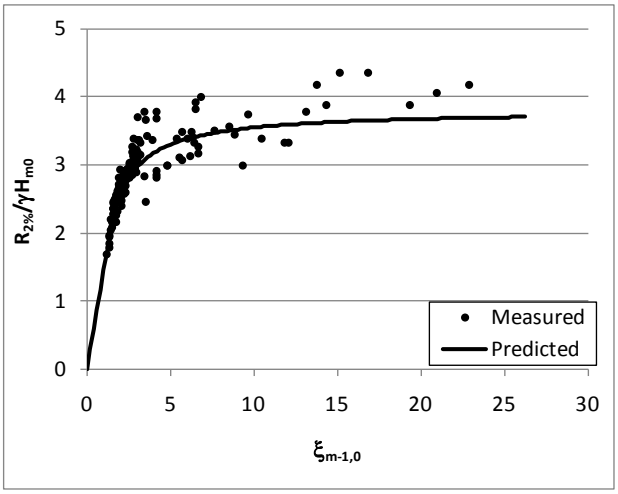

Figure 12. Equation 7 relative runup prediction plotted with van Gent (2001) measurements.

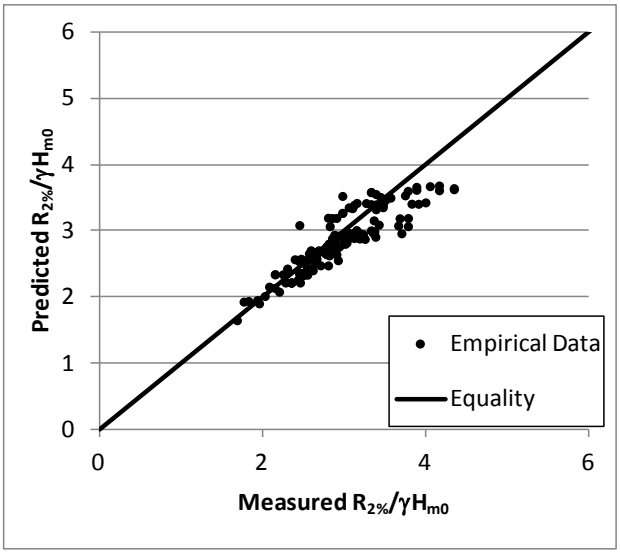

Figure 13. Van Gent (2001) measured relative runup versus Equation 7 prediction for H_{m0} and $T_{m-1,0}$ at structure toe.

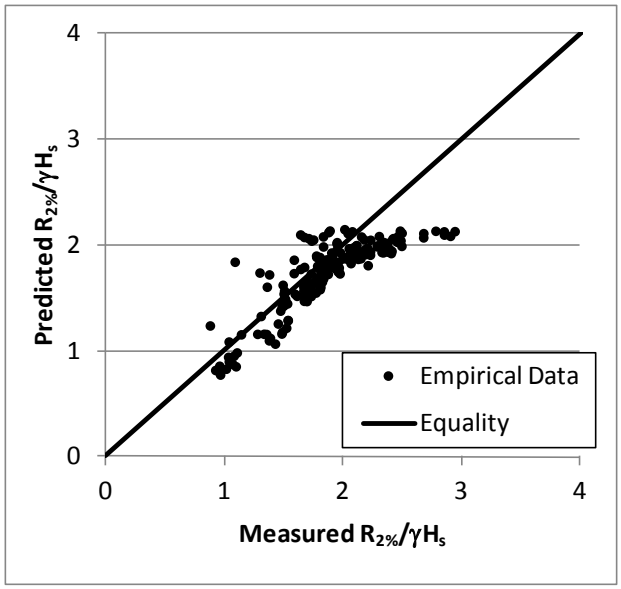

Figure 14. Van der Meer and Stam (1991, 1992) measured relative runup versus Equation 7 prediction for H_{m0} and T_p at structure toe.

3.7 TAW and EurOtop equations for structures

The TAW manual (TAW 2002) has been updated a number of times with variations in the Dutch runup guidance. This guidance has been further updated recently in EurOtop (2007) to include more recent experimental results and to incorporate the findings of van Gent. The EurOtop runup equation is given in Equation 8 and plotted in Figure 15 with the van der Meer and Stam data. Here again, a value of $\gamma_f = 0.55$ was applied to account for roughness of multi-layer rock armor. In addition, the approximation $T_p = 1.1T_{m\text{-}1,0}$ was used. The fit to the data appears to be reasonable in Figure 15 with a modest overprediction bias. The modification from the TAW equation to the EurOtop is to decrease the coefficient on the first equation from 1.75 to 1.65, the two coefficients in the second equation from 4.3 and 1.6 to 4.0 and 1.5 and change the wave period statistic. This modification represents roughly a 14% decrease in predicted runup. Figure 16 shows the EurOtop equation plotted with additional large-scale data referenced in the EurOtop manual. These data are published in a variety of reports, some in Dutch and German languages, so the details of the various studies were unknown at the time of this study. However, the summary data were provided to the author by van der Meer (2012)[1] and are therefore shown here for completeness.

$$\frac{R_{2\%}}{H_{m0}} = 1.65\gamma_b\gamma_f\gamma_\beta\xi_{m-1,0}$$
$$\frac{R_{2\%}}{H_{m0}} \le \gamma_b\gamma_{f\,surging}\gamma_\beta\left(\frac{4-1.5}{\sqrt{\xi_{m-1,0}}}\right) \quad (8)$$

where:

$$\gamma_{f\,surging} = \gamma_f + (\xi_{m-1,0} - 1.8)(1-\gamma_f)/8.2$$
$$\gamma_{f\,surging} = 1.0 \text{ for } \xi_{m-1,0} > 10.$$

[1] Personal Communication. 2012. J. W. van der Meer, van der Meer Consulting b.v.,Marknesse, The Netherlands.

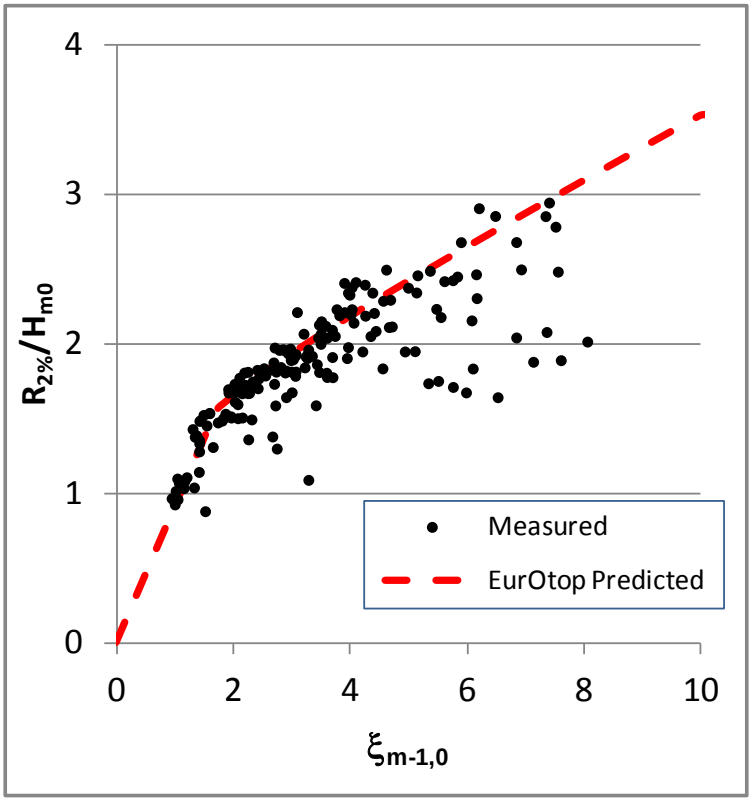

Figure 15. EurOtop runup prediction plotted
with van der Meer and Stam (1991, 1992) measurements.

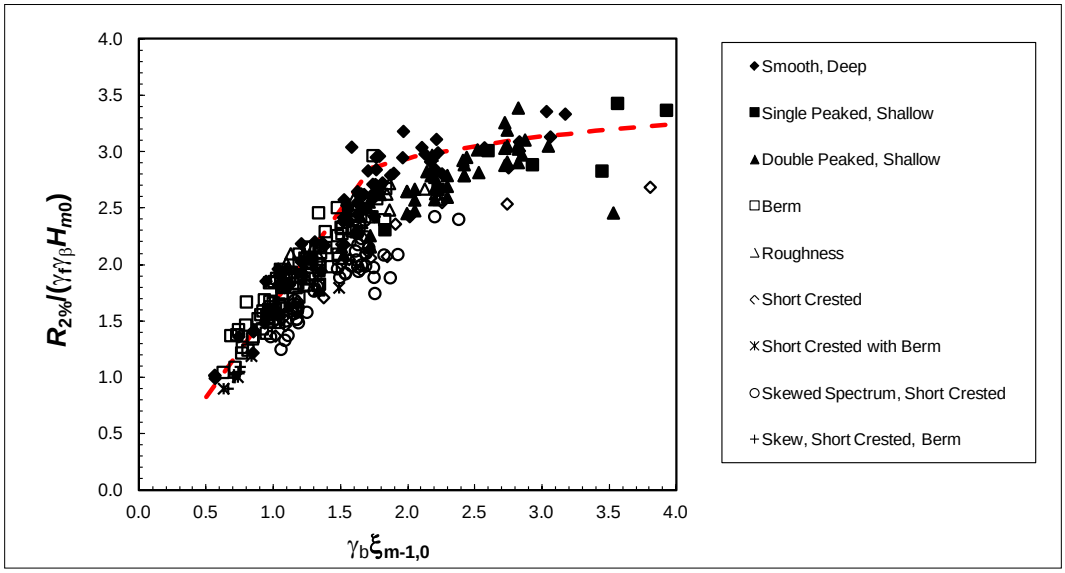

Figure 16. EurOtop runup prediction plotted with large-scale measurements
referenced in the EurOtop manual.

In Figure 16, a wide variety of structure and wave and water level conditions are represented including shallow and deep water at the structure toe, single peaked and double peaked spectra, short-crested and long crested seas, skewed spectra, smooth impermeable and rubble structures, varied roughness, and bermed structures. For all cases, the appropriate influence coefficients were applied. As shown in Figure 16, the EurOtop equation fit appears to be reasonable with a small overprediction bias.

In conclusion, runup is reasonably well predicted for structures using the Hunt-type equation with variations that account for the reduced influence of the surf similarity parameter for steep structures and low steepness waves as well as the many variations of structure and wave spectra conditions. The differences between equations and basis data make selection difficult.

3.8 Hughes equation

Hughes (2004) developed empirical equations for wave runup based on the concept that the weight of fluid in the runup wedge above the still water level at the time of maximum runup should be proportional to the maximum depth-integrated wave momentum flux for wave spectra defined at the structure toe. The basic predictive equations are:

$$\frac{R_{2\%}}{h_t} = A\left(\tan\alpha\right)^B \left[\frac{M_F}{\rho_w g h_t^2}\right]^{1/2} \quad s_{op} \geq 0.0225, \quad 1/5 \leq \tan\alpha \leq 2/3 \tag{9}$$

$$\frac{R_{2\%}}{h_t} = A\left(\tan\alpha\right)^B \left[\frac{M_F}{\rho_w g h_t^2}\right]^{1/2} \quad 1/30 \leq \tan\alpha \leq 1/5 \tag{10}$$

$$\frac{R_{2\%}}{h_t} = C\left(1 - e^{-(1.3\cot\alpha)}\right)^D \left[\frac{M_F}{\rho_w g h_t^2}\right]^{1/2} \quad s_{op} < 0.0225, \; 1/4 \leq \tan\alpha \leq 1 \tag{11}$$

where:

M_F = depth-integrated maximum wave momentum flux per unit width
ρ_w = water density
g = acceleration of gravity
h_t = toe depth.

Equation assumptions include impermeable and plane slopes in the range 1/1.5 to 1/30. Using potential flow theory for waves on a flat bottom, Hughes developed an estimate for the nonlinear wave momentum flux as:

$$\left(\frac{M_F}{\rho_w g h_t^2}\right)_{max} = A_0 \left(\frac{h_t}{g T_m^2}\right)^{-A_1}$$

$$A_0 = 0.639 \left(\frac{H_{m0}}{h_t}\right)^{2.026} \tag{12}$$

$$A_1 = 0.180 \left(\frac{H_{m0}}{h_t}\right)^{-0.391}$$

Hughes fit Equations 9–11 to several data sets with waves defined in relatively deep water including data from experiments of Ahrens, Mase, and van der Meer and Stam, discussed previously, and recommended A = 4.4, $B = D$ = 0.7, and C = 1.75.

The predictive skill of Equations 9–11 is illustrated in Figure 17 for the van der Meer and Stam data and in Figure 18 for the van Gent data. For Figure 17, the wave height and period were defined at the structure toe in relatively deep water. For the van Gent data, the wave height used in Equations 9–11 was defined at the structure toe in relatively shallow water but T_p was the value defined at POS 1–3 in Figure 19, which will be discussed below. A value of γ_f = 0.55 was applied herein to account for roughness of multi-layer rock armor when comparing to van der Meer and Stam data.

Equations 9–11 provide a fairly good fit over the full range of data. The equations also fit the Mase data well. In this case, the mean fit is good but there is considerably more scatter than shown in Figure 13 for van Gent's equation. However, when compared to van Gent data, with wave spectra defined at the structure toe, the scatter soars for a handful of tests. This is due to the fact that van Gent's reported peak wave period shifts by factors of 4–10 between gage positions POS 1–3 and the structure toe for conditions where the water depth becomes very shallow (Figure 19).

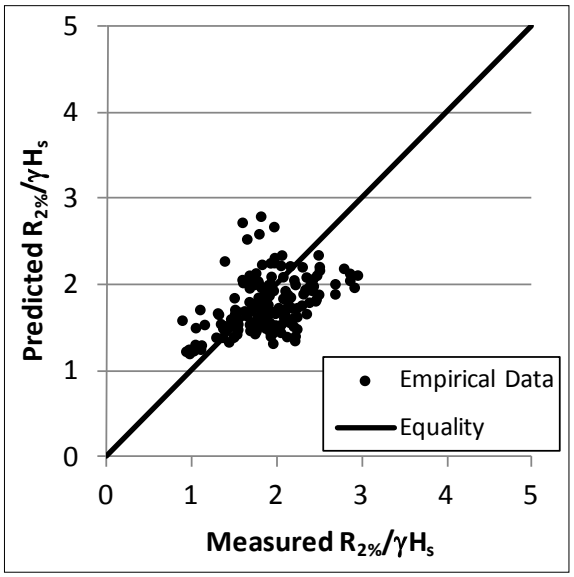

Figure 17. Van der Meer and Stam measured relative runup versus Equations 9–11 prediction for H_{m0} at the structure toe and T_p at POS 1–3.

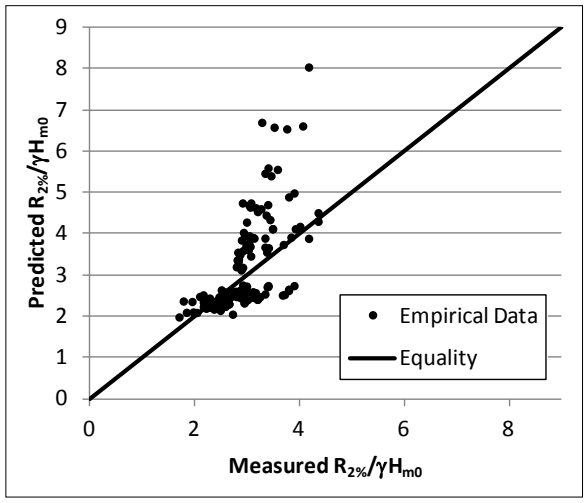

Figure 18. Van Gent measured relative runup versus Equations 9–11 prediction for H_{m0} at the structure toe and T_p at POS 1–3.

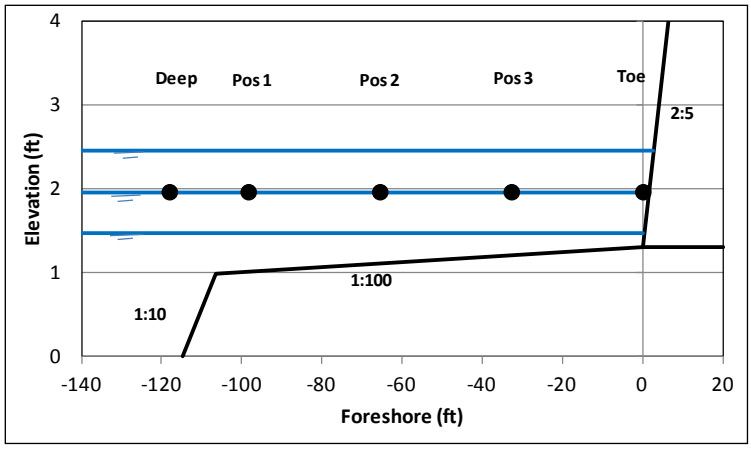

Figure 19. Van Gent Series B nearshore layout with wave gage location.

For example, a wave period of T_p = 1.64 sec at POS 1 became T_p = 16 sec at the structure toe. This shift is so severe that it is difficult to accept without careful re-analysis of the raw wave measurements, primarily because reported wave periods at POS 1–3 differ so dramatically from those at the toe in many cases. This is a characteristic of the peak wave period; it is less stable in shallow water than $T_{m-1,0}$ because the spectral shape and the somewhat arbitrary peak of the spectrum can change significantly in shallow water. The effect in Figure 12 based on Equation 7 is to simply shift the point to the right along the predicted curve. The van Gent

prediction is not very sensitive to over-prediction of wave period for $\xi > 5$. However, the impact on the maximum momentum flux is more severe and requires that these data be analyzed and interpreted very carefully. So herein, the peak wave period at the most shoreward position (POS 1–3) that is similar in magnitude to the deep water period is used for comparing Equations 9–11 to data.

3.9 Analysis of runup prediction for structures

In the following, statistical measures given below in Equations 13–23 are utilized to describe the skill of the various runup models. For these relations, rms = root mean square, p = predicted, m = measured, and n = number of data points.

Dimensional RMS of Measurements: $$m_{rms} = \sqrt{\frac{1}{n}\sum_{i=1}^{n} m_i^2} \tag{13}$$

Dimensional RMS Error: $$E_{rms} = \sqrt{\frac{1}{n}\sum_{i=1}^{n}\left(p_i - m_i\right)^2} \tag{14}$$

Non-dimensional RMS Error: $$e_{rms} = \sqrt{\frac{1}{n}\sum_{i=1}^{n}\left(\frac{p_i}{m_i} - 1\right)^2} \tag{15}$$

Bias: $$B = \frac{1}{n}\sum_{i=1}^{n}\left(p_i - m_i\right) \tag{16}$$

Standard Deviation of Errors: $$\sigma_d = \sqrt{\frac{1}{n-1}\sum_{i=1}^{n}\left(p_i - m_i - b\right)^2} \tag{17}$$

Mean of Measurements: $$\bar{m} = \frac{1}{n}\sum_{i=1}^{n} m_i \tag{18}$$

Scatter Index: $$SI = \frac{\sigma_d}{\bar{m}} \tag{19}$$

Normalized RMS Error Performance: $$\hat{E}_{rms} = \left(1 - \frac{E_{rms}}{m_{rms}}\right) \tag{20}$$

Normalized Bias Error Performance: $$\hat{b} = \left(1 - \frac{|B|}{m_{rms}}\right) \tag{21}$$

Normalized SI Performance: $$\widehat{SI} = \left(1 - SI\right) \tag{22}$$

Summary Performance Score: $$P_S = \frac{\hat{E}_{rms} + \hat{b} + \widehat{SI}}{3} \quad (23)$$

The statistical skill measures summarized in Equations 13–23 were computed for the varied structure empirical models against the structure data sets of van der Meer and Stam and van Gent. The results are summarized in Tables 6 and 7. Generally, the models performed well. All four prediction methods have relatively high skill. The EurOtop equation seems to be the most accurate and versatile, fitting all data well and allowing use of various wave statistics. The EurOtop and van Gent equations also make use of previously published guidance in the CEM (USACE 2002) and TAW (2002) manual for influence coefficients but give somewhat simpler application.

Table 6. Error statistics and skill scores for empirical equations for runup on structures for van der Meer and Stam data.

	Van der Meer and Stam Eq. 6	Van Gent Eq. 7	TAW Eq.	EurOtop Eq. 8	Hughes Eq. 9-11
Dimensional RMS Error, E_{rms} (ft)	0.11	0.10	0.10	0.12	0.15
Bias, B (ft)	0.04	-0.04	0.00	0.04	-0.02
Nondimensional RMS Error, e_{rms}	0.17	0.14	0.16	0.18	0.22
Standard Deviation of Errors, σ_d (ft)	0.10	0.09	0.10	0.11	0.15
Scatter Index = SI	0.15	0.12	0.15	0.16	0.22
Normalized RMS Error Performance, $\hat{E}_{rms}$	0.85	0.86	0.86	0.83	0.79
Normalized Bias Performance, $\hat{b}$	0.95	0.94	0.99	0.94	0.97
Normalized SI Performance, $\widehat{SI}$	0.85	0.88	0.85	0.84	0.78
Summary Performance, P_s	0.88	0.89	0.90	0.87	0.85

Table 7. Error statistics and skill scores for empirical equations for runup on structures for van Gent data.

	Van der Meer and Stam Eq. 6	Van Gent Eq. 7	TAW Eq.	EurOtop Eq. 8	Hughes Eq. 9-11
Dimensional RMS Error, E_{rms} (ft)	0.43	0.06	0.12	0.04	0.24
Bias, B (ft)	-0.40	-0.02	0.07	0.01	0.09
Nondimensional RMS Error, e_{rms}	0.54	0.08	0.15	0.11	0.28
Standard Deviation of Errors, σ_d (ft)	0.05	0.05	0.09	0.03	0.22
Scatter Index = SI	0.01	0.01	0.01	0.01	0.04
Normalized RMS Error Performance, $\hat{E}_{rms}$	0.49	0.93	0.86	0.96	0.71
Normalized Bias Performance, $\hat{b}$	0.52	0.97	0.91	0.99	0.89
Normalized SI Performance, $\widehat{SI}$	0.99	0.99	0.99	0.99	0.96
Summary Performance, P_s	0.67	0.96	0.92	0.98	0.86

3.10 Runup empirical equations for beaches

3.10.1 Holman equation

As discussed previously, Holman (1986) proposed Equation 4 for beaches with a = 0.83, b = 1, and c = 0.2 fit to field data from Duck, NC, using intermediate depth H_{m0} and T_p. Holman retained Hunt's linear relation between relative runup and surf similarity parameter. Figures 20 and 21 show Holman's equation plotted with the data of Mase and Iwagaki (1984) and Stockdon et al. (2006), respectively. The linear relation is only valid for $\xi_{0p} < 2$. Based on Figure 20, it is clear that the proportionality constant, a, varies between smooth impermeable uniform slopes in the laboratory and beaches. The Holman equation fits the beach data well but under-predicts the uniform-slope lab data of Mase.

The Hunt-based relations were fit to the Stockdon beach data with various combinations of parameters and the results are summarized in Table 8. There are four different coefficient combinations. Fit 1 is the Hunt equation with the addition of a zero offset. Fit 2 is the Holman equation. Fit 3 shows improved skill over the Holman equation achieved by optimizing the Holman fit for this data set. Fit 4 is the best fit with b and c set similar to the Mase equation. The various fits provide similar overall predictive skill. Fit 4 is perhaps the most attractive because it goes through the origin. The skill of Fit 4 is illustrated in Figure 22.

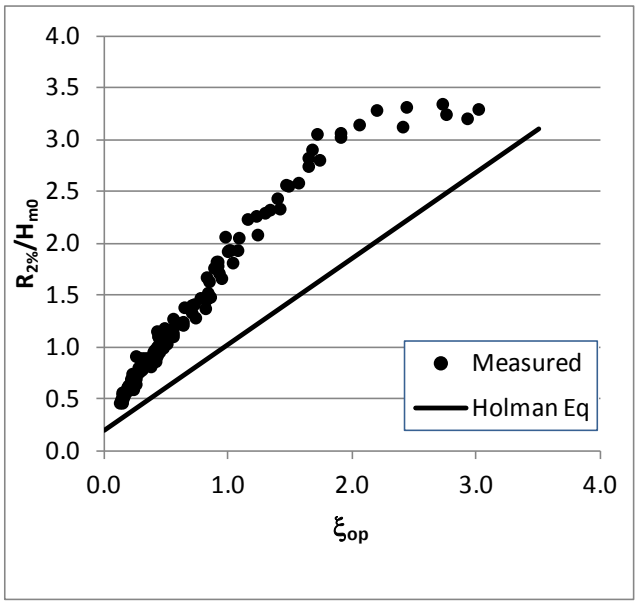

Figure 20. Holman relative runup prediction plotted with Mase measurements.

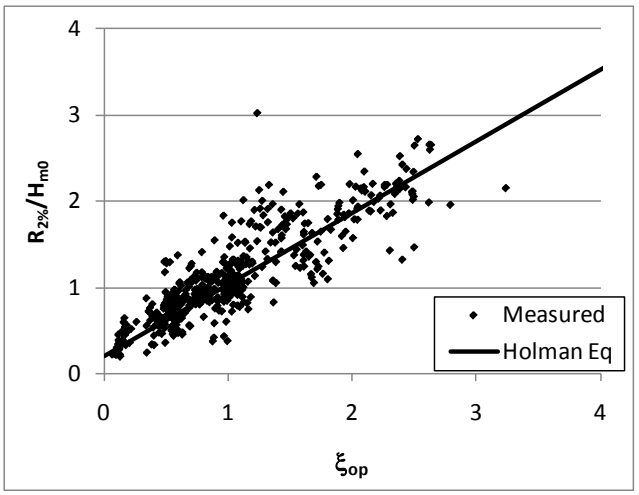

Figure 21. Holman relative runup prediction plotted with Stockdon measurements.

Table 8. Fit coefficients, error statistics and skill scores for Equation 4 compared to Stockdon beach data.

	Fit 1	Fit 2	Fit 3	Fit 4
a	1	0.83	0.90	1.10
b	1	1.00	1.00	0.70
c	0.12	0.20	0.25	0.00
Dimensional RMS Error, E_{rms} (ft)	1.30	1.23	1.19	1.21
Bias, B (ft)	-0.01	-0.48	-0.01	-0.02
Nondimensional RMS Error, e_{rms}	0.30	0.28	0.30	0.28
Standard Deviation of Errors, σ_d (ft)	1.30	1.14	1.19	1.21
Scatter Index = SI	0.27	0.24	0.25	0.26
Normalized RMS Error Performance, $\hat{E}_{rms}$	0.75	0.76	0.77	0.76
Normalized Bias Performance, $\hat{b}$	1.00	0.91	1.00	1.00
Normalized SI Performance, $\widehat{SI}$	0.73	0.76	0.75	0.74
Summary Performance, P_s	0.82	0.81	0.84	0.84

Comparing Table 8 to Tables 6 and 7, the skill of the Hunt-based beach runup models is significantly less than the skill of structure models due to the increased scatter in the beach runup data and the complexity of continuously varying beach morphology and wave and water level conditions.

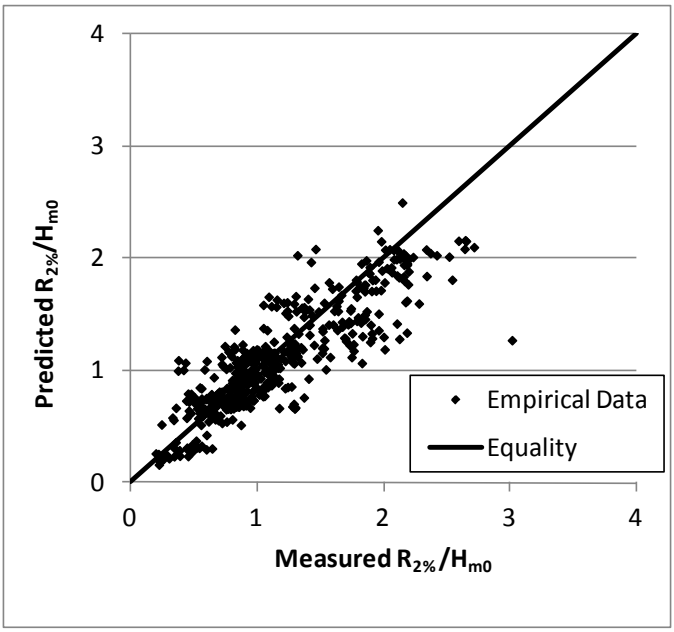

Figure 22. Fit 4 relative runup prediction plotted against Stockdon measurements.

3.10.2 Stockdon equation

Stockdon et al. (2006) developed empirical relations based on data from nine field experiments as summarized in Appendix D. They differentiate the beaches as dissipative or reflective depending on the surf similarity parameter. Dissipative beaches are defined for $\xi_{0p} < 0.3$ and reflective beaches for $\xi_{0p} > 1.25$ where

$$\xi_{0p} = \frac{tan\beta_f}{\sqrt{s_{0p}}} \quad s_{0p} = \frac{H_{m0}}{L_{0p}} \quad L_{0p} = \frac{gT_p^2}{2\pi} \tag{24}$$

and both H_{m0} and T_p are deep water values. They characterize runup as the sum of wave setup and swash and decompose swash into the sum of incident and infragravity contributions:

$$S = \sqrt{\left(S_{inc}\right)^2 + \left(S_{IG}\right)^2} \tag{25}$$

where $S = 4 * \sqrt{m_{os}}$ is the significant swash height determined as a function of the zeroth moment of the swash variance density spectrum, m_{0s}, similar to the calculation of H_{m0}. The separation of swash spectral energy is as follows: $f > 0.05$ Hz for incident wave energy and $f < 0.05$ Hz for infragravity.

The time varying beach profile is averaged over the duration of an experiment. Runup was given as:

$$R_{2\%} = 1.1\left[\overline{\eta} + \frac{S}{2}\right] \tag{26}$$

where the 1.1 factor reflects that the swash distribution is slightly skewed from Gaussian. The final recommended predictive relations are:

$$\overline{\eta} = 0.35\beta_f \left(H_{m0}L_{0p}\right)^{1/2} \tag{27}$$

$$S_{inc} = 0.75\beta_f \left(H_{m0}L_{0p}\right)^{1/2} \tag{28}$$

$$S_{IG} = 0.06\left(H_{m0}L_{0p}\right)^{1/2} \tag{29}$$

They combine Equations 25–29 into a universal beach runup formula as:

$$R_{2\%} = 1.1\left\{0.35\beta_f \left(H_{m0}L_{0p}\right)^{1/2} + \frac{1}{2}\left[H_{m0}L_{0p}\left(0.563\beta_f^2 + 0.004\right)\right]^{1/2}\right\} \quad (30)$$

where the first term in the brackets is wave setup, the β_f^2 term is for incident wave contributions, and the 0.004 term is for infragravity contributions. For dissipative beaches with very shallow slopes, the equation reduces to infragravity-dominated runup:

$$R_{2\%} = 0.043\left(H_{m0}L_{0p}\right)^{1/2} \qquad \xi_{0p} < 0.3 \quad (31)$$

Table 9 summarizes the relative contributions of the various terms in Equation 30 for the beach sites. The incident-wave-dominated sites are grouped together. These are all sites except Scripps, Agate, and Terschelling. The infragravity-dominated sites of Agate and Terschelling are grouped together. Scripps is listed separately as it is between the incident-dominated and infragravity-dominated. As is reflected in the low standard deviation values, the grouping is reasonable. The tabulated average values show that the Stockdon relations predict that setup and swash are of similar relative magnitude with swash contributing about 43 percent more for the incident-wave-dominated sites. For these sites, incident and infragravity swash components have similar weight. From observations of the data, the standard deviation of S_{IG}/S_{inc} of 0.28 is a result of significant variations in each site as opposed to variability from site to site. For infragravity-dominated sites, the swash dominates over setup and infragravity swash is the major contributor to wave runup. Table 9 values for Scripps suggest it is an infragravity-dominated site.

Table 9. Relative contributions to runup of setup, incident swash and infragravity swash based on Equations 27-30 for beach sites.

Site	Average			Standard Deviation		
	$\overline{\eta}/R_{2\%}$	$S/R_{2\%}$	S_{inc}/S_{IG}	$\overline{\eta}/R_{2\%}$	$S/R_{2\%}$	S_{inc}/S_{IG}
Incident-Wave-Dominated Sites	0.41	0.59	1.17	0.03	0.03	0.28
Scripps	0.28	0.72	0.47	0.03	0.03	0.09
Agate and Terschelling	0.16	0.84	0.21	0.04	0.04	0.07

Figures 23 and 24 show dimensional runup as a function of $\beta_f (H_{m0}L_{0p})^{1/2}$ for the incident-wave-dominated sites. The high amount of scatter in the data is clear for all data sets. In addition, the Duck 94 data set shows a strong bias from the overall group. In Figure 23, the maximum difference between the minimum and maximum measurements in runup at $\beta_f (H_{m0}L_{0p})^{1/2}$ = 5 ft is a factor of about 4.5. Figure 25 shows the dimensional runup as a function of $(H_{m0}L_{0p})^{1/2}$ for infragravity-dominated sites. This data group is relatively better behaved than that shown in Figures 23 and 24 but is much less extensive. Additional data may yield even greater variability.

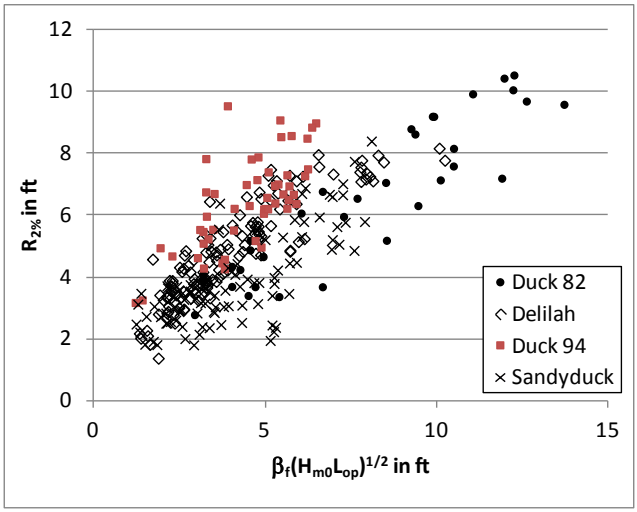

Figure 23. Dimensional runup as a function of $\beta_f (H_{m0}L_{0p})^{1/2}$ for incident-wave-dominated experiments at Duck, NC.

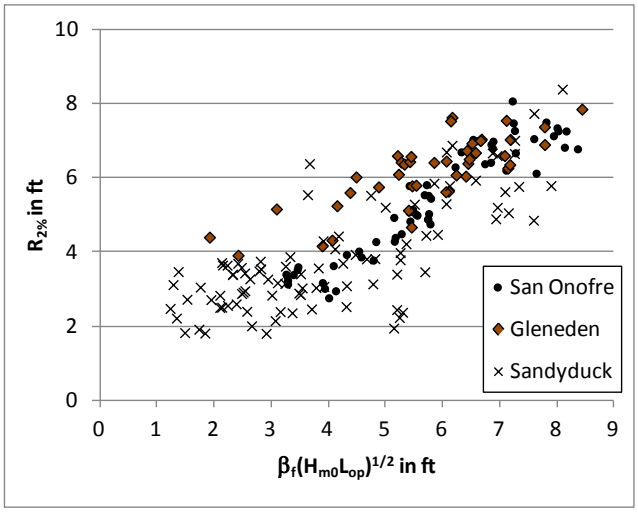

Figure 24. Dimensional runup as a function of $\beta_f (H_{m0}L_{0p})^{1/2}$ for incident-wave-dominated experiments at disparate sites.

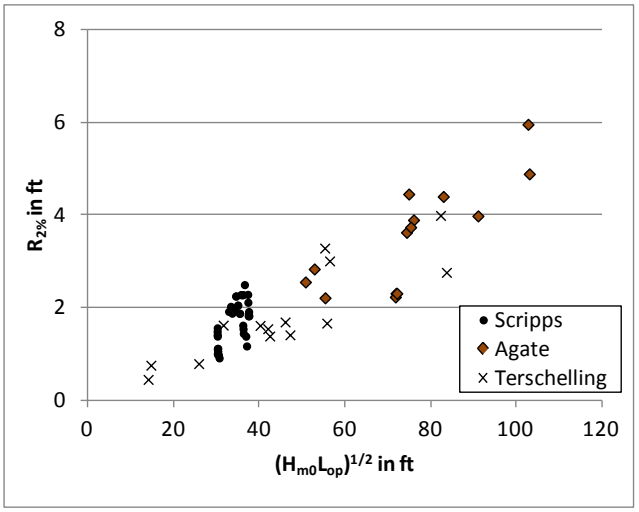

Figure 25. Dimensional runup as a function of $(H_{m0}L_{0p})^{1/2}$ for infragravity-wave-dominated experiments.

Equation 30 is plotted in Figure 26 with the measured beach runup data. The skill of Equation 30 was evaluated and the results are summarized in Table 10. The best fits of the Hunt-based Holman and modified Mase formulae along with a refit of Hughes equations for the beach data are also evaluated in Table 10. The varied predictive equations provide similar skill. Table 11 summarizes the skill of the Stockdon equation by site. It is clear that there is considerable variability in skill between sites.

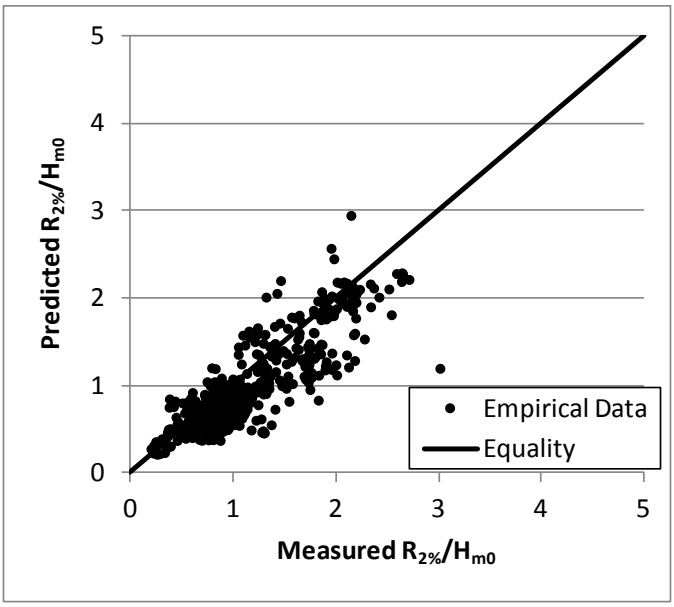

Figure 26. Fit of Stockdon equations to Stockdon beach data.

Table 10. Error statistics and skill scores for empirical equations compared to beach data.

	Hughes[1] Eq. 9–11	Holman[2] Eq. 4	Stockdon Eq. 30	Mase[3] Eq. 4
Dimensional RMS Error, E_{rms} (ft)	1.19	1.19	1.25	1.21
Bias, B (ft)	-0.29	-0.01	-0.58	-0.02
Nondimensional RMS Error, e_{rms}	0.28	0.30	0.27	0.28
Standard Deviation of Errors, σ_d (ft)	1.15	1.19	1.10	1.21
Scatter Index = SI	0.24	0.25	0.23	0.26
Normalized RMS Error Performance, $\hat{E}_{rms}$	0.77	0.77	0.76	0.76
Normalized Bias Performance, $\hat{b}$	0.94	1.00	0.89	1.00
Normalized SI Performance, $\widehat{SI}$	0.76	0.75	0.77	0.74
Summary Performance, P_s	0.82	0.84	0.80	0.84

[1] Equations 9-11 with fit coefficients A = 1.75, B = 0.5.

[2] Equation 4 with fit coefficients a = 0.90, b = 1.0, c = 0.25.

[3] Equation 4 with fit coefficients a = 1.10, b = 0.70, c = 0.0.

Table 11. Error statistics and skill scores for runup estimates using Stockdon Equation 30 compared to beach data by site.

Site	N	Mean Meas, $\overline{m}$ ft	Meas RMS, m_{rms} ft	Dim Diff RMS, E_{rms} ft	Bias, B ft	Nondim RMS Error e_{rms}	St. Dev. of Errors, σ_d ft	SI	Norm. RMS Error Perf. $\hat{E}_{rms}$	Norm. Bias Perf. $\hat{b}$	Norm. SI Perf. $\overline{SI}$	Sum. Perf. P_s
Duck 1982	36	6.41	6.83	1.20	0.30	0.21	1.46	0.23	0.82	0.96	0.77	0.85
Duck 1990	138	4.85	5.10	1.36	-1.06	0.27	0.98	0.20	0.73	0.79	0.80	0.78
Duck 1994	52	6.40	6.57	2.28	-2.04	0.35	1.78	0.28	0.65	0.69	0.72	0.69
SandyDuck	95	3.85	4.12	1.10	-0.06	0.35	1.21	0.32	0.73	0.99	0.68	0.80
San Onofre	59	5.34	5.54	0.57	-0.13	0.12	0.71	0.13	0.90	0.98	0.87	0.91
Scripps	41	1.68	1.75	0.33	0.05	0.25	0.71	0.42	0.81	0.97	0.58	0.79
Gleneden	42	6.17	6.24	0.90	-0.56	0.14	0.70	0.11	0.86	0.91	0.89	0.88
Agate	14	3.53	3.70	0.88	-0.52	0.21	0.71	0.20	0.76	0.86	0.80	0.81
Terschelling	14	1.86	2.10	0.42	-0.02	0.20	0.70	0.38	0.80	0.99	0.62	0.80

Two data sets have relatively high bias: Duck 1990 and Duck 1994. Gleneden and Agate have moderate bias. Scatter is relatively high in the SandyDuck and Terschelling data sets and moderate in the other data sets. Table 12 summarizes skill scores for the modified Mase equation (Equation 4 with a = 1.1, b = 0.7, and c = 0). A relative comparison of the modified Mase and Stockdon equation skill is shown in Figure 27.

Table 12. Error statistics and skill scores for runup estimates using modified Mase equation compared to beach data by site.

Site	N	Mean Meas, $\overline{m}$ ft	Meas RMS, m_{rms} ft	Dim Diff RMS, E_{rms} ft	Bias, B ft	Nondim RMS Error e_{rms}	St. Dev. of Errors, σ_d ft	SI	Norm. RMS Error Perf. $\hat{E}_{rms}$	Norm. Bias Perf. $\hat{b}$	Norm. SI Perf. $\overline{SI}$	Sum. Perf. P_s
Duck 1982	36	6.41	6.83	1.90	1.18	0.28	1.94	0.30	0.72	0.83	0.70	0.75
Duck 1990	138	4.85	5.10	0.95	-0.27	0.18	0.95	0.20	0.81	0.95	0.80	0.86
Duck 1994	52	6.40	6.57	1.64	-1.06	0.25	1.65	0.26	0.75	0.84	0.74	0.78
SandyDuck	95	3.85	4.12	1.56	0.69	0.50	1.58	0.41	0.62	0.83	0.59	0.68
San Onofre	59	5.34	5.54	0.67	-0.32	0.13	0.66	0.12	0.88	0.94	0.88	0.90
Scripps	41	1.68	1.75	0.29	-0.02	0.19	0.30	0.18	0.83	0.99	0.82	0.88
Gleneden	42	6.17	6.24	0.78	0.43	0.14	0.80	0.13	0.88	0.93	0.87	0.89
Agate	14	3.53	3.70	1.48	-1.18	0.34	1.52	0.43	0.60	0.68	0.57	0.62
Terschelling	14	1.86	2.10	0.54	-0.31	0.27	0.55	0.30	0.74	0.85	0.70	0.77

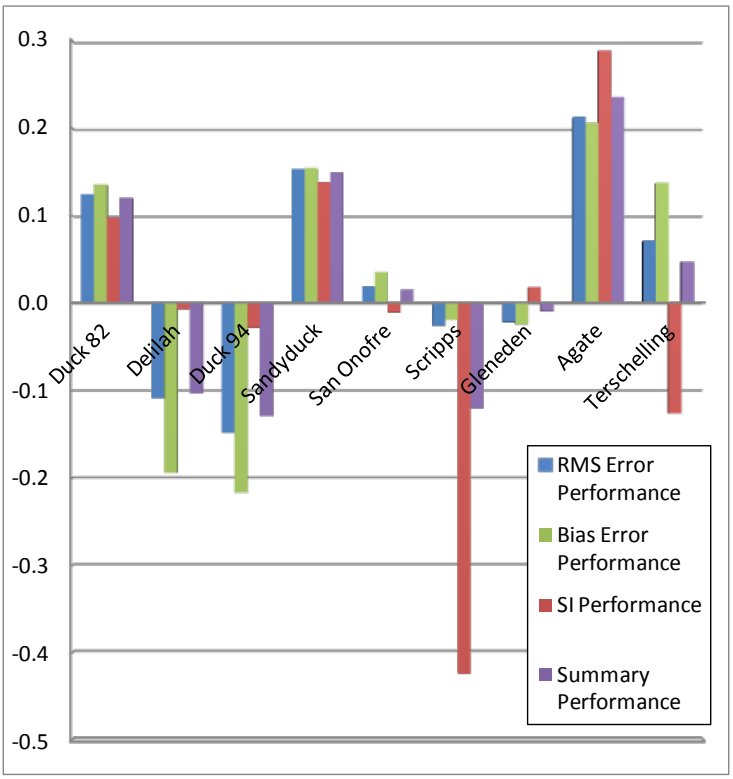

Figure 27. Skill comparison for modified Mase Equation 4 (with a = 1.1, b = 0.7 and c = 0) versus Stockdon Equation 30. The value plotted is 1 - X_M/X_S where X_M is the skill score for Equation 4 and X_S is the skill score for Equation 30.

Here the value plotted is $1 - X_M/X_S$ where X_M is the skill score for Equation 4 and X_S is the skill score for Equation 30. The figure shows varied relative skill over the range of data sets with the Stockdon equation better for Duck 1982, SandyDuck, and Agate but the modified Mase equation better for Delilah, Duck 1994, and Scripps. The models are about the same for San Onofre and Gleneden but show mixed results for Terschelling. The results are not definitive but suggest that either model can be used for all but the most dissipative beaches. For highly dissipative cases where $\xi_{0p} < 0.3$, Equation 31 should be used.

3.11 Computer programs based on empirical equations

3.11.1 ACES

Leenknecht et al. (1995) summarized models used for wave runup in the Automated Coastal Engineering System (ACES). The Mase relation for runup on gently sloping smooth planar slopes was included for beaches but the details of application were left as user inputs (beach slope, fit coefficient). For runup on coastal structures, the relations of Ahrens and

Titus (1985) are recommended for smooth impermeable slopes and Ahrens and McCartney (1975) for rough slopes (riprap). These relations are based on regular wave experiments. The runup relation for rough slopes was given as:

$$\frac{R}{H} = \frac{a\xi}{1 + b\xi} \tag{32}$$

where R is the significant runup, H is the incident significant wave height, and ξ is computed using H_{m0} and T_p. Here a and b are empirical coefficients as listed in Table 13.

Table 13. Coefficients for ACES Equation 32.

Armor Material	*a*	*b*
Riprap	0.956	0.398
Rubble (permeable, no core)	0.692	0.504
Rubble (2 layers, impermeable core)	0.775	0.361

Relations for computing wave height in shallow water were given. Although Ahrens subsequently updated the equations for both structures and beaches (e.g., Ahrens and Seelig 1996; Ahrens et al. 1993), the ACES program was not updated. Application of the ACES model is uncertain because the documentation is not very clear on the parameter statistics. However, an evaluation of the ACES program showed lower skill than the equations discussed above for structures and beaches.

3.11.2 Runup 2.0

Runup 2.0 is the computer program recommended by FEMA for use in Flood Insurance Studies (FEMA 1981, 1991). The program is based on the empirical equations of Stoa (1978) for a wide variety of slope configurations and wave and water level conditions. Stoa used regular wave laboratory experiments to develop the empirical equations. The experiments did not include any of the modern wave generation capabilities, such as active wave absorption and second order correction for spurious bound waves, as discussed earlier. Because the Stoa tests included setup, the Runup 2.0 runup estimate also includes setup.

Stoa conducted experiments for 10 structure profiles, all with flat offshore bathymetry and relatively deep water directly offshore of the structure.

So, the wave is assumed to break on the structure rather than in the nearshore zone. The depth seaward of the structure toe is greater than $3H_s$. Ten empirical curve sets for runup prediction were developed for the 10 structure profiles and the program interpolates or extrapolates to determine runup for input conditions.

If the structure profile matches Stoa's, then the calculation uses one of the digitized Stoa curves. However, if there is no match, then the composite slope method of Saville (1958) is used. This method extends runup estimates from simple structure geometries to more complex profiles. The method defines a uniform slope that provides an equivalent runup to a complex profile. The method was originally developed to correct for horizontal berms on levees. This is similar to the method discussed in the previous section to account for the influence of a berm. In Runup 2.0, this method is extended to complex profiles using empirical rationale with little physical justification. So it should be used with caution.

A number of other adjustments are made within Runup 2.0 including corrections for depth-limited breaking, slope roughness, and scale effects.

As stated earlier, irregular wave runup roughly corresponds to the Rayleigh distribution. For the Rayleigh distribution, $R_{2\%} = 2.2\bar{R}$. Battjes (1974a) noted that $R_{2\%} = 2.0\bar{R}$ to $2.6\bar{R}$. The mean runup from an irregular wave time series ($\bar{R}$) roughly corresponds to the runup resulting from regular waves. According to FEMA (1981), $R_{2\%}$ has equivalent probability to the controlling wave height treated in a flood insurance study. So the $\bar{R}$ output from Runup 2.0 is routinely converted to $R_{2\%}$ assuming Rayleigh-distributed runups using the relation $R_{2\%} = 2.2\bar{R}$.

Figures 28 and 29 show the comparison of relative runup predicted with Runup 2.0 versus Mase and van Gent data, respectively. The Rayleigh assumption was used to determine $R_{2\%}$ from the output $\bar{R}$. For the smooth slope experiments of Mase, Runup 2.0 produced a significant bias with nearly all measurements under-predicted. For higher runup values where $\xi > 2$, Runup 2.0 generally over-predicted runup. For van Gent experiments, the smooth structure was steeper and the offshore shallower. The impact is clear. Here, Runup 2.0 over-predicted almost all of the measurements by a significant amount. The trend was different for cases where the water was very shallow. For these cases, the Runup 2.0 prediction was significantly low, by a factor of 5 – 23.

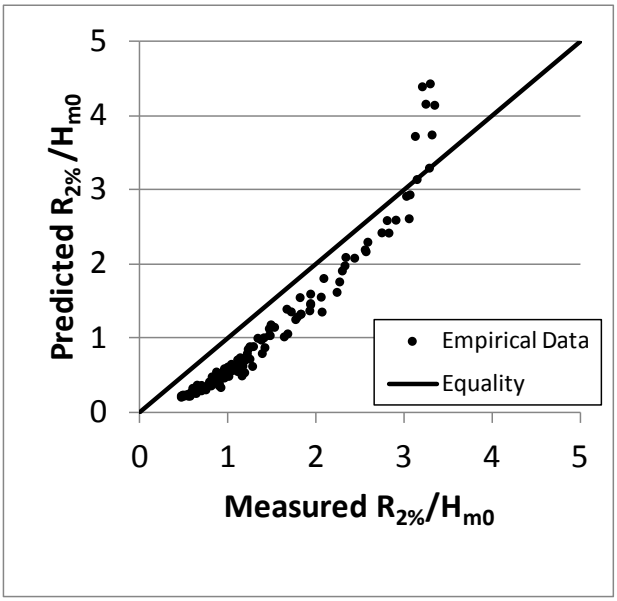

Figure 28. Runup 2.0 prediction versus Mase smooth uniform slope data.

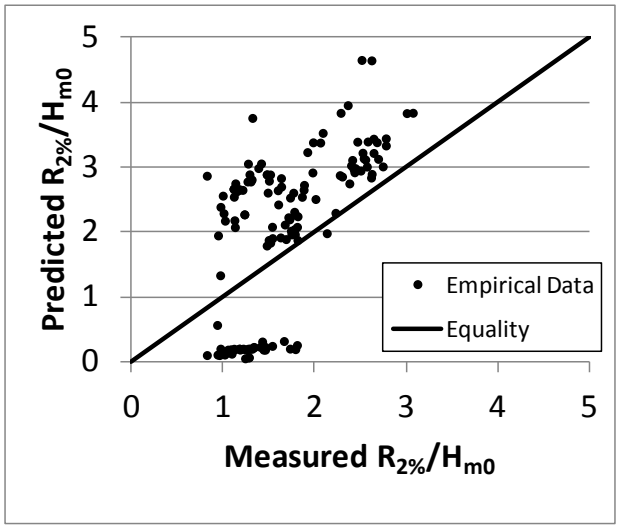

Figure 29. Runup 2.0 prediction versus van Gent smooth structure data.

Runup 2.0 was also compared to Stockdon beach measurements. The results are shown in Figure 30.

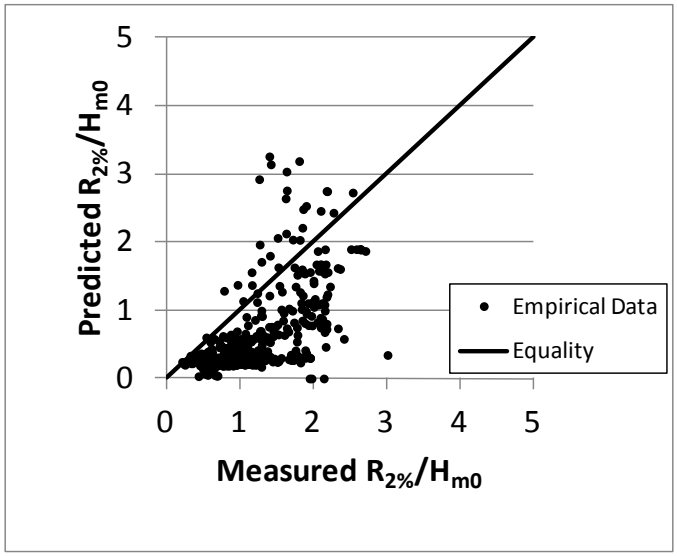

Figure 30. Runup 2.0 prediction versus beach data

The predictive skill of Runup 2.0 for beach data is poor. The digitization of average profiles is shown in Appendix D. A more coarse digitization was also used to determine if the program was sensitive to the slope digitization. There was no significant difference in results between the sparse and fine digitizations.

Table 14 summarizes error statistics and skill scores for Runup 2.0 predictions for the Mase, van Gent and Stockdon data sets. The data sets all produced varied errors with little consistency across the three data sets except that the errors were large and the skill of Runup 2.0 was low. The bias was negative for Mase data. For the beach data, the bias was negative and large. For the van Gent data, the bias was positive. The characteristic negative bias and small scatter errors for Mase appear to be a result of trying to predict irregular wave runup using an empirical model based on regular waves because depth limitations and complex slopes were not an issue for this data set. Mean wave height and period are inputs and mean runup is output for Runup 2.0 so Rayleigh distributed waves and runup were assumed for both inputs and outputs. The bias can be used to develop a correction for the $R_{2\%}$ values. However, given the large errors for the other predictions, it appears as though irregular wave runup on complex profiles with a wide surf zone is just too complex for Runup 2.0 to make accurate and defensible predictions.

Table 14. Error statistics and skill scores for runup 2.0 predictions.

	Mase Data	Van Gent Data	Stockdon Data
Dimensional RMS Error, E_{rms} (ft)	0.09	0.44	3.40
Bias, B (ft)	-0.07	0.16	-2.76
Nondimensional RMS Error, e_{rms}	0.36	0.80	0.62
Standard Deviation of Errors, σ_d (ft)	0.06	0.42	1.98
Scatter Index = SI	0.21	0.54	0.41
Normalized RMS Error Performance, $\hat{E}_{rms}$	-1.57	0.48	0.35
Normalized Bias Performance, $\hat{b}$	-0.92	0.81	0.47
Normalized SI Performance, $\hat{SI}$	0.79	0.46	0.59
Summary Performance, P_s	-0.57	0.58	0.47

3.12 Prediction of runup for other cases

3.12.1 Vertical walls

Vertical walls exist as shoreline structures. Often a seawall exists at the top of a beach. Sometimes the wall is at the crest of a coastal structure. The walls can be vertical, near vertical, or have a recurved shape. Many site-specific laboratory studies have been conducted to develop empirical equations for runup on walls. The *Shore Protection Manual* (SPM) (USACE 1984) gives a variety of predictive runup equations specific to

vertical and recurved wall geometries for seawalls and breakwater crest walls. Because the data are mostly site-specific, application of these equations for general use can be difficult and can require significant experience. However, the predictive equations given in the SPM (USACE 1984)are the state of practice and should be used for flood hazard estimate at this time.

3.12.2 Stepped walls or embankments

Runup on stepped embankments has been investigated for a number of site-specific cases. Melby et al. (2009) suggested using a roughness coefficient of $\gamma_r = 0.60$ for stepped embankments. This value is less than the values given in the CEM (USACE 2002) for rectangular blocks on an otherwise smooth impermeable slope. For blocks, it is suggested using $\gamma_r = 0.70 - 0.95$ depending on the geometry of the blocks and how they are distributed on the slope.

3.12.3 Other roughness factors

Roughness coefficients for stone and concrete armored structures are given in the EurOtop Manual and are repeated in Table 15. Values are given for the primary armoring types used in the United States. For additional guidance on runup on concrete armored structures see Melito and Melby (2002).

Table 15. Roughness factors for varied types of armoring.

Type of armour layer	γ_r
Rocks (1 layer, impermeable core)	0.60
Rocks (1 layer, permeable core)	0.45
Rocks (2 layers, impermeable core)	0.55
Rocks (2 layers, permeable core)	0.40
Cubes (1 layer, random positioning)	0.50
Cubes (2 layers, random positioning)	0.47
Antifer cube	0.47
CORE-LOC®	0.44
Tetrapod	0.38
Dolos	0.43

3.12.4 Tsunami runup

Tsunami runup is not evaluated herein as this report is focused on storm-induced flood hazard. However, several models show reasonable skill for predicting tsunami runup. Synolakis (1986, 1987), Li and Raichlen (2001, 2003), and Carrier et al. (2003) provide wave runup prediction relations for tsunamis. Hughes (2004) provides empirical equations for tsunami prediction based on the maximum wave momentum flux that are simple to apply.

4 Wave Transformation Numerical Models that Include Setup and Runup

4.1 Introduction

The preceding empirical equations are useful for flood risk assessments. However, the nearshore and swash zone consist of spatially varying bathymetry and topography that impact the incident wave climate and runup. Barred-beach and dune conditions are common and usually consist of complex bathymetry from offshore to the landward extent of the dune. During the most extreme storms, there may be significant morphological change and overtopping and erosion of the dune. Empirical equations based on limited experiments using impermeable smooth uniform slopes may not yield accurate solutions in many cases.

An attractive solution is to numerically model the nearshore wave transformation across the surf zone, through the swash zone to the extent of wave runup, including modeling changing morphology and dune erosion if necessary. Several hydrodynamic models for modeling transects are in wide use and they generally fall into two categories: phase-averaged or time-averaged and phase-resolving. Phase-averaged cross-shore models, such as CSHORE, have been widely discussed in the literature (Kobayashi 1997; Kobayashi 2009). The primary advantage of phase-averaged models is that they run very quickly and are very stable. The disadvantage is that they do not model the detailed transformation of each wave so they may miss some important physics in some cases. An example is modeling both incident and infragravity components of a spectrum.

Phase-resolving models based on the Boussinesq equations, have also gained recent popularity for practical application. The primary advantage of the Boussinesq-based models is that they capture the wave-to-wave physics and so can, in some cases, model the details of the spectral wave transformation including infragravity wave contributions. However, surfzone infragravity wave generation, trapped edge waves and other related physical processes may still not be modeled. In addition, offshore wave hindcasts do not typically include information on bound long waves. In this case, it is unlikely that any wave model can adequately resolve the infragravity dominated components of wave runup, particularly for

regional flood inundation studies where thousands of transects must be modeled. A disadvantage of Boussinesq-based models is that they run much slower than phase-averaged models and are less stable. So, for regional inundation studies where thousands of transects are modeled for hundreds of storms, detailed phase-resolving modeling for all transects and all storms may not be practical at this time.

Existing numerical models can provide consistent prediction of runup from steep to shallow slopes, including structure/beach porosity and roughness, and account for complex nearshore processes on irregular bathymetry. CSHORE has the option of including morphology change, bottom porosity, and many other complex nearshore processes. CSHORE runs extremely fast – a few seconds per storm per transect is typical. It is also very stable. A horizontally two-dimensional version of CSHORE is called C2SHORE. The programs have been validated for limited data sets as described in the many references (see Johnson et al. (in preparation) for validation to storm-induced morphology change data sets).

The following description of the CSHORE computational process is extracted from Kobayashi et al. (2008) and Kobayashi (2009). CSHORE solves the following time-averaged continuity, momentum, and energy equations in the region that is always wet:

$$\frac{g\sigma_\eta^2}{C} + \bar{h}\bar{U} = q_o \tag{33}$$

$$\frac{dS_{xx}}{dx} = -\rho g \bar{h}\frac{d\bar{\eta}}{dx} - \tau_b \tag{34}$$

$$\frac{dF}{dx} = -D_B - D_f \tag{35}$$

where σ_η = standard deviation of the free surface elevation η above the still water, C = linear wave phase velocity, $\bar{h}$ =mean water depth, $\bar{U}$ = mean depth-averaged velocity, q_o = wave overtopping rate, S_{xx} = cross-shore radiation stress, ρ = fluid density, $\bar{h}$ =mean free surface elevation, τ_b = time-averaged bottom shear stress, F = wave energy flux per unit width; and D_B and D_f = time-averaged wave energy dissipation rate per unit horizontal area due to wave breaking and bottom friction, respectively. The equations for S_{xx}, τ_b, F, D_B and D_f are given by Kobayashi

(2009). For Equations 33–35, the cross-shore coordinate x is positive onshore and the seaward boundary at $x = 0$ is typically just seaward of the breaker zone. Irregular waves propagate in the positive x direction.

For the wet-dry zone, the time-averaged continuity and momentum equations are:

$$\overline{h}\overline{U} = q_o \tag{36}$$

$$\frac{d}{dx}\left(\overline{hU^2} + \frac{g}{2}\overline{h^2}\right) = -g\overline{h}\frac{dz_b}{dx} - \frac{1}{2}f_b\left|\overline{U}\right|\overline{U} \tag{37}$$

where U is the instantaneous velocity, z_b = bottom elevation, and f_b = bottom friction factor. The averaging suggested by the overbar is only done for the wet period.

Kobayashi (2009) notes that the probability density function (pdf) for h is exponential using P_w as the probability of the presence of water. The velocity is expressed as $U = 2\sqrt{gh} + U_s$ where U_s = steady velocity to account for offshore return flow. Equations 36 and 37 along with the pdf for h and the velocity equation are solved to obtain the cross-shore variations of $\overline{h}$ and P_w.

Runup is computed assuming a runup wire at elevation d_r above the bottom. The mean and standard deviation of runup on the wire ($\overline{\eta}$, σ_r) above the still water elevation are estimated using three intersection points of the free surface on the wire at points (x_1, z_1), (x_2, z_2), and (x_3, z_3) as follows:

$$\overline{\eta}_r = \frac{z_1 + z_2 + z_3}{3},\ \sigma_r = \frac{z_1 - z_3}{2},\ S_r = \frac{z_1 - z_3}{x_1 - x_3} \tag{38}$$

where S_r is the average slope in the region of runup estimate. The runup height above the mean water level is given by $R - \overline{\eta}$ and is assumed to follow the Rayleigh distribution using the relation:

$$P = exp\left[-2\left(\frac{R - \overline{\eta}_r}{R_{1/3} - \overline{\eta}_r}\right)^2\right] \tag{39}$$

where $R_{1/3}$ is the significant runup height given by $R_{1/3} = (1 + 4S_r)$ $(\overline{\eta}_r + 2\sigma_r)$. From the Rayleigh distribution, the 2 percent exceedance value of runup is given by $R_{2\%} = \overline{\eta}_r + 1.40(R_{1/3} - \overline{\eta}_r)$.

Herein we summarize the inputs, outputs, and skill of CSHORE for estimation of runup.

4.2 CSHORE setup

The following is an analysis of CSHORE for a variety of nearshore and structure/beach conditions. The model was compared to measured runup from the benchmark data sets summarized in this report. The settings of the CSHORE model are summarized in Table 16 for parameters that vary. The parameters listed are IWCINT: 0 or 1 for no or yes for wave and current interactions, IROLL: 0 or 1 for no or yes for roller effects in the wet zone, GAMMA: empirical breaker ratio parameter, RWH: runup wire height, DX: constant grid mesh spacing, and Friction Coeff: bottom friction factor. The CSHORE model is metric but the dimensions in Table 16 are English to be consistent herein. The CSHORE model was applied to the field cases using a fixed beach profile (no morphology change was considered).

Table 16. CSHORE settings.

Site	IWCINT	IROLL	GAMMA	RWH (ft)	DX (ft)	Friction Coeff
Van Gent Series A-C[1]	0	0	0.7	0.0082	0.066	0.02
Van Gent Series P[1]	0	0	0.7	0.3281	3.281	0.02
Mase[1]	0	0	0.7	0.0033	0.033	0.002
Duck 1982[2]	1	1	0.8	0.0492	9.843	0.002
Scripps 1989[2]	1	1	0.8	0.0492	9.843	0.002
Duck 1990[2]	1	1	0.8	0.0492	9.843	0.002
San Onofre 1993[2]	1	1	0.8	0.0492	9.843	0.002
Duck 1994[2]	1	1	0.8	0.0492	9.843	0.002
Gleneden 1994[2]	1	1	0.8	0.0492	9.843	0.002
Agate 1996[2]	1	1	0.8	0.015	3.000	0.002
SandyDuck 1997[2]	1	1	0.8	0.015	3.000	0.002

[1] Structures with smooth impermeable slopes.

[2] Beach experiments with fixed bathymetry.

In general, the model is not very sensitive to the breaker ratio parameter or the bottom friction factor. The breaker ratio parameter is typically in the range of 0.6–0.8 with 0.7 being generally used with success herein. The bottom friction factor is less certain but values taken directly from the literature proved satisfactory for this study (e.g., Hughes 1995; Kobayashi 1999). The wave parameters used were H_{m0} and T_p. CSHORE returns the sum of the storm tide and runup so the storm tide must be subtracted out to get runup which includes setup.

For all CSHORE analyses, IPERM=0, IOVER=1, IWTRAN=0, IPOND=0, IWIND=0, ITIDE=0, and ILAB=1, where IPERM = 0 or 1 for an impermeable or permeable bottom, IOVER = 0 or 1 for no wave overtopping or wave overtopping at the landward end of the computation domain, IWTRAN = 0 or 1 for no standing water or wave transmission in a bay or lagoon landward of an emerged dune or coastal structure, IPOND = 0 or 1 for no ponding or ponding on lee side of dune or structure, IWIND = 0 or 1 for no or yes for wind effects, ITIDE = 0 or 1 for no tide or inclusion of tide, ILAB = 0 or 1 for field data or lab data.

The runup wire height RWH was set at 0.003 ft (1 mm) for the Mase experiments. This was done to account for the runup wire being inside of a channel in the slope in the experiments. Runup was measured using video techniques for the beach experiments. The runup wire height in CSHORE should be set very low to match these measurements. A range of runup wire heights was investigated. The runup wire height was arbitrarily set to 0.049 ft (1.5 cm) to most closely match the measured and computed runup for the beach experiments.

4.3 CSHORE results

Input wave conditions for CSHORE were those on the flat part of the flume for Mase and van Gent experiments and those just outside the surf zone for the beach studies. Peak wave period, T_p, was used as input to CSHORE. Further, root-mean-square wave height, H_{rms}, was used and was computed as $H_{m0}/1.41421$ assuming Rayleigh distributed wave heights outside the surf zone. For the beach experiments, waves were measured at varying locations just outside the surf zone. Stockdon transformed these wave conditions to deep water using linear shoaling. Only the deep water wave conditions were provided to us for this study. For the present analysis, these offshore wave conditions were transformed from deep

water to a depth of 8 m using linear wave theory and the 8 m depth conditions were used as input to CSHORE.

The profiles were time-averaged over the duration of the beach experiments. Figures in Appendix D show the profiles and the digitization used in CSHORE input. Each profile was extended to elevation +4 m on the shoreward end and to -8 m on the seaward end using the average swash and offshore slopes, respectively. Note that the Oregon profiles were estimated offshore and assumed linear. For the beach experiment analysis, the measured water levels throughout each experiment were obtained from the NOAA COOPS web site.

Figures 31–35 show measured versus CSHORE computed $R_{2\%}/H_{m0}$ for the study data summarized in Table 16. Each figure shows a solid line for perfect agreement and 20 percent error as dashed lines. Figure 31 shows the relative runup comparison with van Gent data and Figure 32 shows the comparison for the Mase data. The runup is normalized by the wave height at the toe of the slope in relatively deep water. These two figures illustrate that CSHORE predicts $R_{2\%}$ well for smooth structures with nearly all of the predictions within 20 percent error and little bias. Some bias on the high side is observed in the higher relative runup in van Gent data.

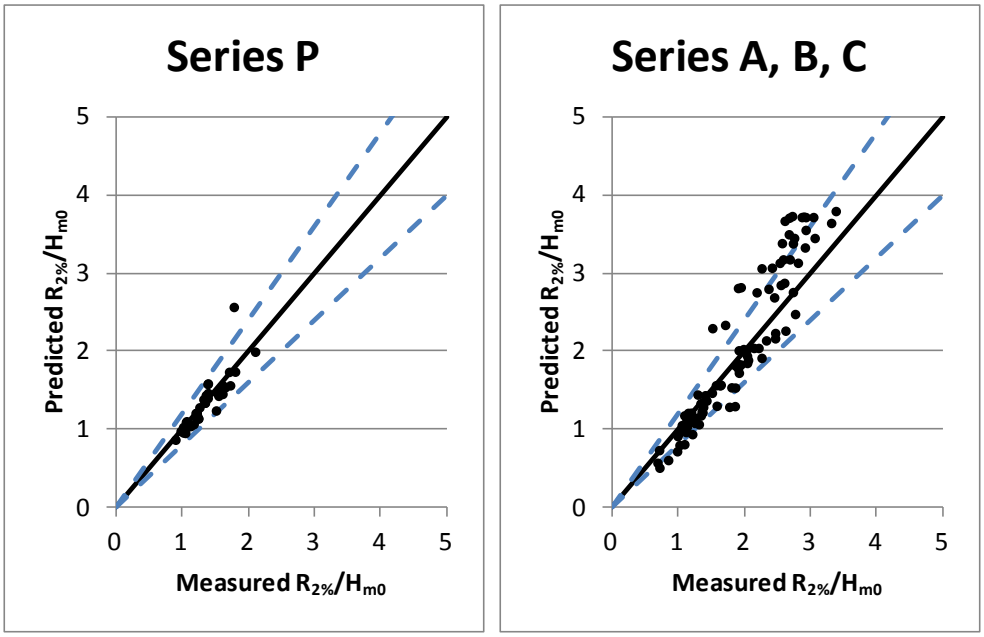

Figure 31. CSHORE predicted relative runup versus van Gent measurements. Solid black line is equality and dashed lines are the 20 percent error.

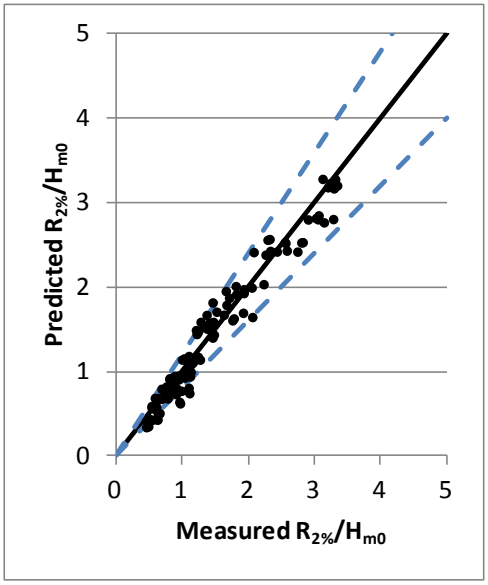

Figure 32. CSHORE predicted relative runup versus Mase measurements. Solid black line is equality and dashed lines are the 20 percent error.

The results have been plotted as relative runup rather than dimensional runup for two reasons. One is to allow comparison of disparate experiments on similar scales and even on the same plot in some cases. The second reason is to spread the points out on the plot to better discern skill. For some studies, the range of relative runup was large but the range of dimensional runup was relatively small. There is an argument against plotting relative runup because it does give weight to very small runup values which have relatively larger measurement error and are of lesser importance to flood hazard assessment. However, comparing dimensional and relative runup plots, the apparent skill of the CSHORE model was the same. The only difference is that the points are more wide spread in the relative runup plots.

Figures 33–35 show CSHORE prediction of relative runup compared to Stockdon beach data. Here, runup is normalized by wave height in 8 m depth. The sites are grouped where predictions were similar in bias and scatter. Figure 33 shows Delilah (Duck 1990), Duck 1994, San Onofre, and Scripps. The skill of CSHORE for these experiments was surprisingly similar with little bias and a reasonable level of overall skill, particularly considering there was no tuning of the model to match these measurements and only average beach profiles and nearby water level data were available.

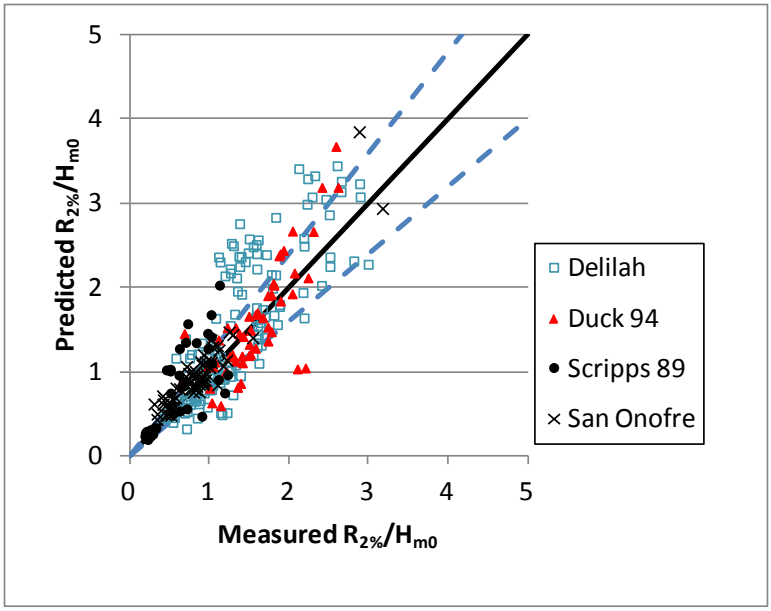

Figure 33. CSHORE predicted runup versus measured runup during Duck 1990, Duck 1994, Scripps, and San Onofre experiments. Solid black line is equality and dashed lines are the 20 percent error.

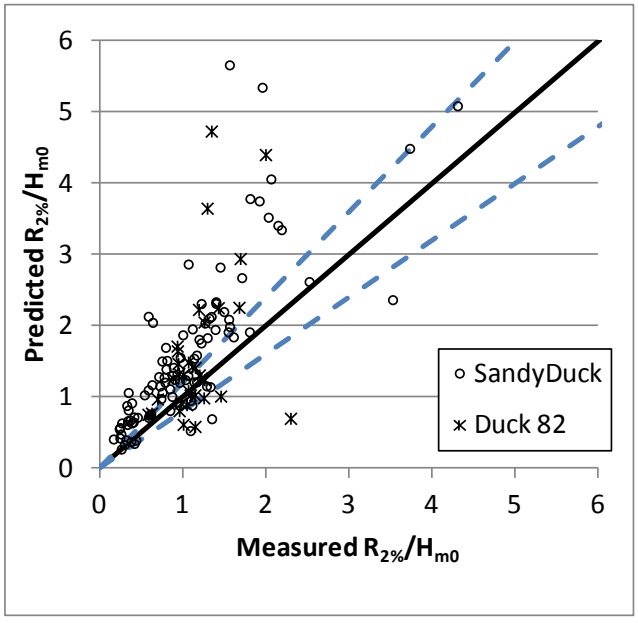

Figure 34. CSHORE predicted runup versus measured during Duck 1982 and SandyDuck experiments. Solid black line is equality and dashed lines are the 20 percent error.

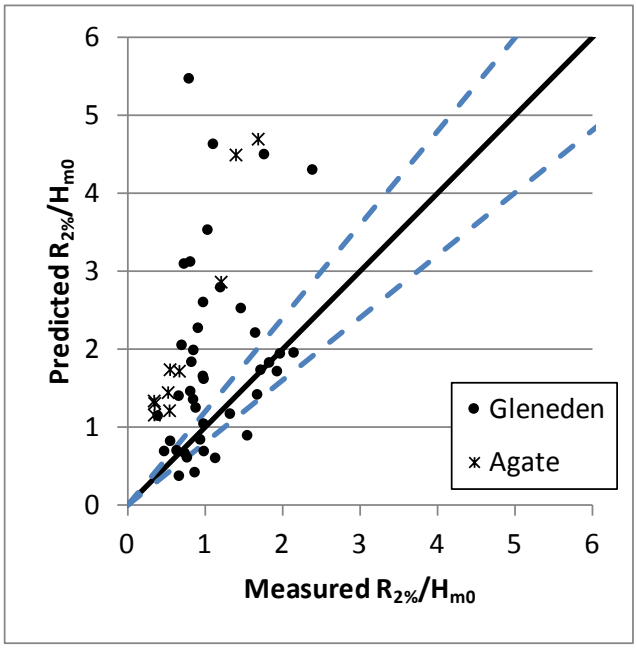

Figure 35. CSHORE predicted runup versus measured during Agate and Gleneden, OR, experiments. Solid black line is equality and dashed lines are the 20 percent error.

Also, measurement and analysis of wave runup, incident waves, and bathymetry were complex for these experiments, spanning nearly two decades when technology was changing rapidly and varying from site to site. Because the conditions were generally not stormy, the waves and runup were often relatively small, producing more relative scatter that would not be significant for flood hazard. Finally, as stated earlier, Scripps data were infragravity-dominated. Given these issues, it is surprising that prediction skill for data from disparate sites on different coasts would be similar. Although the largest error is nearly a factor of two, the predictions show skill similar to the empirical equations that were specifically tuned for these data sets.

Figure 34 shows relative runup predictions for Duck 1982 and SandyDuck experiments, while Figure 35 shows relative runup predictions for Gleneden, OR, and Agate, OR. Here we see much more scatter than is shown in Figure 33, particularly for higher relative runup. Figure 34 shows more scatter than Figure 33 and a few outliers but reasonable overall prediction. Comparison of the modified Mase equation with Duck 1982 and SandyDuck data in Table 12 also showed lower skill than other incident-dominated sites suggesting that poor prediction for several data points is partly due to uncertainty in the data. Figure 35 shows CSHORE has poor skill for the north Pacific coast. The CSHORE model over-predicted relative runup for some cases. Uncertainty in nearshore bathymetry and water levels for these sites adds significant uncertainty to the data. So model predictions were not expected to be accurate for these sites. It is also likely that the CSHORE model provides poor prediction of infragravity-dominated runup on dissipative beaches. For these cases, a formulation specific for dissipative beaches like Equation 31 may be required. The large uncertainty is also a result of relatively small incident waves and resulting small runup values. It is expected that CSHORE runup predictions for storm conditions corresponding to higher flood hazard where a higher water level reaches a steeper beach face and runup is dominated by incident wave conditions would be more accurate with accuracy represented by Figure 33.

4.4 Summary of wave transformation numerical model results

Table 17 summarizes the skill of CSHORE for predicting runup on structures as shown in Figures 31–32. Table 18 summarizes the skill of CSHORE for runup on beaches as shown in Figures 33–35.

Table 17. Error statistics and skill scores for CSHORE predictions of runup on structures.

	Mase Data	Van Gent Data Series P	Van Gent Data Series A, B, C
N	120	40	97
Dimensional RMS Error, E_{rms} (ft)	0.03	2.11	0.20
Bias, B (ft)	0.00	-0.06	0.06
Nondimensional RMS Error, e_{rms}	0.13	0.09	0.19
Standard Deviation of Errors, σ_d (ft)	0.03	2.14	0.23
Scatter Index = SI	0.11	0.20	0.11
Normalized RMS Error Performance, $\hat{E}_{rms}$	0.90	0.45	0.79
Normalized Bias Performance, $\hat{b}$	0.99	0.98	0.94
Normalized SI Performance, $\hat{SI}$	0.89	0.80	0.89
Summary Performance, P_s	0.92	0.74	0.87

Table18. Error statistics and skill scores for CSHORE predictions of runup on beaches. Group 1: Delilah, Duck 1994, Scripps, and San Onofre; Group 2: SandyDuck and Duck 1982; Group 3: Gleneden and Agate.

	Group 1	Group 2	Group 3
N	290	130	56
Dimensional RMS Error, E_{rms} (ft)	1.35	3.26	10.11
Bias, B (ft)	0.28	2.11	6.46
Nondimensional RMS Error, e_{rms}	0.37	0.94	1.83
Standard Deviation of Errors, σ_d (ft)	1.33	2.49	7.85
Scatter Index = SI	0.28	0.55	1.42
Normalized RMS Error Performance, $\hat{E}_{rms}$	0.74	0.34	-0.77
Normalized Bias Performance, $\hat{b}$	0.95	0.57	-0.13
Normalized SI Performance, $\hat{SI}$	0.72	0.45	-0.42
Summary Performance, P_s	0.80	0.46	-0.44

The results summarized above suggest that CSHORE can predict runup with a high degree of skill over a broad range of wave and nearshore profile situations for storm conditions where there is a flood hazard. For the most part, the skill is comparable to empirical models that were tuned to the data. There were areas of weakness with the model though. In particular, CSHORE is not expected to predict runup well for conditions where infragravity conditions dominate, particularly on gently-sloping dissipative beaches that are typical of the northwest Pacific coast. Further research is required in this area.

Note that there are many questions concerning the beach data, including the effect of variable beach profile geometry during the experiment and calculation method of runup, that will impact the comparison. Data acquisition and analysis methods varied between sites. Locally measured water levels were not provided with the data. Some of the beach experiments did not include offshore profile measurement. Some experiments showed relatively more scatter. Ongoing research with improved and consistent data acquisition and analysis methods will help clarify the strengths and weaknesses of CSHORE and improve predictions. Considering the uncertainty in the empirical equation predictions, CSHORE appears to provide roughly equal skill during most conditions and is more versatile because it can be applied to a wide range of wave, water level and profile geometry conditions. As with any engineering hydrodynamic model, care must be exercised in application of CSHORE to assure accurate predictions.

5 Conclusions and Recommendations

The study goal was to establish several benchmark wave runup data sets and evaluate the available tools for predicting wave runup for flood hazard assessment. Benchmark data covered a range of shoreline conditions including sandy beaches on the Pacific and Atlantic coasts, impermeable smooth structures with uniform slopes from 1:30 to 1:5, impermeable structures with steep uniform and compound slopes (clay earthen grass-covered levees), impermeable stone-armored structures (levees and revetments), and permeable stone-armored structures (breakwaters). The beach data sets spanned the range of dissipative to reflective beaches. The structure data sets encompass a wide range of wave and water level conditions from deep water at the slope toe to shallow water with a wide surf zone. The laboratory data sets were limited to data that were carefully obtained using modern wave generation and wave measurement techniques. The data set from van Gent included full-scale and small-scale data and included active wave absorption, second order wave correction, and incident and reflected wave resolution.

Tools for predicting wave runup were analyzed including empirical equations, computer programs based on empirical equations, and the CSHORE numerical hydrodynamic model. Most of the tools showed fairly high degrees of skill but some did not.

Recommendations from this study are as follows:

1. For most shoreline conditions, CSHORE can be used to predict wave runup. This includes coastal structures and beaches. CSHORE also can be used to predict cross-shore beach morphology change where important. In addition, CSHORE can be used to predict wave overtopping of structures and dunes, although that was not analyzed in this report. CSHORE is not likely to predict wave runup on infragravity-dominated dissipative beaches well. For these cases, it is recommended that one of the recommended empirical equations for beaches be used, as discussed below.
2. For structures, the EurOtop equation (Equation 8) can be used for conditions that are within the range of experimental conditions discussed herein. Otherwise use CSHORE. The EurOtop equation is:

$$\frac{R_{2\%}}{H_{m0}} = 1.65\gamma_b\gamma_f\gamma_\beta\xi_{m-1,0}$$
$$\frac{R_{2\%}}{H_{m0}} \le \gamma_b\gamma_{f\,surging}\gamma_\beta\left(\frac{4-1.5}{\sqrt{\xi_{m-1,0}}}\right) \quad \text{(8 bis)}$$

where H_{m0} is defined at the structure toe, $\xi_{m-1,0} = \tan\alpha/\sqrt{s}$, $s = H_{m0}/L_0$, $L_0 = g(T_{m\text{-}1,0})^2/2\pi$, γ_b is the influence coefficient for a berm, if present, γ_f is the influence coefficient for roughness, γ_β is the influence coefficient for wave directionality, $\gamma_{f\,surging} = \gamma_f + (\xi_{m-1,0} - 1.8)(1-\gamma_f)/8.2$ and $\gamma_{f\,surging} = 1.0$ for $\xi_{m-1,0} > 10$.

The EurOtop equation is likely to have better skill than CSHORE for cases that are within the applicable experimental data range of bathymetry and wave-water level conditions. However, for cases with complex nearshore bathymetry, complex structure profile, or wave and water level conditions not represented within experimental data set, CSHORE is likely to show better skill.

3. For beaches where CSHORE is not applicable, or the results are questioned, or if there is a desire to have an independent prediction for comparison, one of the empirical beach runup equations described herein can be used. The Stockdon and modified Mase equations showed similar skill. The simplest method appeared to be the modified Mase formulation, derived herein:

$$\frac{R_{2\%}}{H_{m0}} = 1.1\xi_{0p}^{0.7} \quad (40)$$

where H_{m0} is defined in deep water, $\xi_{0p} = \tan\beta_f/\sqrt{s_{0p}}$, β_f is the foreshore beach slope defined as the average slope over a region between $\pm 2\sigma_s$ of the mean water level, where σ_s is defined as the standard deviation of the continuous water level record, $s_{0p} = H_{m0}/L_{0p}$, and $L_{0p} = gT_p^2/2\pi$. For computing β_f, use may be made of the relation $\sigma_s = 0.5\,H_{m0}$ as given in the CEM (USACE 2002) and H_{m0} is the value used in the runup determination. The foreshore beach slope is usually uncertain and a range of slopes may need to be examined.

Alternatively, the Stockdon equations may be used. The full equation for all beach cases is:

$$R_{2\%} = 1.1\left\{0.35\beta_f (H_{m0}L_{0p})^{1/2} + \frac{1}{2}\left[H_{m0}L_{0p}(0.563\beta_f^2 + 0.004)\right]^{1/2}\right\} \quad (41)$$

where the first term in brackets is setup, the β_f term is for incident-wave contributions, and the 0.004 term is for infragravity wave contributions. The reduced equation for dissipative beaches where infragravity wave conditions dominate is:

$$R_{2\%} = 0.043(H_{m0}L_{0p})^{1/2} \qquad \xi_{0p} < 0.3 \quad (42)$$

4. Integral, energy-based wave parameters, such as H_{m0} and $T_{m\text{-}1,0}$, are more stable than their non-integral counterparts ($H_{1/3}$, T_p, T_m) during wave transformation as a result of energy conservation. As discussed herein, T_p becomes very uncertain in the surf zone as the wave energy density spectrum deforms. So empirical equations based on integral wave parameters, such as the van Gent and EurOtop equations, tend to be better generalized and have more skill. Also, wave transformation models, such as CSHORE and those based on the Boussinesq equations, tend to show more skill across the wide range of possible shoreline conditions than empirical equations partly because they take into account spectral wave transformation and wave breaking across varied bathymetry. Empirical models based on deep-water wave conditions are not very sensitive to the choice of integral or non-integral wave parameters because both are stable in deep water. However, these models will yield significant uncertainty in application to shallow water conditions with varied bathymetry. The recommendations above reflect this.

References

Ahrens, J. P. 1981. *Irregular wave runup on smooth slopes*. CETA No. 81-17. Ft. Belvoir, VA: U.S. Army Corps of Engineers, Coastal Engineering Research Center.

Ahrens, J. P., and B. L. McCartney. 1975. Wave period effect on the stability of riprap. In *Proceedings of Civil Engineering in the Oceans/III, Reston, VA*, 1019–1034. American Society of Civil Engineers.

Ahrens, J. P., and M. F. Titus. 1985. Wave runup formulas for smooth slopes. *J. Wtrwy., Port, Coastal, and Oc. Engrg*. III(1):128–133. ASCE.

Ahrens, J. P., and M. S. Heimbaugh. 1988. *Approximate upper limit of irregular wave runup on riprap*. Technical Report CERC-88-5. Vicksburg, MS: U.S. Army Engineer Waterways Experiment Station, Coastal Engineering Research Center.

Ahrens, J. P., and W. N. Seelig. 1996. Wave runup on beaches. In *Proceedings, 25th International Conference on Coastal Engineering, Orlando, FL*, 981–993. American Society of Civil Engineers.

Ahrens, J. P., W. N. Seelig, D. L. Ward, and W. Allsop. 1993. Wave runup on and wave reflection from coastal structures. In *Proc. of Ocean Wave Measurement and Analysis (Waves '93) Conf.* 489–502. ASCE.

Battjes, J. A. 1974a. Surf similarity. In *Proc. 14th Intl. Coastal Engrg. Conf.* 1:466–480. ASCE.

_____. 1974b. *Computation of set-up, longshore currents, run-up and overtopping due to wind-generated waves*. Report 74-2. Delft, The Netherlands: Committee on Hydraulics, Department of Civil Engineering, Delft University of Technology.

Birkemeier, W., and K. Hathaway. 1996. Delilah, Duck 94, and SandyDuck: Three nearshore field experiments. In *Proc. 25th Int'l Conf. on Coastal Eng.*, 4052–4065.

Carrier, G. F., T. T. Wu, and H. Yeh. 2003. Tsunami run-up and draw-down on a plane beach. *J. of Fluid Mech*. 475:79–99. United Kingdom: Cambridge University Press.

Carstens, T., A. Torum, and A. Traetteberg. 1966. The stability of rubble mound breakwaters against irregular wave. In *Proc. 10th Coastal Engrg. Conf.*, ASCE, 958-971.

De Waal, J. P., and J. W. van der Meer. 1992. Wave runup and overtopping on coastal structures. In *Proc. 23rd Intl. Coastal Engrg. Conf., Venice, Italy*, ASCE, 2:1758–1771.

Douglass, S. L. 1992. Estimating extreme values of run-up on beaches. *J. Wtrwy., Port, Coastal, and Oc. Engrg., ASCE*, 124(2):73–81.

Elgar, S., T. H. C. Herbers, M. Okihiro, J. Oltman-Shay, and R. T. Guza. 1993. Observations of infragravity waves. *Journal of Geophysical Research* 97(C10):15573–15577.

EurOtop Manual. 2007. *Wave overtopping of sea defences and related structures: Assessment manual*. United Kingdon: Environmental Agency. http://www.overtopping-manual.com/.

Federal Emergency Management Agency (FEMA). 1981. *Manual for wave runup analysis, coastal flood insurance studies*. Boston, MA: Stone and Webster Engrg. Corp.

_____. 1991. *Investigation and improvement of capabilities for the FEMA wave runup model*. Washington, DC: Dewberry and Davis, Inc.

Goda, Y., and Y. Suzuki. 1976. Estimation of incident and reflected waves in random wave experiments. In *Proc., 17th Coastal Engrg. Conf*. 1:201–220. ASCE.

Guza, R. T, and E. B. Thornton. 1982. Swash oscillations on a natural beach. *J. Geoph. Res*. 87(C1):483–491. American Geophysical Union.

Holland, K. T., and R. A. Holman. 1999. Wavenumber-frequency structure of infragravity swash motions. *J. Geoph. Res*. 104(C6):13,479–13,488. American Geophysical Union.

Holland, K. T., B. Raubenheimer, R. T. Guza, and R. A. Holman. 1995. Runup kinematics on a natural beach. *J. Geoph. Res*. 100(C3):4985–4993. American Geophysical Union.

Holman, R. A. 1986. Extreme value statistics for wave runup on a natural beach. *Coastal Engrg*. 9(6):527–544. Elsevier.

Holman, R. A., and A. H. Sallenger. 1985. Setup and swash on a natural beach. *J. Geoph. Res*. 90(C1):945–953. American Geophysical Union.

Hughes, M. G. 1995. Friction factors in wave uprush. *J. of Coastal Res*. 11(4):1089–1098. Coastal Ed. and Res. Found., Inc.

Hughes, M. G., A. S. Moseley, and T. E. Baldock. 2010. Probability distributions for wave runup on beaches. *Coastal Engrg*. 57:575–584. Elsevier.

Hughes, S. A. 2004. Estimation of wave run-up on smooth, impermeable slopes using the wave momentum flux parameter. *Coastal Engrg*. 51(11):1085-1104. Elsevier.

Hunt, I. A. 1959. Design of seawalls and breakwaters. *J. of Waterways and Harbours Division*, ASCE, 85(WW3):123–152.

Iribarren, C. R., and C. Nogales. 1949. Protection des Ports. In *XVIIth International Navigation Congress, Section II, Communication*. 31–80.

Jiabao, Z. 1993. Effect of wave groups on wave run-up. *J. of Coastal Res*., 9(4):1110–1114. Coastal Ed. and Res. Found., Inc.

Johnson, B. D., N. Kobayashi, and M. B. Gravens. In preparation. *Cross-shore numerical model CSHORE for waves, currents, sediment transport and beach profile evolution*. ERDC/CHL TR-12-X. Vicksburg, MS: U.S. Army Engineer Research and Development Center.

Johnson, R. R., E. P. D. Mansard, and J. Ploeg. 1978. Effects of wave grouping on breakwater stability. In *Proc. 16th Coastal Engrg. Conf.*, ASCE, 2228-2243.

Kobayashi, N. 1997. *Wave runup and overtopping on beaches and coastal structures*. Research Report No. CACR-97-09. Newark, DE: University of Delaware, Center for Applied Coastal Research.

_____. 1999. Wave runup and overtopping on beaches and coastal structures. *Advances in Coastal and Ocean Engrg*. 5:95–154. World Scientific, Singapore.

_____. 2009. *Documentation of cross-shore numerical model CSHORE*. Research Report No. CACR-09-06. Newark, DE: University of Delaware, Center for Applied Coastal Research.

Kobayashi, N., F. J. de los Santos, and P. G. Kearney 2008. Time-averaged probabilistic model for irregular wave runup on permeable slopes. *J. Wtrwy., Port, Coastal, and Oc. Engrg.*, ASCE, 134(2):88-96.

Kriebel, D. 1994. Swash zone wave characteristics from SUPERTANK. In *Proc. 24th Intl. Conf. on Coastal Engrg., Kobe, Japan*, ASCE, 2207-2221.

Leenknecht, D. A., A. R. Sherlock, and A. Szuwalski. 1995. Automated tools for coastal engineering. *J. of Coastal Res*. 11(4):1108–1124. Coastal Ed. and Res. Found., Inc.

Li, Y., and F. Raichlen. 2001. Solitary wave runup on plane slopes. *J. Wtrwy., Port, Coastal, and Oc. Engrg.*, ASCE, 127(1):33–44.

_____. 2003. Energy balance model for breaking solitary wave runup. *J. Wtrwy., Port, Coastal, and Oc. Engrg.*, ASCE, 129(2):47–59.

Longuet-Higgins, M. S., and R. W. Stewart. 1962. Radiation stress and mass transport in gravity waves with application to 'surf beats'. *J. Fluid Mech*. 13:481–504.

_____. 1964. Radiation stresses in water waves: a physical discussion, with applications. *Deep-Sea Research* 11:529–562. Great Britian: Pergamon Press.

Madsen, P. A., H. A. Schiaffer, and O. R. Sorensen. 1997a. Surf zone dynamics simulated by a Boussinesq type model. Part I: Model description and cross-shore motion of regular waves. *Coastal Engrg*. 32:255–288. Elsevier.

Madsen, P. A., O. R. Sorensen, and H. A. Schaffer. 1997b. Surf zone dynamics simulated by a Boussinesq type model. Part II: surf beat and swash oscillations for wave groups and irregular waves. *Coastal Engrg*. 32:289–319. Elsevier.

Mansard, E. P. D., and E. R. Funke. 1987. *On the reflection analysis of irregular waves*. Tech. Report No. TR-HY-017. Ottawa, Canada: National Research Council of Canada.

Mase, H. 1989. Random wave runup height on gentle slope. *J. Wtrwy., Port, Coastal, and Oc. Engrg.*, ASCE, 115(5):649–661.

Mase, H., and Y. Iwagaki. 1984. Runup of random waves on gentle slopes. In *Proc. 19th Coastal Engrg. Conf.*, ASCE, 593-609.

Mayer, R., and D. Kriebel. 1994. Wave runup on composite-slope and concave beaches. In *Proc. 24th Intl. Conf. on Coastal Engrg., Kobe, Japan*, ASCE, 2325-2339.

Melby, J. A. 2003. Advances in breakwater and revetment design. In *Advances in coastal structure design*, ed. R. Mohan, O. Magoon, and M. Pirello, 161–180. ASCE.

Melby, J. A., E. Burg, D. C. McVan, and W. G. Henderson. 2009. *South Florida reservoir embankment study*. Technical Report ERDC/CHL TR-09-3. Vicksburg, MS: U.S. Army Engineer Research and Development Center.

Melito, I., and J. A. Melby. 2002. Wave runup, transmission, and reflection for structures armored with CORE-LOC. *Coastal Engrg*. 45:33–52. Elsevier.

Nwogu, O. 1993. Alternative form of Boussinesq equations for nearshore wave propagation. *J. Wtrwy., Port, Coastal, and Oc. Engrg*., ASCE, 119(6):618–638.

Nwogu, O., and Z. Demirbelik. 2001. *BOUSS-2D: A Boussinesq wave model for coastal regions and harbors*. Technical Report ERDC/CHL TR-01-25. Vicksburg, MS: U.S. Army Engineer Research and Development Center.

Nielsen, P., and D. J. Hanslow. 1991. Wave runup distributions on natural beaches. *J. of Coastal Res*. 7(4):1139–1152. Coastal Ed. and Res. Found., Inc.

Raubenheimer, B., and R. T. Guza. 1996. Observations and predictions of run-up. *J. Geoph. Res*. 101(C10):25,575–25,587. American Geophysical Union.

Saville Jr., T. 1958. Wave run-up on composite slopes. In *Proc. 6th Intl. Coastal Engrg. Conf.*, ASCE, 691–699.

Stockdon, H. F., R. A. Holman, P. A. Howd, and A. H. Sallenger. 2006. Empirical parameterization of setup, swash, and runup. *Coastal Engrg*. 53:573–588. Elsevier.

Stoa, P. N. 1978. *Reanalysis of wave runup on structures and beaches*. TP 78-2. Ft. Belvoir, VA: U.S. Army Corps of Engineers Coastal Engineering Research Center.

Synolakis, C. E. 1986. The run-up of long waves. PhD Thesis, California Institute of Technology, Pasadena, CA.

_____. 1987. The run-up of solitary waves. *Journal of Fluid Mechanics* 185:523–545. United Kingdom: Cambridge University Press.

TAW. 2002. *Technical report: Wave runup and wave overtopping at dikes*. Technical Advisory Committee on Flood Defence, Delft, The Netherlands.

U.S. Army Corps of Engineers (USACE). 1984. *Shore Protection Manual*. 4th ed. Vicksburg, MS: U.S. Army Engineer Waterways Experiment Station.

_____. 2002. *Coastal Engineering Manual*. Engineer Manual 1110-2-1100. Washington, DC: U.S. Army Corps of Engineers (in 6 volumes).

van der Meer, J. W. 1988. Rock slopes and gravel beaches under wave attack. PhD diss., Delft Hydraulics Communication No. 396, Delft Hydraulics Laboratory, Emmeloord, The Netherlands.

van der Meer, J. W., and C. M. Stam. 1991. *Wave runup on smooth and rock slopes*. Publication No. 454. The Netherlands: WL Delft Hydraulics, Rijkwaterstaat

_____. 1992. Wave runup on smooth and rough slopes of coastal structures. *J. Wtrwy., Port, Coastal, and Oc. Engrg.*, ASCE, 118(5):534–550.

Van Gent, M. 1999a. *Physical model investigations on coastal structures with shallow foreshores-2D model stes on the Petten Sea Defence*. Technical Report H3129. The Netherlands: WL Delft Hydraulics, Rijkwaterstaat, pp. 85.

_____. 1999b. *Physical model investigations on coastal structures with shallow foreshores-2D model tests with single and double-peaked wave energy spectra*. Technical Report H3608. The Netherlands: WL Delft Hydraulics, Rijkwaterstaat.

_____. 2001. Wave runup on dikes with shallow foreshores. *J. Wtrwy., Port, Coastal, and Oc. Engrg.*, ASCE, 127(5):254–262.

Appendix A: Mase Data

The following data (Tables A1–A4) are from laboratory experiments by Mase (1989) and Mase and Iwagaki (1984) for irregular wave run-up on smooth, impermeable plane slopes with slope angles ranging from 1:5 to 1:30.

Table A1. Mase data for slope of 1:5.

Toe Water Depth, d_s ft	Incident Wave Height, H_s ft	Peak Wave Period, T_p sec	Iribarren Parameter ξ_{0p}	2% Exceed-ance Runup $R_{2\%}$ ft
1.48	0.20	2.38	2.44	0.65
1.48	0.16	2.40	2.73	0.53
1.48	0.13	2.39	3.02	0.42
1.48	0.23	1.83	1.72	0.70
1.48	0.19	1.86	1.91	0.59
1.48	0.15	1.87	2.20	0.49
1.48	0.29	1.60	1.34	0.68
1.48	0.23	1.56	1.49	0.58
1.48	0.17	1.58	1.74	0.47
1.48	0.36	1.21	0.92	0.65
1.48	0.28	1.20	1.02	0.55
1.48	0.21	1.17	1.16	0.47
1.48	0.23	0.96	0.92	0.40
1.48	0.19	0.95	1.00	0.36
1.48	0.23	0.87	0.83	0.33
1.48	0.20	0.85	0.86	0.30
1.48	0.20	2.39	2.41	0.63
1.48	0.16	2.44	2.76	0.52
1.48	0.14	2.41	2.93	0.44
1.48	0.25	1.84	1.68	0.71
1.48	0.19	1.86	1.91	0.59
1.48	0.17	1.86	2.06	0.52
1.48	0.30	1.59	1.30	0.70
1.48	0.23	1.55	1.47	0.58
1.48	0.18	1.56	1.65	0.52
1.48	0.36	1.21	0.91	0.66
1.48	0.28	1.19	1.01	0.55
1.48	0.24	1.18	1.09	0.49
1.48	0.24	0.97	0.89	0.43
1.48	0.19	0.94	0.98	0.39
1.48	0.20	2.38	2.44	0.65
1.48	0.16	2.40	2.73	0.53

Table A2. Mase data for slope of 1:10.

Toe Water Depth, d_s ft	Incident Wave Height H_s ft	Peak Wave Period, T_p sec	Iribarren Parameter ξ_{0p}	2% Exceed-ance Runup $R_{2\%}$ ft
1.48	0.17	2.24	1.23	0.38
1.48	0.13	2.23	1.40	0.32
1.48	0.10	2.26	1.65	0.26
1.48	0.22	1.73	0.83	0.37
1.48	0.18	1.73	0.93	0.30
1.48	0.13	1.72	1.08	0.25
1.48	0.29	1.51	0.64	0.35
1.48	0.22	1.48	0.71	0.31
1.48	0.17	1.51	0.84	0.25
1.48	0.36	1.20	0.45	0.40
1.48	0.29	1.17	0.49	0.33
1.48	0.22	1.16	0.56	0.25
1.48	0.22	0.96	0.46	0.25
1.48	0.19	0.93	0.49	0.20
1.48	0.23	0.86	0.41	0.22
1.48	0.19	0.84	0.43	0.19
1.48	0.17	2.29	1.24	0.36
1.48	0.13	2.24	1.42	0.30
1.48	0.10	2.23	1.57	0.27
1.48	0.24	1.78	0.83	0.35
1.48	0.18	1.77	0.95	0.29
1.48	0.15	1.77	1.04	0.27
1.48	0.30	1.53	0.63	0.37
1.48	0.23	1.50	0.71	0.30
1.48	0.19	1.50	0.78	0.28
1.48	0.36	1.20	0.45	0.38
1.48	0.29	1.16	0.49	0.30
1.48	0.24	1.16	0.54	0.26
1.48	0.24	0.94	0.43	0.22
1.48	0.19	0.92	0.48	0.18
1.48	0.17	2.24	1.23	0.38
1.48	0.13	2.23	1.40	0.32

Table A3. Mase data for slope of 1:20.

Toe Water Depth, d_s ft	Incident Wave Height H_s ft	Peak Wave Period, T_p sec	Iribarren Parameter ξ_{0p}	2% Exceed-ance Runup $R_{2\%}$ ft
1.48	0.16	2.27	0.65	0.22
1.48	0.12	2.24	0.73	0.17
1.48	0.09	2.23	0.85	0.14
1.48	0.21	1.78	0.44	0.23
1.48	0.16	1.74	0.49	0.19
1.48	0.12	1.77	0.58	0.15
1.48	0.26	1.58	0.35	0.23
1.48	0.20	1.55	0.39	0.18
1.48	0.15	1.53	0.45	0.14
1.48	0.33	1.21	0.24	0.19
1.48	0.26	1.17	0.26	0.17
1.48	0.19	1.20	0.31	0.15
1.48	0.23	0.97	0.23	0.14
1.48	0.19	0.92	0.24	0.12
1.48	0.23	0.85	0.20	0.14
1.48	0.20	0.82	0.21	0.12
1.48	0.16	2.28	0.64	0.20
1.48	0.12	2.25	0.74	0.15
1.48	0.10	2.25	0.82	0.13
1.48	0.22	1.82	0.44	0.24
1.48	0.17	1.80	0.50	0.19
1.48	0.13	1.80	0.56	0.16
1.48	0.27	1.53	0.33	0.22
1.48	0.20	1.51	0.38	0.16
1.48	0.17	1.52	0.42	0.15
1.48	0.33	1.17	0.23	0.21
1.48	0.25	1.16	0.26	0.17
1.48	0.21	1.17	0.29	0.16
1.48	0.24	0.95	0.22	0.15
1.48	0.19	0.92	0.24	0.12
1.48	0.16	2.27	0.65	0.22
1.48	0.12	2.24	0.73	0.17

Table A4. Mase data for slope of 1:30.

Toe Water Depth, d_s ft	Incident Wave Height H_s ft	Peak Wave Period, T_p sec	Iribarren Parameter ξ_{0p}	2% Exceed-ance Runup $R_{2\%}$ ft
1.41	0.15	2.24	0.43	0.18
1.41	0.12	2.22	0.49	0.14
1.41	0.09	2.18	0.56	0.11
1.41	0.20	1.72	0.29	0.18
1.41	0.16	1.73	0.33	0.14
1.41	0.11	1.78	0.40	0.11
1.41	0.25	1.53	0.23	0.19
1.41	0.19	1.52	0.26	0.18
1.41	0.16	1.47	0.28	0.12
1.41	0.33	1.14	0.15	0.18
1.41	0.26	1.14	0.17	0.14
1.41	0.19	1.15	0.20	0.11
1.41	0.22	0.92	0.15	0.10
1.41	0.18	0.89	0.16	0.09
1.41	0.22	0.82	0.13	0.10
1.41	0.19	0.82	0.14	0.09
1.41	0.16	2.25	0.43	0.16
1.41	0.11	2.28	0.51	0.12
1.41	0.09	2.28	0.56	0.10
1.41	0.20	1.85	0.31	0.18
1.41	0.15	1.82	0.35	0.14
1.41	0.13	1.84	0.39	0.11
1.41	0.27	1.50	0.22	0.18
1.41	0.20	1.54	0.26	0.14
1.41	0.16	1.56	0.29	0.12
1.41	0.33	1.14	0.15	0.18
1.41	0.25	1.18	0.18	0.14
1.41	0.21	1.15	0.19	0.13
1.41	0.23	0.95	0.15	0.11
1.41	0.18	0.90	0.16	0.10
1.41	0.15	2.24	0.43	0.18
1.41	0.12	2.22	0.49	0.14

Appendix B: Van der Meer and Stam Data

The following data (Tables B1–B9) are from laboratory experiment discussed in van der Meer (1988) and van der Meer and Stam (1991, 1992) for irregular wave run-up on smooth, impermeable plane slopes and rubble mound structures with slope angles ranging from 1:1.5 to 1:4. In general, the test conditions were limited to Pierson – Moskowitz spectrum, armor nominal diameter of D_{n50} = 0.11 ft, and stone specific gravity of S = 2.63, unless otherwise noted.

Table B1. Van der Meer and Stam data, small-scale flume model experiment with stone-armored impermeable slope of 1:2, D_{85}/D_{15} = 2.25.

Toe Water Depth, d_s ft	Incident Wave Height, H_s ft	Peak Wave Period, T_p sec	Iribarren Parameter ξ_{0p}	2% Exceedance Runup, $R_{2\%}$ ft
2.62	0.28	2.08	4.44	0.63
2.62	0.15	2.13	6.18	0.37
2.62	0.25	2.13	4.79	0.52
2.62	0.23	2.13	5.03	0.52
2.62	0.24	2.56	5.91	0.60
2.62	0.27	2.53	5.50	0.64
2.62	0.22	2.60	6.34	0.52
2.62	0.18	2.56	6.78	0.45
2.62	0.26	2.56	5.67	0.64
2.62	0.25	3.13	7.14	0.70
2.62	0.22	3.13	7.62	0.54
2.62	0.18	3.13	8.32	0.45
2.62	0.28	3.17	6.83	0.80
2.62	0.31	3.17	6.49	0.82
2.62	0.29	3.85	8.15	0.84
2.62	0.25	3.64	8.27	0.69
2.62	0.31	3.70	7.53	0.83
2.62	0.27	3.70	8.08	0.76

Table B2. Van der Meer and Stam data, small-scale flume model experiment with stone-armored impermeable slope of 1:3, D_{85}/D_{15} = 2.25.

Toe Water Depth, d_s ft	Incident Wave Height, H_s ft	Peak Wave Period, T_p sec	Iribarren Parameter ξ_{0p}	2% Exceedance Runup, $R_{2\%}$ ft
2.62	0.39	2.53	3.07	0.75
2.62	0.33	2.56	3.38	0.59
2.62	0.28	2.53	3.60	0.53
2.62	0.36	2.53	3.20	0.65
2.62	0.23	2.53	3.97	0.41
2.62	0.38	3.17	3.86	0.79
2.62	0.33	3.08	4.06	0.68
2.62	0.28	3.08	4.42	0.61
2.62	0.30	3.13	4.30	0.67
2.62	0.35	3.08	3.94	0.73
2.62	0.38	3.57	4.37	0.89
2.62	0.34	3.51	4.51	0.83
2.62	0.31	3.57	4.82	0.73
2.62	0.27	3.57	5.16	0.62

Table B3. Van der Meer and Stam data, small-scale flume model experiment with stone-armored impermeable slope of 1:3, D_{85}/D_{15} = 1.25.

Toe Water Depth, d_s ft	Incident Wave Height, H_s ft	Peak Wave Period, T_p sec	Iribarren Parameter ξ_{0p}	2% Exceedance Runup, $R_{2\%}$ ft
2.62	0.36	2.53	3.18	0.65
2.62	0.33	2.50	3.29	0.62
2.62	0.28	2.50	3.55	0.52
2.62	0.24	2.50	3.82	0.44
2.62	0.39	2.47	2.98	0.77
2.62	0.42	2.50	2.90	0.00
2.62	0.40	2.04	2.43	0.69
2.62	0.33	2.04	2.68	0.58
2.62	0.26	2.02	2.98	0.45
2.62	0.45	2.02	2.27	0.77
2.62	0.37	2.01	2.50	0.63
2.62	0.32	1.37	1.82	0.42
2.62	0.44	1.38	1.57	0.59
2.62	0.51	1.43	1.51	0.70
2.62	0.55	1.46	1.48	0.76
2.62	0.39	1.41	1.70	0.56
2.62	0.38	3.57	4.39	0.87
2.62	0.34	3.45	4.44	0.82
2.62	0.32	3.51	4.68	0.76
2.62	0.26	3.45	5.08	0.65
2.62	0.37	3.45	4.29	0.88
2.62	0.41	2.11	2.48	0.74
2.62	0.23	2.08	3.30	0.41
2.62	0.28	2.13	3.01	0.52
2.62	0.38	2.17	2.65	0.69
2.62	0.44	2.11	2.41	0.78

Table B4. Van der Meer and Stam data, small-scale flume model experiment with stone-armored impermeable slope of 1:4, D_{85}/D_{15} = 2.25.

Toe Water Depth, d_s ft	Incident Wave Height, H_s ft	Peak Wave Period, T_p sec	Iribarren Parameter ξ_{0p}	2% Exceedance Runup, $R_{2\%}$ ft
2.62	0.62	2.44	1.76	0.94
2.62	0.54	2.50	1.92	0.80
2.62	0.45	2.56	2.16	0.67
2.62	0.38	2.50	2.29	0.57
2.62	0.29	2.44	2.55	0.44
2.62	0.44	3.13	2.67	0.75
2.62	0.39	3.10	2.81	0.70
2.62	0.29	3.13	3.31	0.48
2.62	0.24	3.17	3.69	0.45
2.62	0.34	3.17	3.10	0.62
2.62	0.37	3.64	3.38	0.72
2.62	0.28	3.64	3.86	0.61
2.62	0.25	3.64	4.12	0.51
2.62	0.33	3.64	3.60	0.63
2.62	0.40	3.64	3.24	0.78
2.62	0.61	1.83	1.33	0.67
2.62	0.64	1.82	1.29	0.69
2.62	0.51	1.49	1.18	0.54
2.62	0.54	1.50	1.16	0.51
2.62	0.57	1.48	1.11	0.53
2.62	0.63	1.52	1.09	0.59

Table B5. Van der Meer and Stam data, small-scale flume model experiment with stone-armored impermeable slope of 1:4, D_{85}/D_{15} = 1.25.

Toe Water Depth, d_s ft	Incident Wave Height, H_s ft	Peak Wave Period, T_p sec	Iribarren Parameter ξ_{0p}	2% Exceedance Runup, $R_{2\%}$ ft
2.62	0.38	2.44	2.24	0.61
2.62	0.44	2.53	2.16	0.66
2.62	0.33	2.50	2.48	0.54
2.62	0.23	2.53	3.00	0.36
2.62	0.52	2.53	1.99	0.76
2.62	0.39	3.51	3.18	0.76
2.62	0.27	3.51	3.81	0.55
2.62	0.36	3.51	3.33	0.67
2.62	0.32	3.51	3.53	0.65
2.62	0.45	3.51	2.96	0.84
2.62	0.40	1.42	1.27	0.41
2.62	0.56	1.49	1.12	0.57
2.62	0.65	1.49	1.05	0.62
2.62	0.49	1.42	1.15	0.53
2.62	0.44	1.42	1.21	0.45
2.62	0.50	1.96	1.57	0.74
2.62	0.38	1.92	1.75	0.59
2.62	0.29	1.96	2.06	0.44
2.62	0.44	1.94	1.65	0.68
2.62	0.59	1.96	1.44	0.84
2.62	0.51	2.00	1.59	0.75
2.62	0.50	1.96	1.57	0.64
2.62	0.50	1.96	1.56	0.68

Table B6. Van der Meer and Stam data, small-scale flume model experiment with stone-armored permeable slope of 1:3, D_{85}/D_{15} = 1.25.

Toe Water Depth, d_s ft	Incident Wave Height, H_s ft	Peak Wave Period, T_p sec	Iribarren Parameter ξ_{0p}	2% Exceedance Runup, $R_{2\%}$ ft
2.62	0.40	2.53	3.03	0.52
2.62	0.47	2.53	2.78	0.86
2.62	0.59	2.53	2.49	0.80
2.62	0.42	3.51	4.08	0.75
2.62	0.54	3.51	3.62	0.58
2.62	0.48	3.51	3.82	1.02
2.62	0.37	3.51	4.35	0.71
2.62	0.50	1.46	1.56	0.57
2.62	0.56	1.45	1.47	0.57
2.62	0.42	1.44	1.68	0.37
2.62	0.48	2.06	2.24	0.81
2.62	0.58	2.04	2.02	0.87
2.62	0.53	2.04	2.11	0.90
2.62	0.43	2.06	2.38	0.64

Table B7. Van der Meer and Stam data, small-scale flume model experiment with stone-armored permeable slope of 1:2, D_{85}/D_{15} = 1.25.

Toe Water Depth, d_s ft	Incident Wave Height, H_s ft	Peak Wave Period, T_p sec	Iribarren Parameter ξ_{0p}	2% Exceedance Runup, $R_{2\%}$ ft
2.62	0.29	1.95	4.07	0.56
2.62	0.34	1.94	3.78	0.63
2.62	0.38	1.94	3.57	0.72
2.62	0.45	1.95	3.28	0.89
2.62	0.43	1.95	3.37	0.82
2.62	0.37	2.52	4.69	0.81
2.62	0.30	2.50	5.19	0.63
2.62	0.41	2.53	4.47	0.88
2.62	0.34	2.52	4.89	0.71
2.62	0.44	2.45	4.20	0.95
2.62	0.34	3.48	6.79	0.77
2.62	0.38	3.51	6.42	0.94
2.62	0.43	3.51	6.03	0.97
2.62	0.49	3.48	5.65	1.14
2.62	0.37	1.39	2.57	0.65
2.62	0.45	1.40	2.37	0.74
2.62	0.52	1.46	2.29	0.83
2.62	0.30	1.42	2.94	0.41
2.62	0.41	1.41	2.51	0.68

Table B8. Van der Meer and Stam data, small-scale flume model experiment with stone-armored permeable slope of 1:1.5, D_{85}/D_{15} = 1.25.

Toe Water Depth, d_s ft	Incident Wave Height, H_s ft	Peak Wave Period, T_p sec	Iribarren Parameter ξ_{0p}	2% Exceedance Runup, $R_{2\%}$ ft
2.62	0.37	2.56	6.34	0.63
2.62	0.28	2.53	7.18	0.46
2.62	0.32	2.50	6.71	0.58
2.62	0.34	2.56	6.59	0.57
2.62	0.40	2.53	6.06	0.69
2.62	0.38	1.98	4.86	0.83
2.62	0.28	1.96	5.62	0.54
2.62	0.33	1.96	5.13	0.70
2.62	0.41	1.96	4.64	0.79
2.62	0.43	2.56	5.88	0.75
2.62	0.36	1.43	3.62	0.70
2.62	0.30	1.43	3.96	0.53
2.62	0.40	1.42	3.37	0.72
2.62	0.45	1.43	3.20	0.74
2.62	0.33	1.43	3.76	0.52
2.62	0.30	1.98	5.43	0.59
2.62	0.34	3.45	8.87	0.69
2.62	0.40	3.51	8.37	0.75
2.62	0.46	3.51	7.85	0.85
2.62	0.49	3.51	7.53	1.01
2.62	0.43	3.51	8.10	0.89

Table B9. Van der Meer and Stam data, small-scale flume model experiment with stone homogeneous slope of 1:2, D_{85}/D_{15} = 1.25.

Toe Water Depth, d_s ft	Incident Wave Height, H_s ft	Peak Wave Period, T_p sec	Iribarren Parameter ξ_{0p}	2% Exceedance Runup, $R_{2\%}$ ft
2.62	0.34	2.60	5.02	0.63
2.62	0.45	2.60	4.37	0.90
2.62	0.56	2.63	3.97	1.15
2.62	0.50	2.60	4.15	1.12
2.62	0.44	2.00	3.41	0.97
2.62	0.52	2.00	3.14	1.02
2.62	0.35	2.00	3.85	0.69
2.62	0.47	1.40	2.32	0.82
2.62	0.56	1.47	2.23	0.96
2.62	0.33	1.45	2.85	0.60
2.62	0.62	1.47	2.12	1.03
2.62	0.45	3.64	6.11	0.99
2.62	0.36	3.57	6.69	0.78

Appendix C: van Gent Data

The following data are from the laboratory and prototype experiments by van Gent (1999a 1999b) for irregular wave run-up on smooth, impermeable levees. Two experiments were conducted. Series P was a scale series with small-scale physical model and full scale studies of the Petten levee. The levee has a lower slope of 1:4.5, a berm of about 1:20 from +16.4 ft to +18.7 ft and a 1:3 upper slope (Figures C1–C3). The nearshore bathymetry and gage locations are shown in Figure C3. Both prototype and physical model data were obtained. The model scale was 1:40.

The second experiment was a small-scale laboratory study. The foreshore and structure slopes were as follows: Series A – 1:100, 1:4; Series B – 1:100, 1:2.5; and Series C – 1:250, 1:2.5 (e.g., Figure C3).

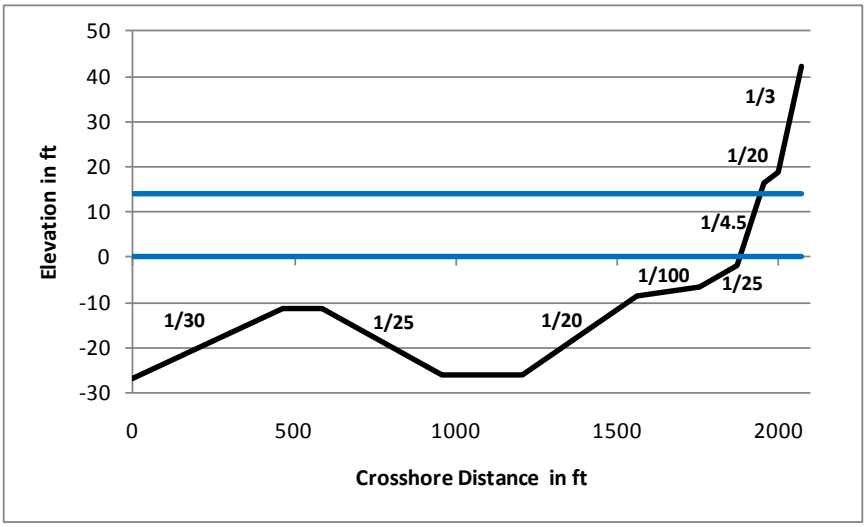

Figure C1. Van Gent Series P (Petten Full Scale) bottom profile and still water level range above datum shown as horizontal lines at elevation 0 and 14 ft for 40 tests.

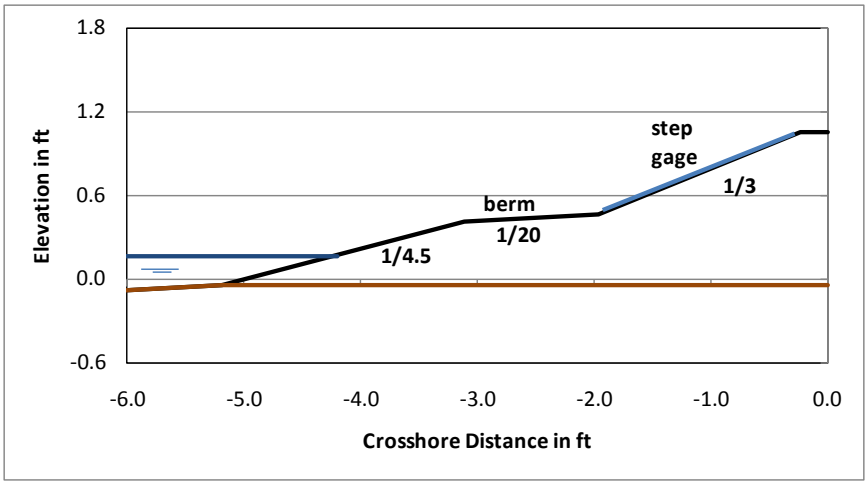

Figure C2. Physical model structure schematic for Series P from van Gent (1999a).

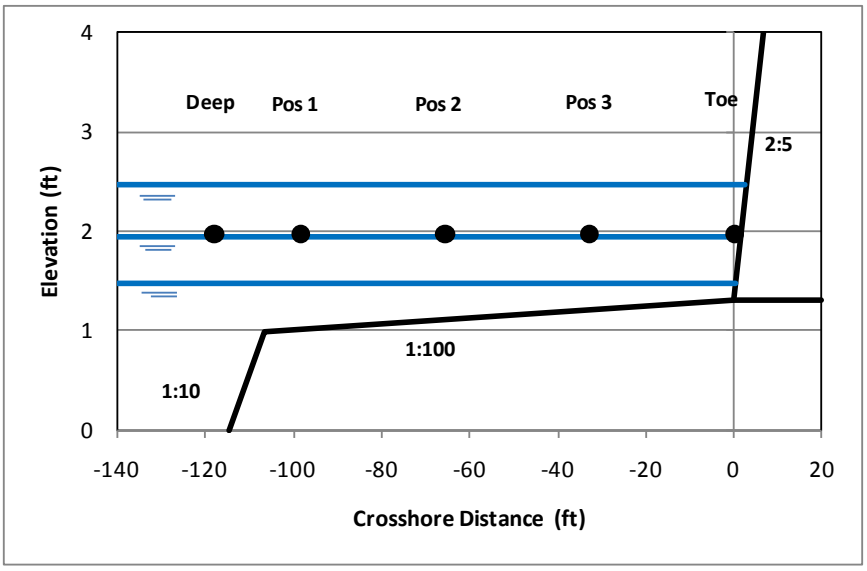

Figure C3. Bottom profile and still water level range above datum shown as horizontal lines at elevation 1.5, 1.9, and 2.5 ft for Series B. Also shown are wave gage locations as large dots. Series A and C are similar: Series A: structure slope of 1:4, Series C: structure slope of 2:5, foreshore slope of 1:250.

Table C1. Measured wave conditions at MP3 location for Series P (Petten Sea).

Series P Test	SWL, ft	Water Depth ft	H_{m0}, ft	$T_{m-1,0}$, sec	T_p, sec
1	6.89	8.92	13.45	9.4	10.8
2	6.69	8.73	13.45	9.5	10.8
3	7.35	9.38	12.14	10.7	14.4
4	5.45	7.48	13.78	11.5	16.2
5	5.25	7.28	9.84	10.3	13.0
6	6.69	8.73	12.14	9.5	9.3
7	6.89	8.92	6.23	7.8	8.6
8	6.89	8.92	9.84	9.7	10.8
9	6.89	8.92	13.45	10.8	11.8
10	6.89	8.92	16.40	11.9	13.0
11	6.89	8.92	18.04	12.5	14.4
12	15.42	17.45	5.91	7.8	8.6
13	15.42	17.45	9.84	9.7	10.8
14	15.42	17.45	13.45	11.0	11.8
15	15.42	17.45	16.73	12.1	13.0
16	15.42	17.45	19.36	12.6	14.4
17	6.89	8.92	11.15	7.1	7.2
18	6.89	8.92	12.47	8.5	8.6
19	6.89	8.92	13.45	10.8	11.8
20	6.89	8.92	13.78	14.4	18.5
21	15.42	17.45	11.15	6.9	7.2
22	15.42	17.45	12.80	8.4	9.3
23	15.42	17.45	13.45	11.0	11.8
24	15.42	17.45	13.78	15.3	18.5
25	15.42	17.45	17.06	8.8	9.3
26	15.42	17.45	19.03	11.0	11.8
27	15.42	17.45	19.36	12.6	14.4
28	15.42	17.45	19.69	14.6	18.5
29	4.27	6.30	12.80	10.7	11.8
30	6.89	8.92	13.45	10.8	11.8
31	9.51	11.55	13.45	10.9	11.8
32	12.47	14.50	13.45	11.0	11.8
33	15.42	17.45	13.45	11.0	11.8
34	18.37	20.41	13.12	11.1	11.8
35	6.89	8.92	12.14	9.4	11.8
36	6.89	8.92	12.47	9.6	10.8
37	6.89	8.92	13.12	10.0	10.8
38	15.42	17.45	12.47	9.3	11.8
39	15.42	17.45	12.80	9.7	11.8
40	15.42	17.45	13.12	10.1	10.8

Table C2. Measured wave heights for Series P.

Gage	MP3	BAR	MP5	MP6	TOE
X (ft)	0	525	1099	1657	1870
Test	Measured H_{m0} (ft) at given X				
1	13.45	10.17	8.86	8.20	5.25
2	13.45	10.50	8.86	8.20	5.25
3	12.14	10.17	8.86	8.20	5.58
4	13.78	9.84	8.20	7.55	4.59
5	9.84	8.86	7.55	7.22	4.27
6	12.14	9.84	8.53	7.87	5.25
7	6.23	6.23	5.91	5.91	4.59
8	9.84	9.19	8.20	7.87	4.92
9	13.45	10.50	9.19	8.53	5.25
10	16.40	10.83	9.19	8.86	5.58
11	18.04	11.15	9.51	8.86	5.58
12	5.91	5.91	5.58	5.91	5.91
13	9.84	10.17	9.51	9.84	7.87
14	13.45	12.80	11.81	12.14	9.19
15	16.73	14.44	13.12	13.12	10.17
16	19.36	15.42	13.45	13.45	10.17
17	11.15	8.53	8.20	7.22	4.92
18	12.47	9.84	8.53	7.87	4.92
19	13.45	10.50	9.19	8.53	5.25
20	13.78	9.84	8.86	8.53	5.25
21	11.15	10.17	9.84	9.51	8.53
22	12.80	11.81	11.15	10.83	8.86
23	13.45	12.80	11.81	12.14	9.19
24	13.78	12.80	11.48	12.14	9.19
25	17.06	14.11	12.80	12.47	9.84
26	19.03	15.09	13.45	13.12	10.17
27	19.36	15.42	13.45	13.45	10.17
28	19.69	15.42	13.45	13.45	10.50
29	12.80	9.19	7.55	6.89	3.94
30	13.45	10.50	9.19	8.53	5.25
31	13.45	11.48	10.17	9.84	6.89
32	13.45	12.14	11.15	11.15	8.20
33	13.45	12.80	11.81	12.14	9.19
34	13.12	13.12	12.14	12.47	9.84
35	12.14	9.84	8.53	8.20	5.25
36	12.47	10.17	8.86	7.87	5.25
37	13.12	10.17	8.86	8.20	5.25
38	12.47	12.14	11.15	11.15	9.19
39	12.80	12.14	11.48	11.15	9.19
40	13.12	12.47	11.81	11.81	9.19

Table C3. Measured 2 percent and 1 percent run-up heights ($R_{2\%}$, $R_{1\%}$) above SWL for Series P.

Series P Test	$R_{2\%}$, ft	$R_{1\%}$, ft
1	15.42	16.73
2	15.75	17.72
3	17.39	18.37
4	17.39	19.03
5	13.45	14.76
6	15.42	16.08
7	11.81	11.81
8	14.11	14.76
9	16.40	17.72
10	18.04	20.01
11	20.67	22.97
12	10.83	11.48
13	17.39	19.03
14	21.65	23.62
15	25.92	26.90
16	26.90	26.90
17	11.81	12.14
18	14.44	15.42
19	16.40	17.72
20	17.72	19.69
21	14.44	15.09
22	17.39	18.37
23	21.65	23.62
24	26.90	26.90
25	20.01	21.00
26	24.93	26.25
27	26.90	26.90
28	26.90	26.90
29	14.44	14.76
30	16.40	17.72
31	18.70	20.01
32	20.34	22.31
33	21.65	23.62
34	23.95	23.95
35	16.40	18.04
36	16.73	18.04
37	16.73	18.37
38	21.00	22.31
39	22.64	24.28
40	21.65	23.62

Table C4. Measured wave conditions at POS1 location for Series A.

Series A Test	SWL, ft	Water Depth, ft	H_{m0}, ft	$T_{m-1,0}$, sec	T_p, sec
1	2.47	1.16	0.49	2.27	2.48
2	2.47	1.16	0.49	1.82	2.00
3	2.47	1.16	0.49	1.55	1.64
4	1.93	0.62	0.47	2.29	2.48
5	1.93	0.62	0.48	1.87	2.00
6	1.93	0.62	0.47	1.54	1.64
7	1.62	0.31	0.46	2.23	2.41
8	1.62	0.31	0.47	1.88	2.00
9	1.62	0.31	0.46	1.60	1.64
10	1.47	0.15	0.44	2.21	2.41
11	1.47	0.15	0.46	1.90	2.00
12	1.47	0.15	0.44	1.64	1.64
13	2.47	1.16	0.48	2.06	2.10
14	2.47	1.16	0.49	1.88	2.48
15	2.47	1.16	0.47	1.75	2.48
16	2.47	1.16	0.49	1.66	2.05
17	2.47	1.16	0.48	1.55	2.05
18	2.47	1.16	0.47	1.37	1.57
19	1.93	0.62	0.46	2.14	2.48
20	1.93	0.62	0.47	2.07	2.10
21	1.93	0.62	0.47	2.00	2.05
22	1.93	0.62	0.47	2.04	2.48
23	1.93	0.62	0.47	1.93	2.48
24	1.93	0.62	0.47	1.81	1.57
25	1.93	0.62	0.46	1.94	2.48
26	1.93	0.62	0.46	1.80	2.48
27	1.93	0.62	0.45	1.65	1.28
28	1.93	0.62	0.47	1.77	2.05
29	1.93	0.62	0.47	1.72	2.05
30	1.93	0.62	0.47	1.66	1.57
31	1.93	0.62	0.47	1.68	2.05
32	1.93	0.62	0.46	1.60	2.05
33	1.93	0.62	0.45	1.51	1.28
34	1.93	0.62	0.45	1.46	1.57
35	1.93	0.62	0.45	1.42	1.57
36	1.93	0.62	0.44	1.37	1.28
37	1.62	0.31	0.46	2.05	2.48
38	1.62	0.31	0.46	1.95	2.48
39	1.62	0.31	0.44	1.83	2.48
40	1.62	0.31	0.46	1.75	2.05
41	1.62	0.31	0.44	1.65	2.05
42	1.62	0.31	0.43	1.48	1.57

Table C5. Measured wave height for Series A.

Gage	POS1	POS2	POS3	TOE
X (ft)	-98.4	-65.6	-32.8	0
Test	Measured H_{m0} (ft) at given X			
1	0.49	0.48	0.48	0.48
2	0.49	0.48	0.47	0.48
3	0.49	0.47	0.45	0.44
4	0.47	0.47	0.45	0.34
5	0.48	0.47	0.44	0.34
6	0.47	0.45	0.42	0.34
7	0.46	0.44	0.35	0.18
8	0.47	0.44	0.35	0.19
9	0.46	0.43	0.35	0.19
10	0.44	0.40	0.28	0.12
11	0.46	0.41	0.28	0.12
12	0.44	0.40	0.28	0.12
13	0.48	0.48	0.47	0.48
14	0.49	0.48	0.47	0.46
15	0.47	0.47	0.45	0.43
16	0.49	0.48	0.46	0.46
17	0.48	0.46	0.44	0.43
18	0.47	0.45	0.43	0.41
19	0.46	0.46	0.44	0.34
20	0.47	0.46	0.44	0.34
21	0.47	0.46	0.44	0.34
22	0.47	0.46	0.44	0.34
23	0.47	0.46	0.44	0.34
24	0.47	0.46	0.44	0.34
25	0.46	0.45	0.42	0.33
26	0.46	0.44	0.41	0.33
27	0.45	0.43	0.40	0.33
28	0.47	0.46	0.44	0.34
29	0.47	0.46	0.43	0.34
30	0.47	0.45	0.43	0.34
31	0.47	0.45	0.42	0.33
32	0.46	0.44	0.41	0.33
33	0.45	0.43	0.40	0.33
34	0.45	0.43	0.41	0.33
35	0.45	0.43	0.40	0.33
36	0.44	0.42	0.39	0.33
37	0.46	0.44	0.36	0.18
38	0.46	0.44	0.35	0.19
39	0.44	0.41	0.34	0.18
40	0.46	0.43	0.36	0.19
41	0.44	0.42	0.34	0.18
42	0.43	0.41	0.34	0.19

Table C6. Measured 2 percent and 1 percent exceedance runups ($R_{2\%}$, $R_{1\%}$) and crest elevation, R_c, for Series A.

Series A Test	$R_{2\%}$, ft	$R_{1\%}$, ft	R_c, ft
1	1.35	1.44	1.31
2	1.08	1.15	1.31
3	0.85	0.89	1.31
4	1.02	1.08	1.02
5	0.92	0.98	1.02
6	0.79	0.85	1.02
7	0.62	0.66	0.52
8	0.59	0.59	0.52
9	0.52	0.56	0.52
10	0.46	0.49	0.66
11	0.46	0.46	0.66
12	0.39	0.43	0.66
13	1.25	1.31	1.31
14	1.18	1.25	1.31
15	1.08	1.15	1.31
16	0.95	1.05	1.31
17	0.92	0.98	1.31
18	0.72	0.79	1.31
19	0.98	1.05	1.02
20	0.95	0.98	1.02
21	0.95	0.98	1.02
22	0.95	1.02	1.02
23	0.92	0.98	1.02
24	0.89	0.92	1.02
25	0.92	0.98	1.02
26	0.89	0.92	1.02
27	0.85	0.89	1.02
28	0.92	0.98	1.02
29	0.89	0.92	1.02
30	0.85	0.92	1.02
31	0.89	0.92	1.02
32	0.89	0.92	1.02
33	0.82	0.85	1.02
34	0.75	0.82	1.02
35	0.72	0.79	1.02
36	0.72	0.75	1.02
37	0.62	0.62	0.52
38	0.56	0.62	0.52
39	0.52	0.56	0.52
40	0.56	0.59	0.52
41	0.52	0.56	0.52
42	0.46	0.49	0.52

Table C7. Measured wave conditions at POS1 location for Series B.

Series B Test	SWL, ft	Water Depth, ft	H_{m0}, ft	$T_{m-1,0}$, sec	T_p, sec
1	2.47	1.16	0.49	2.30	2.48
2	2.47	1.16	0.49	1.85	2.00
3	1.93	0.62	0.47	1.49	1.64
4	1.93	0.62	0.48	2.28	2.41
5	1.93	0.62	0.47	1.87	2.00
6	1.62	0.31	0.46	1.54	1.64
7	1.62	0.31	0.47	2.23	2.48
8	1.62	0.31	0.46	1.88	2.00
9	1.47	0.15	0.44	1.60	1.64
10	1.47	0.15	0.46	2.21	2.41
11	1.47	0.15	0.44	1.89	2.00
12	2.47	1.16	0.49	1.64	1.64
13	2.47	1.16	0.49	2.05	2.05
14	2.47	1.16	0.49	2.01	2.48
15	2.47	1.16	0.49	1.90	2.56
16	2.47	1.16	0.48	1.76	1.54
17	2.47	1.16	0.48	1.92	2.48
18	2.47	1.16	0.47	1.76	2.56
19	2.47	1.16	0.47	1.61	1.28
20	2.47	1.16	0.45	1.89	2.48
21	2.47	1.16	0.44	1.73	2.48
22	2.47	1.16	0.49	1.56	2.48
23	2.47	1.16	0.48	1.67	2.05
24	2.47	1.16	0.48	1.55	2.05
25	1.62	0.31	0.46	1.38	1.57
26	1.62	0.31	0.46	2.05	2.10
27	1.62	0.31	0.44	1.95	2.48
28	1.62	0.31	0.46	1.84	2.48
29	1.62	0.31	0.44	1.74	2.04
30	1.62	0.31	0.43	1.64	2.05
31	2.47	1.16	0.49	1.48	1.54

Table C8. Measured wave height for Series B.

Gage	POS1	POS2	POS3	TOE
X (ft)	-98.4	-65.6	-32.8	0
Test	Measured H_{m0} (ft) at given X			
1	0.49	0.48	0.47	0.48
2	0.49	0.47	0.45	0.44
3	0.47	0.46	0.44	0.34
4	0.48	0.46	0.44	0.34
5	0.47	0.45	0.42	0.34
6	0.46	0.44	0.35	0.18
7	0.47	0.44	0.36	0.19
8	0.46	0.43	0.35	0.19
9	0.44	0.40	0.28	0.12
10	0.46	0.41	0.28	0.12
11	0.44	0.40	0.29	0.12
12	0.49	0.48	0.48	0.48
13	0.49	0.48	0.48	0.46
14	0.49	0.49	0.48	0.46
15	0.49	0.48	0.47	0.46
16	0.48	0.47	0.46	0.43
17	0.48	0.46	0.45	0.43
18	0.47	0.46	0.44	0.43
19	0.47	0.46	0.44	0.41
20	0.45	0.44	0.42	0.41
21	0.44	0.41	0.39	0.41
22	0.49	0.48	0.46	0.46
23	0.48	0.46	0.44	0.43
24	0.48	0.46	0.43	0.41
25	0.46	0.44	0.36	0.18
26	0.46	0.44	0.36	0.19
27	0.44	0.41	0.34	0.18
28	0.46	0.43	0.36	0.19
29	0.44	0.42	0.35	0.18
30	0.43	0.40	0.34	0.19
31	0.49	0.48	0.47	0.48

Table C9. Measured 2 percent and 1 percent exceedance runups ($R_{2\%}$, $R_{1\%}$) and crest elevation, R_c, for Series B.

Series B Test	$R_{2\%}$, ft	$R_{1\%}$, ft	R_c, ft
1	0.49	0.52	0.40
2	0.44	0.48	0.40
3	0.39	0.42	0.40
4	0.39	0.41	0.31
5	0.36	0.38	0.31
6	0.30	0.32	0.31
7	0.21	0.22	0.16
8	0.20	0.21	0.16
9	0.18	0.20	0.16
10	0.15	0.17	0.20
11	0.15	0.17	0.20
12	0.14	0.15	0.20
13	0.45	0.49	0.40
14	0.45	0.49	0.40
15	0.43	0.45	0.40
16	0.41	0.43	0.40
17	0.43	0.47	0.40
18	0.40	0.44	0.40
19	0.38	0.40	0.40
20	0.42	0.46	0.40
21	0.38	0.43	0.40
22	0.36	0.39	0.40
23	0.41	0.45	0.40
24	0.38	0.41	0.40
25	0.35	0.38	0.40
26	0.20	0.22	0.16
27	0.20	0.21	0.16
28	0.18	0.20	0.16
29	0.19	0.20	0.16
30	0.19	0.21	0.16
31	0.17	0.18	0.16

Table C10. Measured wave conditions at POS1 location for Series C.

Series C Test	SWL, ft	Water Depth, ft	H_{m0}, ft	$T_{m-1,0}$, sec	T_p, sec
1	2.47	1.16	0.51	2.27	2.48
2	2.47	1.16	0.49	1.84	2.00
3	2.47	1.16	0.46	1.53	1.64
4	1.93	0.62	0.47	2.18	2.41
5	1.93	0.62	0.44	1.84	2.00
6	1.93	0.62	0.41	1.62	1.64
7	1.62	0.31	0.36	2.28	2.56
8	1.62	0.31	0.33	1.98	2.05
9	1.62	0.31	0.32	1.78	1.64
10	1.47	0.15	0.31	2.68	2.56
11	1.47	0.15	0.28	2.38	2.10
12	1.47	0.15	0.26	2.05	1.44
13	2.47	1.16	0.50	2.06	2.48
14	2.47	1.16	0.49	1.93	2.48
15	2.47	1.16	0.48	1.82	2.48
16	2.47	1.16	0.47	1.70	2.05
17	2.47	1.16	0.47	1.59	2.05
18	2.47	1.16	0.45	1.40	1.28
19	1.62	0.31	0.35	2.14	2.48
20	1.62	0.31	0.36	2.09	2.48
21	1.62	0.31	0.35	1.96	2.48
22	1.62	0.31	0.33	1.89	2.05
23	1.62	0.31	0.33	1.77	2.05
24	1.62	0.31	0.32	1.64	1.26

Table C11. Measured wave height for Series C.

Gage	POS1	POS2	POS3	TOE
X (ft)	-98.4	-65.6	-32.8	0
Test	Measured H_{m0} (ft) at given X			
1	0.154	0.150	0.146	0.144
2	0.150	0.147	0.143	0.140
3	0.141	0.137	0.134	0.132
4	0.143	0.123	0.115	0.095
5	0.135	0.122	0.116	0.098
6	0.126	0.119	0.114	0.099
7	0.110	0.078	0.069	0.045
8	0.102	0.082	0.071	0.047
9	0.099	0.084	0.075	0.050
10	0.093	0.057	0.045	0.023
11	0.084	0.059	0.047	0.023
12	0.079	0.060	0.049	0.024
13	0.151	0.147	0.144	0.141
14	0.149	0.145	0.142	0.138
15	0.147	0.140	0.135	0.129
16	0.144	0.140	0.138	0.135
17	0.143	0.136	0.132	0.126
18	0.138	0.131	0.127	0.122
19	0.107	0.080	0.069	0.046
20	0.109	0.082	0.070	0.046
21	0.107	0.081	0.069	0.046
22	0.102	0.083	0.073	0.048
23	0.102	0.082	0.071	0.048
24	0.099	0.084	0.075	0.049

Table C12. Measured 2 percent and 1 percent exceedance runups ($R_{2\%}$, $R_{1\%}$) and crest elevation, R_c, for Series C.

Series C Test	Water Depth ft	$R_{2\%}$, ft	$R_{1\%}$, ft	R_c, ft
1	0.753	0.48	0.53	0.40
2	0.753	0.40	0.42	0.40
3	0.753	0.37	0.39	0.40
4	0.588	0.35	0.36	0.31
5	0.588	0.33	0.34	0.31
6	0.588	0.28	0.29	0.31
7	0.494	0.18	0.20	0.16
8	0.494	0.18	0.19	0.16
9	0.494	0.17	0.18	0.16
10	0.447	0.10	0.12	0.20
11	0.447	0.10	0.10	0.20
12	0.447	0.10	0.10	0.20
13	0.753	0.43	0.47	0.40
14	0.753	0.41	0.44	0.40
15	0.753	0.39	0.43	0.40
16	0.753	0.38	0.40	0.40
17	0.753	0.38	0.40	0.40
18	0.753	0.34	0.37	0.40
19	0.494	0.18	0.20	0.16
20	0.494	0.16	0.17	0.16
21	0.494	0.16	0.17	0.16
22	0.494	0.16	0.17	0.16
23	0.494	0.15	0.16	0.16
24	0.494	0.15	0.16	0.16

Appendix D: Stockdon Data

The following data are from prototype experiments by Stockdon et al. (2006). The data consist of wave runup measurements with associated incident wave and water level climate for natural beaches. The study sites include Duck, NC; Scipps, CA; San Onofre, CA; Gleneden Beach, OR; Agate Beach, OR; and Terschelling, The Netherlends. A total of nine studies are summarized herein (Table D1). In Table D1, N is the number of individual data values, H_{m0}, T_p and ξ_0 are the significant wave height, peak wave period and surf similarity parameter offshore and β_f is the nearshore slope at the mean water level averaged over a region ± one standard deviation of swash, including setup. H_{m0} is the value reverse shoaled to deep water from a depth of approximately 8 m. Agate Beach and Terschelling have very shallow sloping beaches, considered dissipative. Experiments at Duck, NC, constitute 65 percent of all data values, experiments on the southern California coast 20 percent, and experiments on the central Oregon coast 11 percent. Experiments at Terschelling are included but there is little understanding of, and little confidence in, these data.

Table D1. Summary of prototype experiments.

			Average Conditions			
Site	Dates	N	H_{m0} (ft)	T_p (s)	β_f	$\xi_0 \pm \sigma$
Duck, NC (Duck 1982)	5-25 Oct 1982	36	5.60	11.9	0.12	1.95, 1.02
Duck, NC (Duck 1990)	6-19 Oct 1990	138	4.58	9.2	0.09	1.21, 0.59
Duck, NC (Duck 1994)	3-21 Oct 1994	52	6.19	10.5	0.08	1.15, 0.50
Duck, NC (SandyDuck)	3-30 Oct 1997	95	4.51	9.5	0.09	1.70, 0.53
San Onofre, CA	16-20 Oct 1993	59	2.64	14.9	0.10	2.44, 1.90
Scripps Beach, CA	26-29 Jun 1989	41	2.26	10.0	0.04	0.68, 0.46
Agate Beach, OR	11-17 Feb 1996	14	8.13	11.9	0.02	0.18, 0.13
Gleneden, OR	26-28 Feb 1994	42	6.77	12.4	0.08	1.08, 0.64
Terschelling, NL	Apr&Oct 1994	14	6.02	8.3	0.02	0.18, 0.09

Tables D2–D10 describe the average bottom profiles used during this study as reported by Stockdon et al. (2006). The profiles are given relative to mean sea level. Tables D11–D19 summarize the measurements. In these tables, H_{m0} and T_p are the deep water values as described above. Time is given in Greenwhich mean time. Water level is the locally measured value from the NOAA COOPS web site relative to mean sea level. For sites

Scripps and San Onofre there was no local measurement of water level so the values were interpolated from the nearest gages. For these sites, the two neighboring gages had water levels that were very close in both phase and amplitude so this was a very good estimate of water levels. The water levels at Agate and Gleneden are not accurate and represent crude guesses because there are no nearby gages. There were no water level measurements for Terschelling.

Table D2. Duck 1982 bottom profile.

Cross-Shore Position (ft)	Elevation (ft)
0.0	-13.1
41.0	-13.1
82.0	-13.1
123.0	-13.1
164.0	-13.0
205.1	-12.6
246.1	-12.3
287.1	-11.5
328.1	-10.7
369.1	-9.0
410.1	-7.4
451.1	-5.7
492.1	-4.1
533.1	-3.4
574.1	-2.8
615.2	-2.5
635.7	-3.3
656.2	0.0
697.2	3.3
738.2	7.4
795.6	13.1

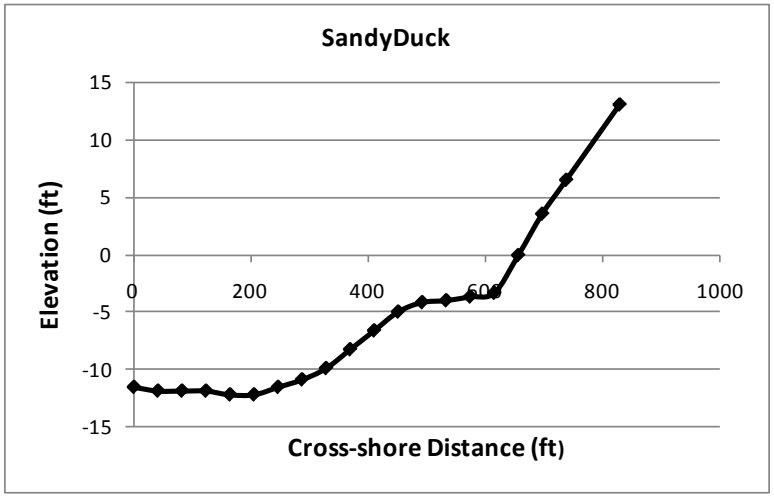

Table D3. Delilah (Duck 1990) bottom profile.

Cross-Shore Position (ft)	Elevation (ft)
0.0	-12.5
41.0	-12.3
82.0	-12.3
123.0	-11.8
164.0	-11.5
205.1	-9.8
246.1	-8.2
287.1	-6.6
328.1	-5.6
369.1	-4.3
410.1	-4.6
451.1	-5.6
492.1	-6.2
533.1	-6.6
574.1	-4.9
615.2	-2.5
656.2	0.0
697.2	3.3
738.2	6.6
820.2	13.1

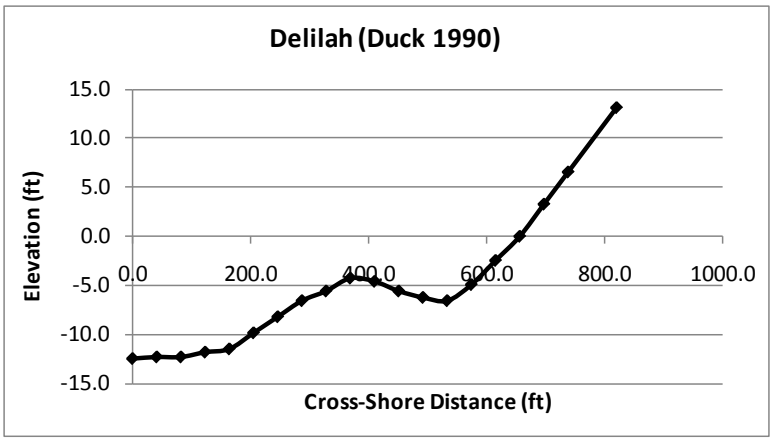

Table D4. Duck 1994 bottom profile.

Cross-Shore Position (ft)	Elevation (ft)
0.0	-12.1
41.0	-11.5
82.0	-10.7
123.0	-9.8
164.0	-9.0
205.1	-8.2
246.1	-7.9
287.1	-7.2
328.1	-7.9
369.1	-8.2
410.1	-7.9
451.1	-6.9
492.1	-6.6
533.1	-5.7
574.1	-4.3
615.2	-2.5
656.2	0.0
697.2	2.5
738.2	4.9
874.9	13.1

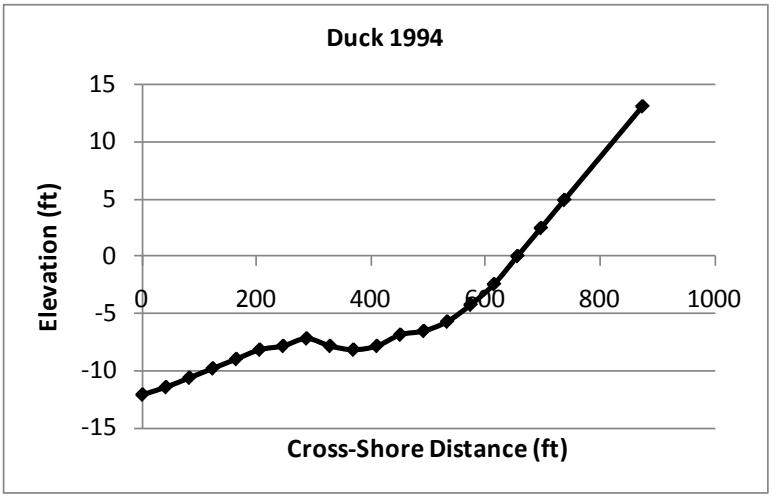

Table D5. SandyDuck bottom profile.

Cross-Shore Position (ft)	Elevation (ft)
0.0	-11.5
41.0	-11.8
82.0	-11.8
123.0	-11.8
164.0	-12.1
205.1	-12.1
246.1	-11.5
287.1	-10.8
328.1	-9.8
369.1	-8.2
410.1	-6.6
451.1	-4.9
492.1	-4.1
533.1	-3.9
574.1	-3.6
615.2	-3.3
656.2	0.0
697.2	3.6
738.2	6.6
829.3	13.1

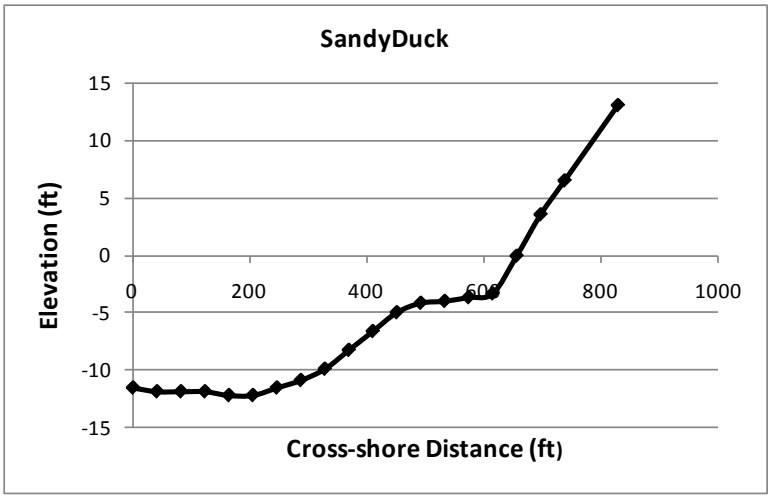

Table D6. Scripps, CA bottom profile.

Cross-Shore Position (ft)	Elevation (ft)
0.0	-4.9
41.0	-4.8
82.0	-4.8
123.0	-4.7
164.0	-4.6
205.1	-4.5
246.1	-4.4
287.1	-4.3
328.1	-4.3
369.1	-4.2
410.1	-4.1
451.1	-3.3
492.1	-2.5
533.1	-1.6
574.1	-0.8
615.2	-0.5
656.2	0.0
697.2	1.6
738.2	3.3
984.3	13.1

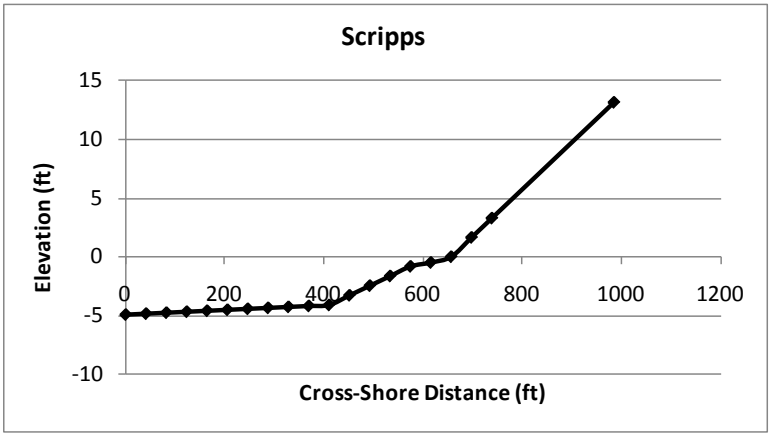

Table D7. San Onofre, CA bottom profile.

Cross-Shore Position (ft)	Elevation (ft)
0.0	-7.2
41.0	-7.1
82.0	-7.1
123.0	-7.0
164.0	-6.9
205.1	-6.8
246.1	-6.7
287.1	-6.6
328.1	-6.6
369.1	-5.7
410.1	-5.2
451.1	-4.9
492.1	-4.3
533.1	-4.3
574.1	-3.9
615.2	-0.8
656.2	0.0
697.2	1.6
738.2	5.7
812.0	13.1

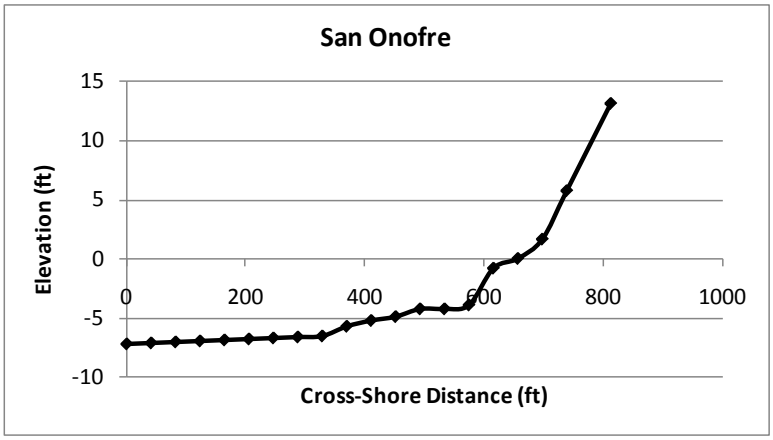

Table D8. Agate Beach, OR bottom profile.

Cross-Shore Position (ft)	Elevation (ft)
0.0	-13.1
41.0	-12.3
82.0	-11.5
123.0	-10.7
164.0	-9.8
205.1	-9.0
246.1	-8.2
287.1	-7.4
328.1	-6.6
369.1	-5.7
410.1	-4.9
451.1	-4.1
492.1	-3.3
533.1	-2.5
574.1	-1.6
615.2	-0.8
656.2	0.0
697.2	0.8
738.2	1.6
1312.3	13.1

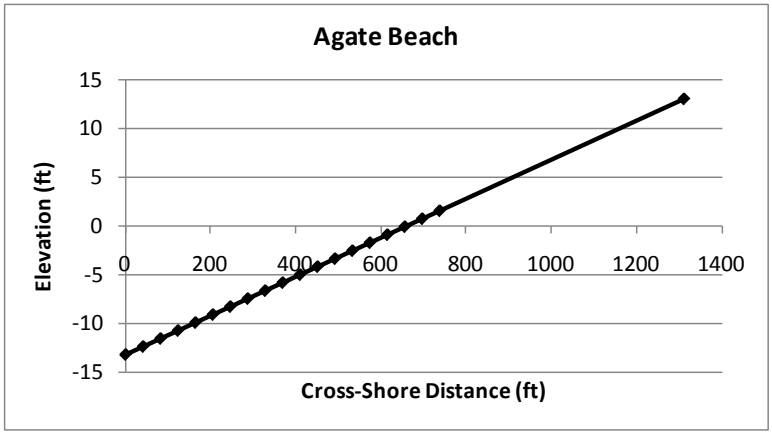

Table D9. Gleneden, OR bottom profile.

Cross-Shore Position (ft)	Elevation (ft)
0.0	-3.5
41.0	-3.5
82.0	-3.4
123.0	-3.3
164.0	-3.2
205.1	-3.1
246.1	-3.0
287.1	-3.0
328.1	-2.9
369.1	-2.8
410.1	-2.7
451.1	-2.6
492.1	-2.5
533.1	-2.5
574.1	-0.8
615.2	-0.5
656.2	0.0
697.2	1.6
738.2	3.3
984.3	13.1

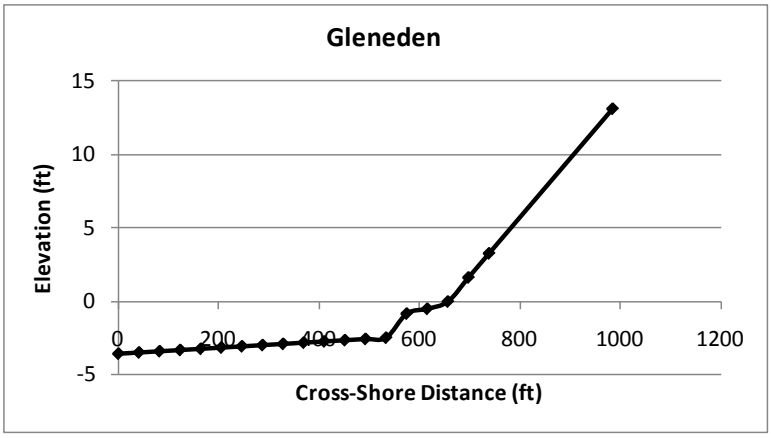

Table D10. Terschelling, NL, bottom profile.

Cross-Shore Position (ft)	Elevation (ft)
0.0	-5.7
41.0	-4.6
82.0	-4.3
123.0	-5.6
164.0	-6.6
205.1	-6.6
246.1	-5.7
287.1	-4.9
328.1	-4.1
369.1	-3.3
410.1	-1.6
451.1	-0.7
492.1	-0.7
533.1	-1.6
574.1	-1.6
615.2	-0.7
656.2	0.0
697.2	1.0
738.2	1.6
1455.9	13.1

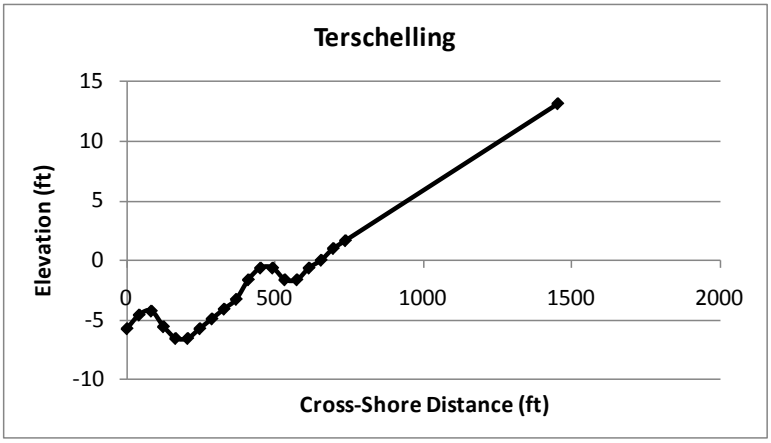

Table D11. Duck 1982 measurements.

Experiment *n*	Wave Runup $R_{2\%}$ (ft)	Deep Water Significant Wave Height, H_{m0} (ft)	Deep Water Peak Wave Period, T_p (s)	Average Slope β (rad)	Date (yymmdd)	Time GMT (hhmm)	Water Level, *h* (ft)
1	3.37	3.22	9.5	0.140	821004	1555	0.61
2	3.68	2.80	11.0	0.160	821005	1632	0.59
3	6.77	2.80	11.0	0.160	821006	1025	-0.44
4	3.69	1.86	9.3	0.140	821008	1308	0.49
5	2.79	1.57	7.4	0.140	821009	1315	-0.30
6	6.55	7.21	7.9	0.160	821010	947	0.85
7	8.62	8.13	12.1	0.120	821010	1355	0.97
8	8.79	8.62	11.6	0.120	821010	1542	2.33
9	8.16	6.68	13.8	0.130	821011	925	1.64
10	9.20	6.21	14.6	0.120	821011	1705	1.76
11	9.19	6.43	14.4	0.120	821011	1756	2.38
12	7.14	5.92	15.3	0.120	821012	846	1.81
13	10.43	7.40	16.2	0.120	821012	1405	-1.07
14	9.92	7.26	15.1	0.120	821012	1531	-0.56
15	10.05	7.44	16.5	0.120	821012	1722	0.80
16	10.53	7.67	16.3	0.120	821012	1815	1.41
17	7.59	5.83	16.0	0.120	821013	915	2.08
18	6.31	5.69	14.6	0.120	821013	1114	1.42
19	7.06	5.16	13.8	0.120	821013	1445	-1.40
20	7.19	8.77	14.8	0.120	821013	1649	-0.67
21	5.19	4.77	14.4	0.120	821014	911	2.26
22	6.07	3.78	12.5	0.110	821014	1703	-0.78
23	4.66	2.52	12.5	0.110	821015	850	1.61
24	3.40	2.35	11.8	0.110	821015	1535	-0.83
25	4.24	2.38	11.1	0.110	821016	847	0.32
26	4.56	4.96	6.3	0.120	821017	929	0.63
27	3.69	2.36	12.3	0.110	821019	1300	1.78
28	4.08	3.52	6.8	0.110	821020	1128	0.19
29	3.90	3.52	6.8	0.110	821020	1303	1.45
30	4.34	3.45	8.7	0.110	821021	1045	-0.92
31	4.29	3.91	8.1	0.110	821021	1350	1.31
32	5.18	5.54	9.5	0.090	821022	1145	0.00
33	4.88	5.54	9.5	0.090	821022	1516	1.86
34	5.96	10.70	8.2	0.120	821024	846	0.63
35	9.58	13.40	13.8	0.120	821025	850	2.30
36	9.69	12.21	13.3	0.120	821025	1220	0.81

Table D12. Duck 1990 measurements.

Experiment *n*	Wave Runup $R_{2\%}$ (ft)	Deep Water Significant Wave Height, H_{m0} (ft)	Deep Water Peak Wave Period, T_p (s)	Average Slope β (rad)	Date (yymmdd)	Time GMT (hhmm)	Water Level, *h* (ft)
1	2.96	1.96	12.2	0.068	901006	1418	1.54
2	2.79	1.71	12.2	0.064	901006	1452	1.20
3	2.51	1.97	12.2	0.061	901006	1526	0.68
4	3.47	2.01	12.2	0.076	901006	1215	1.62
5	3.58	1.94	12.2	0.076	901006	1249	1.77
6	3.77	2.07	12.2	0.076	901006	1323	1.78
7	1.37	1.75	11.6	0.054	901006	1736	-1.69
8	3.42	2.76	9.5	0.054	901008	1314	0.99
9	3.33	2.86	10.3	0.054	901008	1348	1.35
10	2.83	2.92	10.2	0.054	901008	1422	1.53
11	3.18	2.88	11.1	0.055	901008	1523	1.52
12	3.30	2.82	11.1	0.052	901008	1557	1.40
13	3.06	2.71	10.9	0.054	901008	1631	1.06
14	2.80	2.64	11.0	0.046	901008	1831	-0.67
15	1.82	2.86	10.6	0.040	901008	1905	-1.26
16	2.28	2.78	11.0	0.037	901008	1939	-1.67
17	2.18	2.76	10.1	0.035	901008	2033	-2.14
18	2.02	3.06	10.4	0.033	901008	2107	-2.32
19	2.10	3.14	11.1	0.035	901008	2141	-2.29
20	3.74	4.09	10.6	0.065	901009	1401	0.99
21	3.83	4.37	10.2	0.067	901009	1435	1.31
22	4.12	4.56	11.1	0.070	901009	1509	1.57
23	3.45	4.57	9.6	0.067	901009	1608	1.66
24	3.78	4.33	10.7	0.065	901009	1642	1.56
25	3.80	4.52	9.9	0.065	901009	1716	1.36
26	3.53	4.56	9.8	0.055	901009	1831	0.45
27	3.42	4.31	9.3	0.055	901009	1905	-0.07
28	3.01	4.15	10.0	0.054	901009	1939	-0.56
29	2.94	4.31	10.8	0.052	901009	2038	-1.25
30	3.35	4.24	10.5	0.052	901009	2112	-1.56
31	2.89	4.01	9.5	0.050	901009	2146	-1.82
32	4.24	4.38	10.1	0.076	901010	1455	1.09
33	4.49	4.02	9.5	0.078	901010	1529	1.40

Table D12. Continued.

34	4.83	4.34	9.3	0.078	901010	1603	1.66
35	4.56	4.34	8.1	0.076	901010	1714	1.73
36	4.16	4.26	9.2	0.074	901010	1748	1.63
37	3.85	4.82	10.0	0.072	901010	1822	1.42
38	3.97	7.31	8.0	0.066	901011	1131	-1.80
39	3.32	7.27	8.4	0.066	901011	1205	-1.78
40	3.25	6.87	7.7	0.066	901011	1239	-1.36
41	4.71	6.58	7.8	0.079	901011	1348	-1.03
42	4.69	6.54	8.3	0.088	901011	1422	-0.54
43	5.40	6.88	8.1	0.098	901011	1456	0.19
44	4.83	6.42	9.3	0.107	901011	1556	0.99
45	6.20	5.92	8.7	0.113	901011	1630	1.28
46	5.33	6.02	7.6	0.116	901011	1704	1.52
47	5.47	5.86	7.8	0.113	901011	2015	1.18
48	5.64	5.66	8.2	0.107	901011	2049	0.69
49	6.01	5.31	8.3	0.098	901011	2123	0.21
50	5.24	5.73	9.5	0.120	901011	1806	1.68
51	5.14	6.20	8.9	0.120	901011	1840	1.81
52	4.87	5.80	9.1	0.116	901011	1914	1.77
53	4.80	4.80	8.1	0.081	901012	1220	-1.03
54	5.26	4.74	8.7	0.079	901012	1254	-1.12
55	5.04	4.87	7.7	0.086	901012	1328	-1.01
56	6.50	4.95	8.3	0.124	901012	1727	1.52
57	7.77	6.03	14.8	0.125	901012	2039	1.75
58	8.16	6.57	14.8	0.118	901012	2147	1.16
59	7.94	7.90	11.6	0.112	901013	1146	-0.01
60	7.40	8.06	11.1	0.109	901013	1220	-0.38
61	7.11	8.11	11.6	0.109	901013	1254	-0.69
62	7.35	7.60	11.1	0.115	901013	1617	-0.03
63	7.72	8.16	11.1	0.117	901013	1651	0.35
64	7.77	7.12	10.8	0.120	901013	1725	0.68
65	7.17	7.30	10.5	0.124	901013	1840	1.54
66	7.57	6.74	10.4	0.107	901013	1914	1.89
67	7.33	6.50	11.3	0.107	901013	1948	2.05
68	7.29	5.54	10.0	0.107	901013	2055	2.01
69	7.96	6.10	10.9	0.107	901013	2129	1.87
70	7.25	8.25	11.6	0.107	901013	1402	-0.89
71	7.09	8.12	11.1	0.109	901013	1436	-0.82

Table D12. Continued.

72	7.55	7.69	11.4	0.109	901013	1510	-0.68
73	5.64	4.20	9.8	0.105	901014	1301	-0.50
74	5.04	4.03	9.5	0.102	901014	1335	-0.79
75	5.51	3.65	9.6	0.099	901014	1409	-1.04
76	6.75	3.97	9.1	0.117	901014	1831	0.70
77	6.97	3.99	9.7	0.119	901014	1905	1.18
78	6.54	3.88	9.2	0.119	901014	1939	1.50
79	4.82	3.99	9.7	0.099	901014	1512	-1.18
80	5.34	3.69	9.8	0.101	901014	1546	-1.08
81	5.76	3.77	10.1	0.105	901014	1620	-0.85
82	7.29	3.99	9.2	0.122	901014	2046	1.79
83	7.48	3.82	9.6	0.122	901014	2120	1.80
84	6.71	3.43	10.5	0.122	901015	1213	0.79
85	7.26	3.93	11.2	0.121	901015	1247	0.27
86	5.78	3.24	10.5	0.112	901015	1321	-0.21
87	4.77	3.60	11.1	0.099	901015	1642	-1.37
88	4.71	3.83	11.1	0.099	901015	1716	-1.19
89	5.66	3.62	11.1	0.108	901015	1750	-0.87
90	6.48	3.88	10.7	0.119	901015	1852	-0.12
91	6.76	3.77	10.7	0.122	901015	1926	0.32
92	6.37	3.67	11.1	0.122	901015	2000	0.76
93	5.35	5.73	5.8	0.105	901016	1229	1.70
94	5.26	5.50	5.9	0.101	901016	1303	1.32
95	4.16	5.60	6.0	0.088	901016	1337	0.79
96	4.18	4.81	6.0	0.086	901016	1438	-0.21
97	3.94	4.96	6.9	0.084	901016	1512	-0.68
98	4.21	5.00	9.9	0.082	901016	1546	-0.98
99	3.75	4.82	8.2	0.081	901016	1649	-1.21
100	3.66	4.52	8.1	0.084	901016	1723	-1.15
101	3.89	4.46	8.1	0.084	901016	1757	-1.03
102	4.89	4.48	8.5	0.091	901016	1915	-0.02
103	5.66	4.46	10.0	0.096	901016	1949	0.50
104	5.38	4.32	9.7	0.105	901016	2023	0.95
105	5.33	4.30	9.4	0.105	901016	2107	1.48
106	5.21	4.03	9.5	0.111	901016	2141	1.74
107	7.11	4.10	9.4	0.137	901017	1211	2.00
108	7.11	3.76	9.1	0.133	901017	1245	1.72
109	6.44	3.53	6.3	0.126	901017	1319	1.37

Table D12. Concluded.

110	4.58	3.54	4.7	0.086	901017	1839	-1.67
111	4.81	3.73	9.5	0.086	901017	1913	-1.37
112	4.91	3.86	9.4	0.094	901017	1947	-0.98
113	5.68	3.76	8.8	0.104	901017	2051	-0.15
114	6.59	3.82	9.0	0.112	901017	2125	0.29
115	4.00	3.51	9.1	0.094	901017	1419	0.55
116	3.93	3.42	9.1	0.090	901017	1453	-0.04
117	3.93	3.52	8.9	0.083	901017	1527	-0.68
118	3.53	3.67	9.7	0.076	901017	1630	-1.59
119	3.26	3.75	6.3	0.073	901017	1704	-1.87
120	3.32	3.75	8.8	0.073	901017	1738	-1.91
121	4.85	3.83	5.2	0.116	901018	1201	1.62
122	4.71	3.87	5.1	0.116	901018	1235	1.45
123	4.28	4.23	5.2	0.108	901018	1309	1.23
124	3.55	4.61	6.0	0.078	901018	1812	-2.24
125	3.88	4.56	5.9	0.081	901018	1846	-2.15
126	3.38	4.41	5.6	0.081	901018	1920	-2.10
127	3.89	4.29	5.5	0.085	901018	1617	-1.37
128	3.72	4.48	5.8	0.081	901018	1651	-1.82
129	3.81	4.71	5.8	0.081	901018	1725	-2.08
130	4.53	4.77	6.6	0.110	901019	1420	1.47
131	5.11	4.73	6.4	0.104	901019	1454	1.21
132	5.46	5.10	7.1	0.104	901019	1528	0.75
133	4.32	4.14	6.6	0.083	901019	1924	-1.53
134	3.78	4.50	7.3	0.083	901019	1958	-1.36
135	4.37	4.60	6.8	0.083	901019	2032	-1.16
136	4.22	5.13	6.1	0.124	901019	1211	2.18
137	4.42	4.93	6.2	0.124	901019	1245	2.07
138	5.05	4.94	6.6	0.117	901019	1319	1.89

Table D13. Duck 1994 measurements.

Experiment *n*	Wave Runup $R_{2\%}$ (ft)	Deep Water Significant Wave Height, H_{m0} (ft)	Deep Water Peak Wave Period, T_p (s)	Average Slope β (rad)	Date (yymmdd)	Time GMT (hhmm)	Water Level, *h* (ft)
1	3.26	2.39	4.5	0.090	941008	1506	2.37
2	3.18	2.45	3.8	0.089	941008	1709	0.90
3	4.94	5.70	6.4	0.056	941010	2134	-0.63
4	4.29	8.08	7.0	0.071	941011	1306	-0.15
5	5.23	6.97	7.0	0.079	941011	1514	1.75
6	4.68	6.20	6.2	0.065	941012	1126	-0.55
7	5.47	8.23	6.7	0.073	941012	1330	-0.38
8	5.97	8.65	6.6	0.074	941012	1530	0.99
9	6.75	8.44	6.7	0.074	941012	2140	0.92
10	5.54	6.90	7.7	0.076	941013	1313	-0.72
11	7.83	6.69	8.0	0.070	941013	1521	-0.15
12	6.70	7.12	8.3	0.070	941013	2143	1.44
13	5.18	7.47	8.5	0.089	941014	1300	-0.66
14	4.97	7.82	8.6	0.089	941014	1504	-0.72
15	7.28	13.01	10.7	0.071	941015	1334	0.42
16	8.49	13.32	10.8	0.070	941015	1536	-0.11
17	9.08	10.75	10.8	0.068	941016	1149	1.91
18	8.98	10.39	11.5	0.077	941016	1223	1.46
19	8.85	9.89	11.0	0.081	941016	1257	0.88
20	6.67	9.84	10.7	0.077	941016	1351	0.14
21	6.94	10.32	11.1	0.070	941016	1555	-1.03
22	6.51	9.32	11.1	0.074	941016	1759	-0.71
23	7.50	8.88	10.7	0.087	941016	2002	0.91
24	7.15	6.42	10.7	0.078	941017	1153	1.63
25	6.39	6.66	10.7	0.085	941017	1227	1.30
26	7.01	6.41	10.7	0.088	941017	1301	0.93
27	7.30	6.54	10.7	0.091	941017	1355	0.16
28	6.22	6.37	10.7	0.092	941017	1557	-1.38
29	6.38	6.75	10.6	0.095	941017	2001	0.23
30	6.96	5.45	11.9	0.084	941018	1535	-0.50
31	6.20	5.54	11.3	0.082	941018	1609	-0.87

Table D13. Concluded.

32	6.06	5.68	11.6	0.079	941018	1643	-1.13
33	6.21	5.54	11.5	0.082	941018	1736	-1.28
34	6.57	5.59	11.1	0.085	941018	1938	-0.59
35	8.57	4.88	14.6	0.079	941019	1339	1.43
36	8.54	4.52	14.6	0.078	941019	1413	1.09
37	6.31	4.70	12.9	0.072	941019	1926	-1.27
38	7.40	5.04	13.5	0.074	941019	2000	-1.01
39	6.69	4.93	14.8	0.074	941019	2034	-0.63
40	6.20	4.82	14.2	0.072	941019	1718	-1.38
41	7.88	3.62	14.1	0.079	941020	1331	1.77
42	7.82	3.69	13.5	0.078	941020	1405	1.56
43	6.99	3.50	13.5	0.078	941020	1439	1.24
44	9.54	3.17	12.4	0.078	941020	1937	-1.00
45	5.52	3.26	12.8	0.078	941020	2011	-0.75
46	6.22	3.26	12.8	0.078	941020	2045	-0.51
47	4.63	2.94	10.7	0.073	941021	1344	2.19
48	5.09	2.90	11.3	0.073	941021	1418	2.00
49	5.54	2.76	11.5	0.072	941021	1452	1.81
50	4.46	2.67	11.1	0.091	941021	1748	-0.28
51	4.57	2.67	11.1	0.093	941021	1822	-0.52
52	4.27	2.67	11.1	0.093	941021	1856	-0.71

Table D14. SandyDuck measurements.

Experiment *n*	Wave Runup $R_{2\%}$ (ft)	Deep Water Significant Wave Height, H_{m0} (ft)	Deep Water Peak Wave Period, T_p (s)	Average Slope β (rad)	Date (yymmdd)	Time GMT (hhmm)	Water Level *h* (ft)
1	2.73	1.94	5.3	0.092	971003	1200	1.58
2	3.65	2.09	7.1	0.092	971003	1300	1.84
3	3.05	1.98	5.9	0.094	971003	1400	1.62
4	3.15	1.94	10.5	0.098	971003	1500	1.15
5	2.60	1.84	7.1	0.109	971003	1600	0.48
6	2.53	1.73	12.5	0.116	971003	1700	-0.43
7	2.40	1.33	11.1	0.089	971004	1300	1.58
8	2.36	1.21	14.3	0.095	971004	1500	1.46
9	2.39	1.21	14.3	0.089	971004	1200	1.05
10	2.46	1.15	15.4	0.099	971004	1600	0.83
11	1.83	1.57	5.9	0.089	971005	1300	1.33
12	2.84	1.73	10.5	0.096	971006	1200	0.10
13	3.58	1.88	10.0	0.080	971006	1400	1.46
14	3.17	1.94	12.5	0.079	971006	1500	1.66
15	3.55	1.64	10.0	0.097	971007	1500	1.43
16	3.49	1.60	10.0	0.097	971007	1600	1.53
17	3.04	1.67	10.0	0.129	971007	1100	-1.13
18	3.41	1.56	10.0	0.124	971007	1200	-0.57
19	3.75	1.65	9.1	0.106	971007	1300	0.14
20	3.39	1.61	9.1	0.089	971007	1400	0.86
21	3.27	1.49	10.0	0.106	971007	1700	1.29
22	3.47	2.73	4.0	0.092	971008	1600	1.65
23	3.57	2.77	10.0	0.101	971008	1700	1.63
24	3.62	2.80	9.1	0.094	971009	1800	1.73
25	4.30	2.84	10.0	0.102	971009	1900	1.51
26	4.43	2.55	11.1	0.104	971010	1700	1.17
27	3.65	4.33	5.0	0.095	971011	1900	2.18
28	3.44	4.80	5.6	0.092	971011	2000	2.31
29	2.92	4.52	5.0	0.104	971011	1600	0.05
30	3.70	4.39	5.3	0.097	971011	1700	0.93
31	3.72	4.19	5.0	0.092	971011	1800	1.71

Table D14. Continued.

32	2.96	4.63	5.6	0.094	971011	2100	2.14
33	3.70	3.84	10.0	0.096	971012	1900	1.59
34	3.82	3.56	11.8	0.096	971012	2000	2.17
35	3.14	2.73	11.1	0.115	971013	1800	-0.36
36	4.08	2.89	10.5	0.102	971013	1900	0.69
37	3.88	2.08	10.5	0.097	971014	1100	2.39
38	5.53	4.66	10.5	0.092	971016	1100	3.38
39	5.21	4.69	10.0	0.102	971016	1200	3.72
40	4.90	6.36	12.5	0.097	971017	1400	3.50
41	6.39	6.06	6.3	0.105	971017	1300	3.66
42	3.07	5.66	11.8	0.062	971017	1600	1.41
43	3.82	5.84	11.1	0.077	971017	1500	2.60
44	3.98	5.56	11.1	0.089	971017	1800	-0.85
45	3.47	5.80	11.8	0.089	971017	1900	-1.14
46	6.70	6.42	10.5	0.100	971017	1100	2.78
47	3.40	5.87	11.8	0.081	971017	2000	-1.02
48	2.89	6.33	10.0	0.061	971017	2100	-0.48
49	5.63	6.39	11.8	0.105	971017	1200	3.64
50	5.55	5.04	7.7	0.093	971018	1300	3.88
51	2.15	8.94	7.1	0.063	971019	1100	1.72
52	2.85	8.73	7.1	0.074	971019	1200	2.77
53	4.47	9.45	7.7	0.110	971019	1400	4.49
54	4.45	10.22	7.1	0.110	971019	1500	4.48
55	5.29	9.51	7.1	0.110	971019	1600	4.09
56	3.79	10.71	8.3	0.085	971019	1700	3.66
57	3.93	11.71	8.3	0.069	971019	1800	2.73
58	4.22	9.01	7.1	0.110	971019	1300	3.88
59	5.77	7.94	11.8	0.098	971020	1200	1.17
60	6.67	8.11	11.1	0.096	971020	1300	2.22
61	7.01	7.98	11.8	0.097	971020	1400	3.07
62	7.74	7.89	12.5	0.096	971020	1500	3.49
63	8.40	7.72	13.3	0.097	971020	1600	3.38
64	6.66	7.04	12.5	0.097	971020	1700	2.92
65	6.60	6.53	12.5	0.096	971020	1800	2.24
66	5.79	7.05	13.3	0.099	971020	1900	1.33
67	5.94	5.92	14.3	0.084	971021	1500	2.60
68	4.86	6.56	12.5	0.105	971021	1200	0.33
69	6.88	6.33	12.5	0.087	971021	1600	2.89

Table D14. Concluded.

70	5.79	6.28	11.8	0.092	971021	1300	1.02
71	5.86	6.11	11.8	0.089	971021	1400	1.93
72	5.30	6.05	12.5	0.087	971021	1700	2.90
73	5.21	5.91	13.3	0.095	971021	1800	2.44
74	5.06	6.22	12.5	0.101	971021	1900	1.78
75	2.48	3.45	5.3	0.056	971023	1700	1.50
76	2.22	3.63	5.9	0.053	971023	1800	1.56
77	2.01	1.92	11.1	0.076	971024	1700	0.61
78	2.51	1.94	10.5	0.064	971024	1800	0.88
79	1.92	1.52	10.5	0.059	971024	1900	1.09
80	1.81	1.29	11.1	0.064	971024	2000	1.09
81	1.81	1.27	10.5	0.108	971024	2100	0.71
82	2.72	2.97	7.7	0.065	971025	2000	1.36
83	2.50	4.33	7.1	0.062	971026	2100	2.18
84	2.56	4.58	7.1	0.065	971026	2000	1.99
85	2.88	3.31	8.3	0.072	971027	2100	2.17
86	3.40	3.54	7.7	0.071	971027	2000	1.75
87	3.03	6.03	6.3	0.102	971028	1200	1.92
88	3.09	6.87	6.7	0.109	971028	1300	1.09
89	2.45	5.92	7.1	0.132	971028	1400	0.46
90	2.23	6.03	7.1	0.132	971028	1500	-0.21
91	2.37	5.53	7.1	0.139	971028	1600	-0.78
92	1.95	5.21	7.1	0.139	971028	1700	-0.92
93	2.83	1.86	6.7	0.102	971029	1200	1.17
94	3.28	1.29	9.1	0.112	971030	1200	1.35
95	3.12	2.43	3.7	0.098	971031	1200	2.08

Table D15. San Onofre measurements.

Experiment *n*	Wave Runup $R_{2\%}$ (ft)	Deep Water Significant Wave Height, H_{m0} (ft)	Deep Water Peak Wave Period, T_p (s)	Average Slope β (rad)	Date (yymmdd)	Time GMT (hhmm)	Water Level *h* (ft)
1	6.21	3.49	17.0	0.099	931016	1448	2.51
2	7.28	3.46	17.0	0.101	931016	1505	2.51
3	7.06	3.43	17.0	0.107	931016	1522	2.85
4	7.14	3.40	17.0	0.112	931016	1539	3.12
5	6.83	3.29	17.0	0.117	931016	1723	3.38
6	6.13	3.30	17.0	0.109	931016	1740	3.78
7	6.68	3.30	17.0	0.104	931016	1757	3.64
8	6.38	3.31	17.0	0.096	931016	1814	3.50
9	6.30	3.31	17.0	0.089	931016	1831	3.19
10	6.42	3.49	17.0	0.095	931017	1507	3.45
11	7.48	3.48	17.0	0.101	931017	1524	2.11
12	8.08	3.46	17.0	0.101	931017	1541	2.43
13	7.51	3.44	17.0	0.109	931017	1558	2.75
14	7.27	3.43	17.0	0.113	931017	1615	3.07
15	7.35	3.41	17.0	0.113	931017	1632	3.28
16	6.79	3.38	17.0	0.118	931017	1820	3.47
17	7.27	3.38	17.0	0.115	931017	1837	3.57
18	5.79	2.68	15.0	0.097	931018	1613	3.44
19	5.82	2.65	15.0	0.103	931018	1630	2.41
20	7.04	2.60	15.0	0.119	931018	1700	2.66
21	6.90	2.62	15.0	0.125	931018	1734	3.09
22	6.81	2.63	15.0	0.125	931018	1808	3.34
23	6.99	2.64	15.0	0.125	931018	1825	3.51
24	7.01	2.66	15.0	0.119	931018	1905	3.47
25	6.70	2.67	15.0	0.114	931018	1922	3.33
26	5.53	2.68	15.0	0.103	931018	2000	3.12
27	5.04	2.69	15.0	0.103	931018	2017	2.64
28	5.14	2.70	15.0	0.098	931018	2034	2.30
29	4.29	2.70	15.0	0.092	931018	2051	1.95
30	3.78	2.71	15.0	0.086	931018	2108	1.61
31	3.02	2.45	15.0	0.074	931019	1357	2.04

Table D15. Concluded.

32	3.17	2.43	14.9	0.074	931019	1414	-0.10
33	2.77	2.41	14.7	0.078	931019	1446	0.05
34	2.95	2.40	14.6	0.081	931019	1503	0.38
35	3.63	2.38	14.5	0.081	931019	1520	0.56
36	3.93	2.37	14.4	0.086	931019	1537	0.78
37	3.87	2.36	14.3	0.092	931019	1554	1.01
38	4.40	2.33	14.1	0.106	931019	1628	1.24
39	5.15	2.31	14.0	0.114	931019	1657	1.70
40	5.03	2.32	13.9	0.116	931019	1714	2.10
41	4.89	2.32	13.7	0.121	931019	1748	2.29
42	4.89	2.33	13.6	0.122	931019	1805	2.65
43	4.76	2.33	13.5	0.124	931019	1822	2.80
44	5.45	2.34	13.3	0.126	931019	1900	2.88
45	5.55	2.35	13.1	0.125	931019	1934	3.05
46	4.99	2.34	13.0	0.123	931019	1958	2.94
47	4.84	2.33	13.0	0.121	931019	2015	2.86
48	5.08	2.31	13.0	0.121	931019	2032	2.69
49	4.49	2.30	13.0	0.118	931019	2049	2.50
50	4.93	2.29	13.0	0.116	931019	2106	2.31
51	4.28	2.27	13.0	0.109	931019	2123	2.08
52	4.02	2.26	13.0	0.103	931019	2140	1.78
53	3.24	1.75	13.0	0.084	931020	1447	1.99
54	3.36	1.74	13.0	0.084	931020	1504	0.18
55	3.40	1.72	13.0	0.084	931020	1521	0.25
56	3.14	1.71	13.0	0.085	931020	1538	0.36
57	3.39	1.69	13.0	0.088	931020	1555	0.48
58	3.60	1.68	13.0	0.091	931020	1612	0.60
59	3.53	1.67	13.0	0.091	931020	1629	0.50

Table D16. Scripps measurements.

Experiment *n*	Wave Runup $R_{2\%}$ (ft)	Deep Water Significant Wave Height, H_{m0} (ft)	Deep Water Peak Wave Period, T_p (s)	Average Slope β (rad)	Date (yymmdd)	Time GMT (hhmm)	Water Level *h* (ft)
1	1.92	2.11	10.0	0.055	890626	2056	1.24
2	2.03	2.17	10.0	0.049	890626	2113	1.45
3	1.88	2.21	10.0	0.045	890626	2130	1.63
4	1.95	2.27	10.0	0.038	890626	2146	1.81
5	1.97	2.27	10.0	0.038	890626	2147	1.82
6	2.25	2.33	10.0	0.038	890626	2203	1.98
7	2.25	2.33	10.0	0.038	890626	2204	1.98
8	2.05	2.39	10.0	0.038	890626	2220	2.06
9	2.05	2.39	10.0	0.038	890626	2221	2.06
10	1.88	2.45	10.0	0.038	890626	2237	2.14
11	1.88	2.45	10.0	0.038	890626	2238	2.14
12	2.28	2.49	10.0	0.038	890626	2254	2.22
13	2.28	2.51	10.0	0.038	890626	2255	2.22
14	2.28	2.55	10.0	0.041	890626	2311	2.22
15	2.28	2.55	10.0	0.041	890626	2312	2.21
16	2.50	2.61	10.0	0.041	890626	2328	2.17
17	1.82	2.76	10.0	0.039	890627	1944	-0.18
18	1.92	2.75	10.0	0.043	890627	2001	0.06
19	1.87	2.74	10.0	0.046	890627	2018	0.31
20	1.82	2.74	10.0	0.045	890627	2035	0.57
21	2.12	2.72	10.0	0.041	890627	2109	1.07
22	2.29	2.72	10.0	0.041	890627	2126	1.31
23	1.17	2.68	10.0	0.029	890628	1901	-0.91
24	1.38	2.65	10.0	0.035	890628	1935	-0.80
25	1.44	2.57	10.0	0.032	890628	2109	0.39
26	1.54	2.56	10.0	0.032	890628	2126	0.63
27	1.62	2.55	10.0	0.029	890628	2143	0.86
28	0.91	1.83	10.0	0.032	890629	1951	-0.75
29	0.98	1.81	10.0	0.032	890629	2008	-0.67
30	0.99	1.79	10.0	0.032	890629	2025	-0.56
31	1.12	1.79	10.0	0.034	890629	2042	-0.45
32	1.06	1.79	10.0	0.034	890629	2059	-0.34
33	1.06	1.79	10.0	0.035	890629	2116	-0.12
34	1.12	1.79	10.0	0.030	890629	2133	0.11
35	1.01	1.79	10.0	0.028	890629	2152	0.36
36	1.01	1.78	10.0	0.025	890629	2209	0.62
37	1.11	1.78	10.0	0.027	890629	2226	0.89
38	1.39	1.78	10.0	0.031	890629	2243	1.16
39	1.56	1.78	10.0	0.039	890629	2300	1.43
40	1.42	1.78	10.0	0.045	890629	2317	1.71
41	1.49	1.78	10.0	0.054	890629	2334	1.99

Table D17. Agate Beach measurements.

Experiment *n*	Wave Runup $R_{2\%}$ (ft)	Deep Water Significant Wave Height, H_{m0} (ft)	Deep Water Peak Wave Period, T_p (s)	Average Slope β (rad)	Date (yymmdd)	Time GMT (hhmm)	Water Level *h* (ft)
1	3.89	7.57	12.2	0.017	960211	2357	1.32
2	3.63	6.75	12.7	0.015	960211	2145	-0.77
3	2.31	6.07	12.9	0.013	960211	1732	-1.80
4	2.23	6.14	12.8	0.012	960211	1806	-2.29
5	2.31	6.20	12.8	0.012	960211	1840	-2.49
6	4.45	6.97	12.5	0.015	960211	2219	-0.16
7	3.74	7.20	12.4	0.016	960211	2253	-0.50
8	4.40	7.91	13.0	0.017	960211	2431	0.68
9	3.98	8.25	14.0	0.017	960211	2505	1.76
10	5.96	10.04	14.3	0.015	960212	1713	-0.34
11	4.89	10.15	14.3	0.014	960212	1747	-1.14
12	2.55	10.09	7.1	0.019	960217	1536	2.33
13	2.83	10.19	7.3	0.023	960217	1610	3.30
14	2.21	10.31	7.6	0.023	960217	1644	4.29

Table D18. Gleneden Beach measurements.

Experiment *n*	Wave Runup $R_{2\%}$ (ft)	Deep Water Significant Wave Height, H_{m0} (ft)	Deep Water Peak Wave Period, T_p (s)	Average Slope β (rad)	Date (yymmdd)	Time GMT (hhmm)	Water Level *h* (ft)
1	5.76	6.26	12.4	0.070	940226	1751	2.16
2	7.63	6.27	12.3	0.088	940226	1808	2.68
3	6.74	6.29	12.2	0.093	940226	1825	3.17
4	6.05	6.29	12.2	0.093	940226	1842	3.65
5	7.04	6.27	12.1	0.097	940226	1859	4.13
6	7.01	6.19	12.0	0.099	940226	1951	5.01
7	6.94	6.16	11.9	0.097	940226	2008	5.12
8	6.68	6.13	11.9	0.099	940226	2025	5.01
9	6.39	6.12	11.9	0.097	940226	2042	4.91
10	5.64	6.09	11.8	0.093	940226	2059	4.81
11	6.46	6.06	11.8	0.093	940226	2116	4.47
12	5.13	6.00	11.7	0.084	940226	2159	3.56
13	4.67	6.00	11.8	0.084	940226	2216	3.01
14	4.17	5.99	11.9	0.059	940226	2233	2.45
15	4.40	7.40	10.5	0.030	940227	1744	-0.18
16	5.16	7.34	10.5	0.048	940227	1801	0.37
17	5.25	7.30	10.5	0.064	940227	1818	0.93
18	6.03	7.24	10.6	0.069	940227	1835	1.49
19	6.60	7.18	10.7	0.081	940227	1852	2.05
20	6.10	7.17	10.7	0.081	940227	1909	2.57
21	6.43	7.17	10.8	0.081	940227	1947	3.65
22	7.54	7.17	10.8	0.093	940227	2004	4.08
23	6.60	7.17	10.9	0.107	940227	2021	4.29
24	7.55	7.17	10.9	0.107	940227	2038	4.51
25	6.27	7.17	11.0	0.107	940227	2055	4.72
26	6.08	7.17	11.0	0.093	940227	2112	4.70
27	6.37	7.17	11.1	0.079	940227	2131	4.56
28	6.44	7.17	11.1	0.081	940227	2148	4.43
29	6.58	7.17	11.2	0.081	940227	2205	4.22
30	5.79	7.15	11.2	0.081	940227	2222	3.79
31	5.61	7.13	11.3	0.064	940227	2239	3.36
32	4.32	7.12	11.3	0.060	940227	2256	2.93
33	3.91	7.10	11.4	0.035	940227	2313	2.37
34	5.63	6.15	16.0	0.067	940228	1922	0.94
35	6.51	6.24	16.0	0.071	940228	1939	1.49
36	6.90	6.96	16.0	0.081	940228	2201	4.30
37	7.86	6.97	16.0	0.088	940228	2218	4.11
38	7.38	6.99	16.0	0.081	940228	2235	3.92
39	6.36	7.00	16.0	0.075	940228	2252	3.73
40	7.04	7.01	16.0	0.075	940228	2309	3.65
41	6.42	7.03	16.0	0.061	940228	2326	3.65
42	5.80	7.04	16.0	0.058	940228	2343	2.55

Table D19. Terschelling measurements.

Experiment *n*	Wave Runup, $R_{2\%}$ (ft)	Deep Water Significant Wave Height, H_{m0} (ft)	Deep Water Peak Wave Period, T_p (s)	Average Slope β (rad)	Date (yymmdd)
1	1.62	4.61	6.5	0.030	940402
2	3.29	10.06	7.7	0.032	940407
3	2.76	12.89	10.3	0.015	940408
4	3.99	11.77	10.6	0.016	940411
5	3.01	7.85	8.9	0.016	940412
6	1.67	8.60	8.4	0.020	940413
7	1.69	3.82	10.4	0.013	941005
8	1.55	3.51	9.9	0.014	941006
9	1.41	6.46	8.2	0.009	941011
10	1.62	3.15	10.0	0.017	941012
11	0.45	1.68	4.8	0.014	941015
12	0.76	1.69	5.0	0.013	941016
13	0.79	3.51	6.1	0.011	941017
14	1.39	4.65	8.7	0.011	941021

REPORT DOCUMENTATION PAGE

Form Approved
OMB No. 0704-0188

1. REPORT DATE *(DD-MM-YYYY)*	**2. REPORT TYPE**	**3. DATES COVERED** *(From - To)*
October 2012	Final report	

4. TITLE AND SUBTITLE

Wave Runup Prediction for Flood Hazard Assessment

5a. CONTRACT NUMBER

5b. GRANT NUMBER

5c. PROGRAM ELEMENT NUMBER

6. AUTHOR(S)

Jeffery A. Melby

5d. PROJECT NUMBER

5e. TASK NUMBER

5f. WORK UNIT NUMBER

7. PERFORMING ORGANIZATION NAME(S) AND ADDRESS(ES)

U.S. Army Engineer Research and Development Center
Coastal and Hydraulics Laboratory
3909 Halls Ferry Road
Vicksburg, MS 39180--6199

8. PERFORMING ORGANIZATION REPORT NUMBER

ERDC/CHL TR-12-24

9. SPONSORING / MONITORING AGENCY NAME(S) AND ADDRESS(ES)

U.S. Army Engineer District, Detroit
477 Michigan Avenue, Detroit, MI 48226;
Federal Emergency Management Agency
536 Clark Street, 6th Floor, Chicago, IL 60605

10. SPONSOR/MONITOR'S ACRONYM(S)

11. SPONSOR/MONITOR'S REPORT NUMBER(S)

12. DISTRIBUTION / AVAILABILITY STATEMENT

Approved for public release; distribution is unlimited.

13. SUPPLEMENTARY NOTES

14. ABSTRACT

Wave runup determines the extent over which waves act. Wave runup is therefore an important parameter to determine flood inundation extents from coastal storms. Cross-shore and longshore sediment transport are a function of the hydrodynamics on the beach and are therefore related to wave runup. In this report, several benchmark wave runup data sets are summarized and used to evaluate the available tools for predicting wave runup for flood hazard assessment. Benchmark data cover a range of shoreline conditions including sandy beaches on the Pacific and Atlantic coasts, dissipative to reflective beaches, as well as structures ranging from impermeable smooth levees to rough permeable rubble mounds. Data include laboratory and prototype measurements. Tools for predicting wave runup are analyzed including empirical equations, computer programs based on empirical equations, and the CSHORE numerical hydrodynamic model. Most of the tools show fairly high degrees of skill but some do not. The study recommends using the numerical hydrodynamic program CSHORE to model runup for most beach and structure conditions. However, CSHORE is not likely to predict wave runup on infragravity-dominated dissipative beaches well. For these cases, it is recommended that one of the recommended empirical equations for beaches be used.

15. SUBJECT TERMS

Beaches
Coastal structures
Flood hazard
Flooding
Wave height
Wave runup
Wave setup
Waves

16. SECURITY CLASSIFICATION OF:			**17. LIMITATION OF ABSTRACT**	**18. NUMBER OF PAGES**	**19a. NAME OF RESPONSIBLE PERSON: Jeffrey A. Melby**
a. REPORT	**b. ABSTRACT**	**c. THIS PAGE**			**19b. TELEPHONE NUMBER** *(include area code)*
UNCLASSIFIED	UNCLASSIFIED	UNCLASSIFIED		122	

Standard Form 298 (Rev. 8-98)
Prescribed by ANSI Std. 239.18